EMISSIVITIES AND ABSORPTIVITIES OF GASES

Thesis by
J. Alex Thomson

In Partial Fulfillment of the Requirements
For the Degree of
Doctor of Philosophy

California Institute of Technology
Pasadena, California
1958

ACKNOWLEDGEMENTS

The author is indebted to Dr. S. S. Penner for suggesting these studies and for his continued interest and advice during the progress of the work. He is grateful to Messrs. W. J. Hooker, F. Williams and M. Lapp for many illuminating discussions and to Miss Barbara Rickert for her untiring efforts in typing the thesis.

Support for part of the studies, through the U. S. Navy (Office of Naval Research) under Contract Nonr-220(03), NR 015 401 and the U. S. Air Force under Contract AF 18(603)-2 is gratefully acknowledged.

ABSTRACT

Equilibrium emissivities and absorptivities of heated gases have been computed from spectroscopic data. Several problems have been studied:

(1) The relation between equilibrium absorptivities and equilibrium emissivities for diatomic and polyatomic molecules has been investigated. Our theoretical results provide a satisfactory correlation of available experimental data for heated water vapor but not for carbon dioxide. The origin of the failure of the theory for carbon dioxide is discussed in detail.

(2) The available, empirically determined, emissivity data for water vapor have been correlated in terms of a statistical model for the distribution of spectral lines within well-defined wavelength regions corresponding to the stronger vibration-rotation bands. This correlation provides a useful framework for the extrapolation of measured emissivity data to temperatures and pressures somewhat different from those used to obtain the experimental data.

(3) The equilibrium emissivity of heated NO has been calculated for the conditions under which this molecule exists in high-temperature air during reentry of hypersonic missiles. An extension of the Mayer-Goody statistical model was used for emissivity calculations on NO. Our semi-analytical results are in acceptable agreement with a simpler numerical analysis of Kivel, Mayer and Bethe.

The original investigations of gas absorptivities and emissivities are introduced with a brief survey of basic theoretical results. An attempt has also been made to calculate the dipole moments and low energy transition probabilities for HF, HCl and HBr. In this study it was found that the intensities of lines lying in the infrared are very sensitive to the details of the approximating wavefunctions. A considerably more detailed description of the wavefunctions than is available at present is required to make confident predictions of absolute intensities from first principles.

TABLE OF CONTENTS

Page

Acknowledgements

Abstract

Table of Contents

List of Figures

I. INTRODUCTION 1

A. Blackbody Radiation Laws 1

B. Basic Laws for Distributed Radiators 3

C. Einstein Coefficients and Integrated Absorption 5

D. Oscillator Strengths 10

E. Spectral Line Profiles 11

F. Matrix Elements 12

II. DIPOLE MOMENTS AND EFFECTIVE CHARGES FOR HF, HCl AND HBr 17

A. Introduction 17

B. Electronic Wave Functions 19

C. Dipole Moments and Effective Charges 26

D. Outline of Calculations 27

E. Discussion 33

a. Change of Ionicity with r_e 33

b. Polarization of the Inner Core of the Halogen 35

c. Polarization of the Valence Shell Electrons 36

d. The Slater Wave Functions 37

e. The Percentage Ionicity and Percentage s-p Hybridization 37

F. Reduction of Molecular Matrix Elements to Functions of One-Electron Matrix Elements 38

III. EMISSIVITIES AND ABSORPTIVITIES 40

A. Introduction 40

B. The Statistical Model 44

Page

C. The Regularly Spaced Model 47

D. Approximate Expressions for Vibration-Rotation Band Radiancies 48

E. Absorptivity of Molecular Vibration-Rotation Bands for Radiation Emitted by Molecular Vibration-Rotation Bands 51

a. Absorptivity of Water Vapor for Blackbody Radiation 57

b. Absorptivity of Carbon Dioxide Vapor for Blackbody Radiation 58

c. Improved Representation of the Absorptivity 59

F. Limits of Validity of the Effective Band-Width Approximation 65

G. Semi-Empirical Correlation of Infrared Emissivities for Heated Water Vapor 69

a. Mean Emissivity $\bar{\varepsilon}^{(1)}$ for the Distribution $P^{(1)}(\bar{S}, S) = (1/\bar{S}) \exp(-S/\bar{S})$ 70

b. Mean Emissivity $\bar{\varepsilon}^{(2)}$ for the Distribution $P^{(2)}(\bar{S}, S) = \delta(S-\bar{S})$ 71

c. The Engineering Emissivity for Water Vapor 72

d. Outline of Emissivity Calculations for Water Vapor 73

H. Emissivity Estimates for Heated NO 77

a. Introduction 77

b. Outline of the Calculations 80

c. Structure of the Spectrum 82

1. Line Widths 82

2. Electronic Structure 83

3. Vibrational Structure 83

4. Rotational Structure 84

d. The Total Absorption of an Isolated Band of Non-Overlapping Spectral Lines Having Combined Doppler and Collision Broadening 87

e. Approximation Procedures 91

Page

f. The Total Emissivity of a Band System in Which the Bands are Distributed Statistically 95

g. The Total Emissivity of the NO β- and γ-Bands Systems (at 8000°K) 96

References 108

Tables 113

Figures 129

LIST OF FIGURES

Page

1. Geometry of the molecule HX. 129

2. The reduced dipole moment μ/ea_H of HF as a function of percentage s-p hybridization for different ionicities. 130

3. The reduced effective charge $\frac{1}{e}\frac{\partial \mu}{\partial r}_e$ of HF as a function of the percentage s-p hybridization for different ionicities. 131

4. The reduced dipole moment μ/ea_H of HCl as a function of the percentage s-p hybridization for different ionicities. 132

5. The reduced effective charge $\frac{1}{e}\frac{\partial \mu}{\partial r}_e$ of HCl as a function of the percentage s-p hybridization for different ionicities. 133

6. The reduced dipole moment μ/ea_H of HBr as a function of the percentage s-p hybridization for different ionicities. 134

7. The reduced effective charge $\frac{1}{e}\frac{\partial \mu}{\partial r}_e$ of HBr as a function of the percentage s-p hybridization for different ionicities. 135

8. The reduced effective charge as a function of the percentage s-p hybridization when the ratio α/β is chosen in such a way that the calculated values of the dipole moments agree with the measured values (the dashed portions of the curves correspond to negative values of λ). 136

9. The ratios α_H/α_{obs} and α/α_{obs} for blackbody radiation at a temperature T_s=1160°R. 137

10. The ratios α_H/α_{obs} and α/α_{obs} for blackbody radiation at a temperature T_s=1760°R. 138

Page

11. The ratios α_H/α_{obs} and α/α_{obs} for blackbody radiation at a temperature $T_s = 2500^\circ R$. 139

12. Comparison of calculated and measured hemispherical absorptivity data for water vapor. The open points are calculated for an over-lapping line model according to Eq. (140) and the solid points for a non-overlapping model according to Eq. (159). 140

13. The quantity $P_{j\rightarrow j-1}(\omega) + P_{j\rightarrow j+1}(\omega)$ evaluated at $\omega = \omega_o + 100\delta$ as a function of j for $b/\delta = 2.5$ and $(2\gamma u_e)^{-1/2} = 25$. The dashed curve represents $j \exp\left[-\gamma u_e j^2\right]$. 141

14. The emissivity of water vapor calculated from Eq. (188) by use of "best" values of the adjustable parameters. The circles represent experimental points according to Hottel[58] for pure water vapor at a pressure of 0.5 atmos. 142

15. Plot for determining the intensity distribution function $P(\alpha, \bar{\alpha})$ for the β-band system of NO at $8000^\circ K$. The solid curves correspond to the distribution $P(\beta, \bar{\beta}) = (\bar{\beta})^{-1}\exp(-\beta/\bar{\beta})$. The points are computed according to Eq. (257a) for $v' \leq 6$ utilizing the values of $q^2_{v''v'}$ listed by Kivel, Mayer and Bethe.[26] 143

16. Plot for determining the intensity distribution function $P(\alpha, \bar{\alpha})$ for the β-band system of NO at $8000^\circ K$. The solid curves correspond to the distribution $P(\beta, \bar{\beta}) = (\bar{\beta})^{-1}$ $\exp(-\beta/\bar{\beta})$. The points are computed according to Eq. (257a) for $v' \leq 6$ utilizing the values of $q^2_{v''v'}$ listed by Kivel, Mayer and Bethe.[26] 144

Page

17. Plot for determining the intensity distribution function $\rho(\alpha, \bar{\alpha})$ for the β-band system of NO at 8000°K. The solid curves correspond to the distribution $\rho(\beta, \bar{\beta})=(\bar{\beta})^{-1}$ $\exp(-\beta/\bar{\beta})$. The points are computed according to Eq. (257a) for $v' \leq 6$ utilizing the values of $q^2_{v''v'}$ listed by Kivel, Mayer and Bethe.[26] 145

18. The mean value of the parameter β for $v' \leq 6$ as a function of ω for the β-band system of NO at 8000°K. 146

19. The function $H(\gamma, a)$. 147

20. The parameter $1-\varepsilon(\bar{\gamma})$ as a function of $\bar{\gamma}$. 148

21. The hemispherical emissivity of the γ- and β-bands of NO (for $f_{elec\,\gamma} = 0.312\, f_{elec\,\beta}$). The lower boundaries of the hatched regions refer to zero pressure and the upper boundaries to high pressure. For intermediate pressures the emissivity lies within the hatched regions. 149

22. Partial emission spectrum of the β-bands of NO at 8000°K and high pressure. Only transitions from the first six upper vibrational states have been included. The values of vibrational overlap integrals were taken from ref. (26). 150

23. The "smoothed" spectral radiancy $\bar{R}_\omega = \bar{\varepsilon}_\omega R^0_\omega$ for the NO β-bands at 4000°K. The lower boundaries of the hatched regions correspond to zero pressure and the upper boundaries to very high pressure. For intermediate pressures the radiancy lies within the hatched regions. 151

24. The "smoothed" spectral radiancy $\bar{R}_\omega = \bar{\varepsilon}_\omega R^0_\omega$ for the NO β-bands at 8000°K. The lower boundaries of the hatched regions correspond to zero pressure and the upper boundaries to very high pressure. For intermediate pressures the radiancy lies within the hatched regions. 152

I. INTRODUCTION

Radiant energy transfer is of fundamental importance in the solution of many problems in applied science. Examples of interesting practical applications are theoretical calculations of (equilibrium) radiant heat transfer, flame temperature measurements, determinations of gas composition and excitation behind shock fronts, spectroscopic analysis of isothermal multicomponent gas mixtures, etc. Usually a satisfactory description of the phenomena involved is feasible only for equilibrium (thermal) radiation. In the following discussion we shall outline the fundamental approach used for the calculation of the thermal radiation characteristics of gases. In this introductory section we discuss the physical laws which are basic to a calculation of radiant heat transfer. In Section II we are concerned with the calculation of the infrared transition probabilities for the hydrogen halides HF, HCl and HBr. In Section III we develop various procedures for the calculation of total emissivities and absorptivities and apply these methods to specific gases.

A. Blackbody Radiation Laws

A blackbody is defined as a body which absorbs all of the radiation which it receives. It can be shown that the equilibrium energy of radiation emitted from unit area of a blackbody in unit time at a fixed

temperature represents an upper limit for the thermally emitted energy from unit area for any substance which is at the same temperature as the blackbody. This definition of a blackbody and the quantum-mechanical principle of equipartition of energy[2-4] are sufficient to establish the Planck blackbody distribution law for the spectral (or monochromatic) radiancy $R^{o}_{\lambda}\, d\lambda$, which is defined as the energy emitted, per unit time, from unit area of a blackbody, in the wavelength range between λ and $\lambda + d\lambda$, at the absolute temperature T (in ^{o}K), into a solid angle of 2π steradians. The Planck blackbody distribution law is

$$R^{o}_{\lambda}\, d\lambda = \frac{c_1}{\lambda^5} \frac{d\lambda}{\left[\exp(c_2/\lambda T)\right] - 1} \qquad (1)$$

where c_1/π and c_2 are known as the first and second radiation constants, respectively. The quantities c_1 and c_2 may be expressed in terms of the fundamental physical constants c (velocity of light), h (Planck's constant), and k (Boltzmann constant). Thus $c_1 = 2\pi c^2 h \simeq 3.740 \times 10^{-5}$ erg-cm^2-sec^{-1} and $c_2 = hc/k \simeq 1.439$ cm-^{o}K.

The total radiant energy emitted from unit area in unit time by a blackbody over all wavelengths into a solid angle of 2π steradians is

$$W = \int_0^{\infty} R^{o}_{\lambda}\, d\lambda = \sigma T^4 \qquad (2)$$

where σ is known as the Stefan-Boltzmann constant and has the numerical value $\sigma \simeq 5.670 \times 10^{-5}$ erg-cm^{-2}-(^{o}K)$^{-4}$-sec^{-1}. The quantity W is variously referred to as the radiant flux per unit area, total emissive power of a blackbody, or radiancy.

The quantities R^o_λ , $R^o_{\lambda\,max}$, $R^o_\lambda / R^o_{\lambda\,max}$, $\int_0^\lambda R^o_{\lambda'} d\lambda'$, W, and $(1/W)\int_0^\lambda R^o_{\lambda'} d\lambda'$ have been tabulated for the wavelengths and/or temperatures which are likely to be encountered in practice.(5)

The frequency ν is related to the wavelength λ through the expression $\nu = c/\lambda$ where c is the velocity of light ($c \simeq 2.998 \times 10^{10}$ cm-sec^{-1}); the wave number ω is the reciprocal of the wavelength. Hence we may rewrite Eq. (1) in the equivalent forms

$$R^o_\nu \, d\nu = \frac{2\pi h \nu^3}{c^2} \frac{d\nu}{\left[\exp(h\nu/kT)\right] - 1} \tag{1a}$$

and

$$R^o_\omega \, d\omega = 2\pi hc\omega^3 \frac{d\omega}{\left[\exp(hc\omega/kT)\right] - 1} \, . \tag{1b}$$

B. Basic Laws for Distributed Radiators

From thermodynamic arguments one can deduce Kirchhoff's law, which states that the spectral radiancy of any substance equals the product of the spectral absorptivity P'_ω and the spectral radiancy of a blackbody. In other words, the spectral emissivity ε_ω and the spectral absorptivity P'_ω are identically equal. It is convenient in practice to introduce the product of two dimensional parameters for the dimensionless spectral absorptivity P'_ω. Following customary procedure we write for distributed radiators

$$P'_\omega = P_\omega \, dX$$

where P_ω is termed the spectral absorption coefficient and is expressed in cm^{-1}-atmos^{-1} or in ft^{-1}-atmos^{-1}, with the pressure referring to the actual pressure of radiators responsible for absorption at the

wave number ω ; correspondingly, the optical density dX, which represents the product of a geometric length and the partial pressure of the radiators, must have the dimensions of cm-atmos or ft-atmos, respectively.

Consider now a system of isothermal radiators at pressure p distributed uniformly through a region of geometric length ℓ . The optical density of a region of infinitesimal geometric length dx is $dX = p\,dx$; the optical density of the region of geometric length ℓ is $X = p\ell$. It is desired to obtain an expression for the total spectral radiancy from the isothermal distributed radiators located in a column of geometric length ℓ . Let the spectral radiancy incident on the face be R_ω . The change in spectral radiancy corresponding to the region of optical depth dX is then

$$dR_\omega = (P_\omega\, dX)R^o_\omega - (P_\omega\, dX)R_\omega$$

where the first term on the right-hand side represents the emitted spectral radiancy in dX and the second term measures the attenuation by the absorbers of radiation in dX. Since $R_\omega = 0$ for $X = 0$ it follows that

$$R_\omega = R^o_\omega \left[1-\exp(-P_\omega X)\right] . \qquad (3)$$

Equation (3) is the basic phenomenological law for the emission of radiation from distributed sources.

Reference to Eq. (3) shows that the spectral emissivity of the uniformly distributed radiators is given by the relation

$$\varepsilon_\omega = \left[1-\exp(-P_\omega X)\right] . \qquad (4)$$

Similarly, the total or engineering emissivity ε used in practical calculations on radiant heat transfer is

$$\varepsilon = \frac{1}{W} \int_0^\infty E^\circ_\omega \left[1-\exp(-P_\omega X)\right] d\omega. \qquad (5)$$

Theoretical calculations of gas emissivities therefore require determination of P_ω in terms of atomic or molecular parameters, followed by evaluation of the integral appearing in Eq. (5). In this connection it is of particular importance to note that absorption coefficients P_ω for gas mixtures are additive but that neither spectral nor total emissivities can be added. As the result of this requirement, neither ε_ω nor ε can exceed unity for equilibrium radiation.

C. Einstein Coefficients[7] and Integrated Absorption

Let N_l = number of molecules per unit volume in the lower quantum state,

N_u = number of molecules per unit volume in the upper quantum state,

$B_{l \to u}$ = Einstein coefficient for induced absorption,

$B_{u \to l}$ = Einstein coefficient for induced emission

$A_{u \to l}$ = Einstein coefficient for spontaneous emission.

The Einstein coefficient $B_{l \to u}$ is defined in such a way that the probability of a transition from the lower state with energy E_l to the upper state with energy E_u in unit time (sec), in a radiation field of density $\rho_{\nu_{lu}}$ at the frequency ν_{lu}, equals $B_{l \to u}\ \rho_{\nu_{lu}}$. For black radiating systems in equilibrium at the temperature T,

$$\rho_{\nu_{\ell u}} = \frac{8\pi h \nu_{\ell u}^3}{c^3} \frac{1}{\left[\exp\left(h\nu_{\ell u}/kT\right)\right] - 1} \tag{6}$$

according to the Planck blackbody distribution curve. In Eq. (6) the dimensions of $\rho_{\nu_{\ell u}}$ are, for example, erg-sec/cm^3 whence it follows that the dimensions of $B_{\ell \longrightarrow u}$ are cm^3/erg-sec^2.

The Einstein coefficients are related in such a way that the number of transitions in unit time in unit volume from energy E_ℓ to energy E_u is

$$N_\ell B_{\ell \longrightarrow u} \rho_{\nu_{\ell u}}$$

and the number of transitions in unit time in unit volume from energy E_u to energy E_ℓ equals

$$N_u\left(A_{u \longrightarrow \ell} + B_{u \longrightarrow \ell} \rho_{\nu_{\ell u}}\right).$$

At equilibrium

$$N_\ell B_{\ell \longrightarrow u} \rho_{\nu_{\ell u}} = N_u\left(A_{u \longrightarrow \ell} + B_{u \longrightarrow \ell} \rho_{\nu_{\ell u}}\right)$$

whence it follows that

$$\frac{N_\ell}{N_u} = \frac{A_{u \longrightarrow \ell} + B_{u \longrightarrow \ell} \rho_{\nu_{\ell u}}}{B_{\ell \longrightarrow u} \rho_{\nu_{\ell u}}}. \tag{7}$$

But, at equilibrium, we have also

$$\frac{N_\ell}{N_u} = \frac{g_\ell}{g_u} e^{-(E_\ell - E_u)/kT} = \frac{g_\ell}{g_u} e^{h\nu_{\ell u}/kT}$$

and Eq. (7) becomes therefore

$$\rho_{\nu_{\ell u}} = \frac{A_{u \longrightarrow \ell}/B_{u \longrightarrow \ell}}{\frac{g_\ell}{g_u}\frac{B_{\ell \longrightarrow u}}{B_{u \longrightarrow \ell}}\left[\exp(h\nu_{\ell u}/kT)\right] - 1}. \tag{8}$$

Comparison of Eqs. (7) and (8) shows that the following expressions are consistent with the required form of the relation for the volume density of blackbody radiation at the frequency $\nu_{\ell u}$:

$$A_{u \to \ell} = \frac{8\pi h \nu_{\ell u}^3}{c^3} B_{u \to \ell} \tag{9}$$

and

$$g_\ell B_{\ell \to u} = g_u B_{u \to \ell}. \tag{10}$$

Thus $B_{\ell \to u}$ like $B_{u \to \ell}$ has the dimensions $cm^3/erg\text{-}sec^2 = cm/g$ in metric units whereas $A_{u \to \ell}$ is a frequency (sec^{-1}).

The total number of transitions N_{tr} from E_ℓ to E_u induced in unit time in unit volume by a radiation field of volume density ρ_ν is

$$N_{tr} = (N_\ell B_{\ell \to u} - N_u B_{u \to \ell}). \tag{11}$$

Consider an isotropic medium in thermal equilibrium at the temperature T. Then the radiant intensity I_ν (in erg/cm^2) passing through the solid angle $d\Omega$ per sec in the frequency interval between ν and $\nu + d\nu$ is

$$I_\nu d\nu \, d\Omega' = \left(\frac{c}{4\pi}\right) \rho_\nu d\nu \, d\Omega,$$

i.e.,

$$I_\nu = \frac{c}{4\pi} \rho_\nu. \tag{12}$$

The spectral absorption coefficient k_ν (in cm^{-1}) is defined by the relation

$$-dI_\nu/d\ell = k_\nu I_\nu$$

where $-dI_\nu$ measures the decrease in I_ν in the path length $d\ell$ (in cm). Hence

$$-(dI_\nu/d\ell)d\nu \, d\Omega = I_\nu k_\nu d\nu d\Omega$$

equals the rate of absorption of radiant energy per unit volume (erg/cm^3-sec) of light quanta of energy $h\nu$ (erg) in the frequency interval between ν and $\nu + d\nu$, in the solid angle $d\Omega$. Integrating over Ω, the preceding relation becomes

$$-4\pi(dI_\nu/d\ell)d\nu = c\rho_\nu k_\nu d\nu \qquad (13)$$

where use has been made of Eq. (12). Therefore the number of light quanta absorbed in unit volume in unit time, which equals the number of induced transitions N_{tr} in unit volume in unit time leading from energy level E_ℓ to energy level E_u, is

$$N_{tr} = c \int_{\Delta\nu_{\ell u}} \frac{\rho_\nu}{h\nu} k_\nu d\nu$$

where we have integrated over the frequency interval $\Delta\nu_{\ell u}$ in which the actual energy transitions lie. For narrow frequency intervals $\Delta\nu_{\ell u}$, the preceding expression may be rewritten as

$$N_{tr} \simeq \frac{1}{h\nu_{\ell u}} c\rho_{\nu_{\ell u}} \int_{\Delta\nu_{\ell u}} k_\nu d\nu .$$

Comparison with Eq. (11) now leads to the desired relation, viz.,

$$S'_{\ell u} \equiv \int_{\Delta\nu_{\ell u}} k_\nu d\nu = (N_\ell B_{\ell \to u} - N_u B_{u \to \ell})(h\nu_{\ell u}/c)$$

or, in view of Eqs. (9) and (10),

$$S'_{\ell u} = N_\ell B_{\ell \rightarrow u}\left(1 - \frac{N_u}{N_\ell}\frac{g_\ell}{g_u}\right)(h\nu_{\ell u}/c)$$

$$= \left(\frac{c^2}{8\pi\nu_{\ell u}^2}\right) N_\ell A_{u \rightarrow \ell}\left(\frac{g_u}{g_\ell}\right)\left(1 - \frac{N_u}{N_\ell}\frac{g_\ell}{g_u}\right). \qquad (14)$$

For thermal equilibrium Eq. (14) may also be rewritten in the form

$$S'_{\ell u} = N_\ell B_{\ell \rightarrow u}\left[1-\exp(-h\nu_{\ell u}/kT)\right](h\nu_{\ell u}/c)$$

$$= \left(\frac{c^2}{8\pi\nu_{\ell u}^2}\right) N_\ell A_{u \rightarrow \ell}\left(\frac{g_u}{g_\ell}\right)\left[1-\exp(-h\nu_{\ell u}/kT)\right]. \qquad (15)$$

The quantity $S'_{\ell u}$ represents the integral of the spectral absorption coefficient over the effective width $\Delta\nu_{\ell u}$ of the spectral line whose center lies at $\nu_{\ell u}$. It has the dimensions cm^{-1} sec^{-1} and will be referred to as the integrated absorption.

In practical work it is often advantageous to define a spectral absorption coefficient P_ω (in cm^{-1}-$atmos^{-1}$) at S. T. P. by the relation

$$\frac{-dI_\omega}{d(p\ell)} = P_\omega I_\omega$$

where p is the partial pressure of absorber (in atmos), ℓ represents again the path length (in cm), and $\omega = \nu/c$. Proceeding as before, we find now that

$$-c\left[dI_\omega/d(p\ell)\right] d\omega\, d\Omega = cI_\omega P_\omega d\omega d\Omega$$

equals the rate of absorption of radiant energy per unit volume per unit pressure (erg/cm^3-atmos-sec) in the wave number interval between ω and $\omega + d\omega$. Hence the number of induced transitions in unit volume per unit of pressure in the absorber in unit time, is

$$N_{tr} = \frac{pc^2 \rho_{\nu_{lu}}}{h\nu_{lu}} \int_{\Delta\omega_{lu}} P_\omega \, d\omega$$

for a sufficiently narrow wave number range $\Delta\omega_{lu}$. Comparison with Eq. (11) at thermal equilibrium now leads to the conclusion that

$$S_{lu} = \int_{\Delta\omega_{lu}} P_\omega \, d\omega = \frac{h\nu_{lu}}{c} \left(\frac{1}{pc}\right) N_l B_{l\longrightarrow u} \left[1-\exp(-hc\omega_{lu}/kT)\right]$$

$$= \frac{c}{8\pi\nu_{lu}^2} \left(\frac{N_l}{p}\right) A_{u\longrightarrow l} \frac{g_u}{g_l} \left[1-\exp(-hc\omega_{lu}/kT)\right] . \quad (16)$$

Evidently also

$$S_{lu} = S'_{lu}/pc.$$

The values of S_{lu} in cm^{-2}-$atmos^{-1}$ may be converted to $A_{u\longrightarrow l}$ at S.T.P. for $h\nu_{lu} \gg kT$, $g_u = g_l$, in the case where practically all of the molecules present are in the ground energy level, by noting that

$$\frac{N_l}{p} = \frac{6.0247 \times 10^{23}}{82.056 \times 273.16}$$

whence

$$S_{lu}(cm^{-2}\text{-}atmos^{-1}) = 3.210 \times 10^{28} \frac{A_{u\longrightarrow l}(sec^{-1})}{\nu_{lu}^2 \, (sec^{-2})} .$$

D. Oscillator Strengths[8]

The dimensionless absorption oscillator strength* $f_{l\longrightarrow u}$ is defined through the relation

* Physically the absorption oscillator strength $f_{l\longrightarrow u}$ represents the ratio of the number of classical oscillators (whose absorption strength is equivalent to the absorbing atoms) to the number N_l of absorbers in the lower energy level E_l.

$$S'_{\ell u} = \frac{\pi e^2}{mc} N_\ell f_{\ell \rightarrow u} \left[1-\exp(-h\nu_{\ell u}/kT)\right]$$

where e and m denote, respectively, the electronic charge (in esu) and mass (in g/electron). Hence the integrated absorption and dimensionless f-number are related through the expression

$$S_{\ell u} = \frac{\pi e^2}{mc^2} \frac{N_\ell}{p} f_{\ell \rightarrow u} \left[1-\exp(-h\nu_{\ell u}/kT)\right] \qquad (17)$$

At S.T.P., if practically all of the molecules present are in the ground energy level E_ℓ, then it is readily seen that

$$S_{\ell u} = 2.3795 \times 10^7 f_{\ell \rightarrow u}.$$

The emission oscillator strength $f_{u \rightarrow \ell}$ is related to $f_{\ell \rightarrow u}$ through the expression

$$f_{u \rightarrow \ell} = -\frac{g_\ell}{g_u} f_{\ell \rightarrow u}; \qquad (18)$$

thus $f_{u \rightarrow \ell}$ can be computed from measured values of $S_{\ell u}$ by using Eqs. (17) and (18).

E. Spectral Line Profiles[9-19]

A detailed quantitative description of spectral line profiles requires consideration of a variety of line-broadening effects including natural broadening, Doppler broadening, collision broadening, Stark broadening, etc.[9-19] For the practical calculations which we shall consider (i.e., moderate temperatures and pressures), it is probably sufficient to include only Doppler and dispersion contributions. In this case it may be shown that

$$P_{|\xi|} = P' \left(\frac{a}{\pi}\right) \int_{-\infty}^{\infty} \frac{\exp(-y)^2}{a^2 + (\xi - y)^2}\, dy, \qquad (19)$$

where

$$P' = \frac{S}{\omega_o} \left(\frac{mc^2}{2\pi kT}\right)^{1/2},$$

$$a = (b_N + b_C)(\ln 2)^{1/2}/b_D,$$

$$\xi = \frac{\omega - \omega_o}{\omega_o} \left(\frac{mc^2}{2kT}\right)^{1/2} = \frac{\omega - \omega_o}{b_D} (\ln 2)^{1/2},$$

and ω_o identifies now the wave number at the line center. A variety of theoretical representations may be obtained for $P_{|\xi|}/P'$ which are suitable for numerical calculations. The resulting expressions are useful for evaluation of the quantity

$$\frac{A(\ln 2)^{1/2}}{b_D} = \int_{-\infty}^{\infty} \left[1 - \exp(-P_{|\xi|} X)\right] d\xi$$

where

$$A = \int_{-\infty}^{\infty} \left[1 - \exp(-P_{|\omega - \omega_o|} X)\right] d(\omega - \omega_o).$$

The results of computations of $A(\ln 2)^{1/2}/b_D$ may be summarized conveniently[20-22] by the "curves of growth" where the dimensionless parameter $A(\ln 2)^{1/2}/2b_D$ is plotted as a function of $P'X$ for various values of the line-shape parameter a.

F. Matrix Elements

The line absorption spectrum of a molecule results from changes

in its electronic, vibrational and/or rotational motions induced by an interaction with an external radiation field. In general, if the electronic configuration is affected by the transition, the spectral lines will occur in the visible or ultraviolet regions of the spectrum. If only the vibrational and rotational motions are altered during the transition, the lines will lie in the near infrared. If only the rotational structure is changed the spectra are in the (far) infrared.

The Einstein coefficients B_{mn} or A_{mn} may be related directly to the matrix element of the transition, viz.,

$$B_{mn} = \frac{8\pi^3}{3h^2c} \left|\vec{M}_{n'';n'}\right|^2. \tag{20}$$

Here the matrix element $\left|\vec{M}_{n'';n'}\right|$ is given by

$$\vec{M}_{n'';n'} = \int \psi^*(n'')\, \vec{M}\, \psi(n')\, d\tau \tag{21}$$

where n'' and n' represent the totality of all quantum numbers of the initial and final states, respectively; $\psi(n'')$ and $\psi(n')$ are the wavefunctions of the initial and final states and M is the dipole moment of the molecule. The integration is to be performed over the coordinates corresponding to all the degrees of freedom of the molecule. The integrated absorption $S_{n'';n'}$ of the spectral line is related to the matrix element $\vec{M}_{n'';n'}$ by the expression

$$S_{n'';n'} = \frac{8\pi^3 \nu N g_{n''}(1-e^{-h\nu/kT}) \exp(-E_{n''}/kT) \left|\vec{M}_{n'';n'}\right|^2}{3hc \sum_n g_n \exp(-E_n/kT)}. \tag{22}$$

Here $E_{n''}$ represents the energy of the initial (lower) state, $g_{n''}$ is the corresponding statistical weight, N is the number of molecules per unit

volume, and ν is the frequency (at the center) of the absorption or emission line for the specified transition.

The matrix element $\vec{M}_{n'';n'}$ may be expressed in terms of its components along a set of axes (x', y', z') which are fixed in space, viz.,

$$\left|\vec{M}_{n'';n'}\right|^2 = \left|M_{x'_{n'';n'}}\right|^2 + \left|M_{y'_{n'';n'}}\right|^2 + \left|M_{z'_{n'';n'}}\right|^2 . \qquad (23)$$

In good approximation the molecular wave function ψ_n may be written as a product of a rotational factor $\psi_R(\theta, \varphi)$, a vibrational factor $\psi_v(\xi_1, \ldots \xi_n)$ and an electronic factor $\psi_e(\vec{r}_1, \ldots, \vec{r}_N)$. Here θ and φ represent, respectively, the polar and azimuthal angles of one of the principal axes of the molecule; $\xi_1, \ldots, \xi_n$ are the characteristic vibrational coordinates (n = number of nuclei - 5); $\vec{r}_1, \ldots, \vec{r}_N$ are the radius vectors of the N electrons in the molecule measured relative to a set of axes x, y, z fixed to the molecule. We shall find it convenient to choose the z-axis to be parallel to the dipole moment of the molecule.

The electronic velocities are generally much larger than the nuclear velocities so that, in good approximation, the electronic wave functions depend only parametrically on the nuclear coordinates $\xi_1, \ldots, \xi_n$. The F-component of $\vec{M}_{n'';n'}$ (F equals x', y' or z') is

$$M_{F_{n'';n'}} = \int \psi^*_{R''} \cos(F, z)\, \psi_{R'}\, d\Omega(\theta, \varphi) \int \psi^*_{v''} \mu(\xi_1, \ldots, \xi_n)\, \psi_{v'}\, d\tau_1 \ldots d\tau_n . \qquad (24)$$

In Eq. (24) we have written $\mu(\xi_1, \ldots, \xi_n)$ for

$$\int \psi^*_{e''} M_z \psi_{e'}\, d\tau_1 \ldots d\tau_N .$$

If $A_{R'';R'}$ is defined by

$$A^2_{R'';R'} = \sum_F \left| \int \psi^*_{R''} \cos(F,z)\, \psi_{R'}\, d\Omega \right|^2 , \tag{25}$$

then $\left|\vec{M}_{n'';n'}\right|^2$ is given by

$$\left|\vec{M}_{n'';n'}\right|^2 = A^2_{R'';R'} \left| \int \psi^*_{v''}\, \mu(\xi_1, \ldots, \xi_n)\, \psi_{v'}\, d\tau_1 \ldots d\tau_n \right|^2 . \tag{26}$$

The procedure that is normally followed in evaluating the second factor in Eq. (26) depends on the type of transition. For purely rotational transitions ($v'' = v'$, $e'' = e'$) Eq. (26) becomes

$$\left|\vec{M}_{n'';n'}\right|^2 = A^2_{R'';R'}\, \mu_e . \tag{27}$$

Here μ_e is the equilibrium dipole moment of the molecule, given by

$$\mu_e = \int \psi^*_v\, \mu(\xi_1, \ldots, \xi_n)\, \psi_v\, d\tau_1 \ldots d\tau_n . \tag{28}$$

Since, for most molecules, the parameters $A^2_{R'';R'}$ are well-known and the dipole moments have been measured with reasonable accuracy, there is little difficulty involved in predicting the absolute intensity of pure rotation spectra. For vibration-rotation bands ($e'' = e'$), $\mu(\xi_1, \ldots, \xi_n)$ may be expanded in a Taylor series about the equilibrium values of $\xi_1, \ldots, \xi_n$ viz.,

$$\mu(\xi_1, \ldots, \xi_n) = \mu_e + \sum_{i=1}^{n} \frac{\partial \mu}{\partial \xi_i} \left(\xi_i - \xi_{i_e} \right) + \cdots . \tag{29}$$

For transitions between low-lying vibrational states Eq. (26) becomes (for $v'' \neq v'$)

$$\left|\vec{M}_{n'';n'}\right|^2 = A^2_{R'';R'}\left|\sum_i \frac{\partial\mu}{\partial\xi_i}\int \psi^*_{v''}(\xi_i-\xi_{i_e})\,\psi_{v'}\,d\tau_1\ldots d\tau_n\right|^2 + \ldots \quad (30)$$

since $\psi_{v''}$ and $\psi_{v'}$ are mutually orthogonal. For small amplitude vibrations the internuclear potential of most diatomic molecules is known with reasonable accuracy[24] in terms of term values, force constants, expansion coefficients, etc. For diatomic molecules it has been possible to obtain reasonable analytic expressions for the wave-functions ψ_v. Thus, since the parameters $A_{R'';R'}$ are well-known, the chief difficulty arising in the prediction of $\left|\vec{M}_{n'';n'}\right|^2$ lies in the evaluation of $\partial\mu/\partial\xi_i$, the so-called "effective charge" associated with the i'th normal coordinate ξ_i.

For electronic transitions, the usual procedure[27] involves the assumption that the dipole moment $\mu(\xi_1\ldots\xi_n)$ in the integrand of Eq. (26) may be replaced by a mean value $\bar{\mu}$. In this approximation

$$\left|\vec{M}_{n'';n'}\right|^2 = A^2_{R'';R'}\left|\bar{\mu}\right|^2\left|\int \psi^*_{v''}\,\psi_{v'}\,d\tau_1\ldots d\tau_n\right|^2. \quad (31)$$

The vibrational overlap integrals appearing in Eq. (31) have been evaluated for various diatomic molecules by Jarmain et al[25] and for NO by Kivel, Mayer and Bethe.[26] Jarmain et al discuss the problem of estimating the term $\left|\bar{\mu}\right|^2$. It is expected that $\left|\bar{\mu}\right|^2$ will be only a slowly varying function of the vibrational quantum numbers v'', v' so that, from measurements of $\left|\bar{\mu}\right|^2$ for specific transitions (e.g., those that may be observed at room temperature), estimates of $\left|\bar{\mu}\right|^2$ for some other transitions may be made. The available experimental evidence

for the variation of $|\bar{\mu}|^2$ with vibrational excitation is, however, meagre.

II. DIPOLE MOMENTS AND EFFECTIVE CHARGES FOR HF, HCl AND HBr

A. Introduction

In this Section II, theoretical calculations of dipole moments and infrared intensities for HF, HCl and HBr are described. Approximate representations (containing two arbitrary parameters) of the molecular electronic wavefunctions are used to evaluate the dipole moments and the effective charges. It is found that confident predictions of absolute intensities cannot be carried out at the present time and must await a considerably more accurate representation of the electronic wavefunctions. However, some correlation between dipole moments and effective charges may be possible on the basis of the present crude analysis.

In the present section we are concerned only with transitions in which the electronic state remains unchanged, the vibrational state necessarily changes and the rotational state may or may not change. Such transitions give rise to a spectrum composed of vibration-rotation bands which generally appear in the near infrared. The matrix element for the line corresponding to the transition $R' \longrightarrow R''$ and $v' \longrightarrow v''$ is given by Eq. (30) which, for diatomic molecules, reduces to

$$\left|\vec{M}_{n'';n'}\right|^2 = A^2_{R'';R'}\left|\int \psi^*_{v''}\,\mu(r)\,\psi_{v'}\,r^2\,dr\right|^2 \qquad (32)$$

where r is the internuclear distance, $\psi_{v''}$ and $\psi_{v'}$ are the initial and final vibrational wavefunctions, and the remaining symbols have their previously defined meanings. There is no strict selection rule governing the change of the vibrational quantum number for a general diatomic molecule; in the special case that the internuclear potential is harmonic, the vibrational quantum number v can change by one unit only in a transition but, in general, any change is allowed. Transitions for which $\Delta v = \pm 1$ give rise to the fundamental vibration-rotation bands and transitions for which $|\Delta v| > 1$ give rise to overtone or harmonic bands.

The selection rules which result from the symmetric top eigenfunctions ψ_R have been shown[27,28] to be

$$\Delta j = j'' - j' = \begin{cases} \pm 1 \text{ for } \Lambda = 0 \\ \pm 1, 0 \text{ for } \Lambda \neq 0, \end{cases} \qquad (33)$$

where j'' and j' are the nuclear angular momentum quantum numbers of the initial and final states, respectively, and Λ is the component of the electronic angular momentum along the internuclear axis. The series of lines corresponding to the transitions for which $\Delta j = +1$, $\Delta j = 0$, and $\Delta j = -1$ are known, respectively, as the P, Q and R branches of the vibration-rotation band corresponding to the vibrational transition $v'' \rightarrow v'$. The amplitude factors $A^2_{R'';R'}$ are well-known.[24,29] In the case of the simple rotator ($\Lambda = 0$) they are:

$$A^2_{R'';R'} = \begin{cases} j'' + 1 \text{ for } \Delta j = +1, \\ j'' \quad \text{for } \Delta j = -1 . \end{cases} \tag{34}$$

For diatomic molecules, there is one characteristic vibrational coordinate so that Eq. (29) becomes

$$\mu(r) = \mu(r_e) + \frac{\partial \mu}{\partial r}(r - r_e) + \ldots \tag{35}$$

and the matrix element of the dipole moment is given by

$$\left| \vec{M}_{n'';n'} \right|^2 = \left| \int \psi_{v''}(r - r_e)\, \psi_{v'}\, r^2 dr \right|^2 \left| (A_{R'';R'}) \right|^2 \left| \frac{\partial \mu}{\partial r} \right|^2 + \ldots \tag{36}$$

In the present analysis we attempt to calculate $\partial \mu / \partial r$ by using properly antisymmetrized Slater-type electronic wave functions as was done earlier by Kastler[30] in his computations of dipole moments.

B. Electronic Wave Functions

Before proceeding with the evaluation of the dipole moments and effective charges, we shall review, from the point of view of perturbation theory, the arguments that lead to the selection of relatively simple wave functions. As will become apparent, the extreme difficulties encountered in the evaluation of the matrix elements involved in the interaction of one atom with another, prevent any real justification of the steps we use to reduce the problem to workable proportions. However, the established success obtained by these arguments in the description of chemical bonding indicates that the physical picture is qualitatively correct and should at least be useful for correlating, and possible extrapolating, experimental data. We limit our discussion

here specifically to the hydrogen halides HF, HCl, HBr and HI. We shall follow a standard procedure for the calculation of molecular parameters, a procedure which starts with a separated or non-interacting molecule and introduces the interactions as perturbations.

A neutral isolated halogen atom has seven outer (ns and np) electrons occupying the valence shell (here n refers to the radial quantum number and s and p refer to the states with orbital angular momentum quantum numbers 0 and 1, respectively). The remaining electrons occupy all the allowed states of the inner shells. We may view molecule formation qualitatively in the following manner: as the two atoms approach each other the electronic wave functions become distorted. The distortion will be large for the electrons in the valence shell and, for weak interactions, small for the tightly bound inner electrons. We shall assume that the distortion of the inner electrons may be neglected for all values of the interatomic distance which may be encountered. The electronic wave function of the molecule HX may then be written as

$$\psi(\vec{r}_1,\ldots,\vec{r}_{Z+1}) = \psi_{\text{inner}}(\vec{r}_1,\ldots,\vec{r}_{Z-7})\ \psi_m(\vec{r}_{Z-6},\ldots,\vec{r}_{Z+1}) \tag{37}$$

if the interaction of the inner core electrons with the valence shell electrons is also neglected. Here $\psi_{\text{inner}}(\vec{r}_1,\ldots,\vec{r}_{Z-7})$ represents the undisturbed wave function of the Z-7 electrons of the inner core of the halogen atom with atomic number Z. The wave functions of the

separated molecule form a complete and orthonormal set and may be written as products of the wave functions for the 7 valence electrons of the halogen and the single hydrogen electron. Hence the molecular wave function ψ_m may be expressed as a linear combination of the undisturbed wave functions, viz.,

$$\psi_m = a_o \psi_o + a_1 \psi_1 + a_2 \psi_2 + \ldots \tag{38}$$

where ψ_o is the ground state wave function of the separated molecule (i.e., the non-interacting atoms) and the ψ_K's, for $K \neq 0$, correspond to excited states with energy ε_K. The coefficients a_K are given by

$$a_K = \alpha_K \left(\sum_{K=0}^{\infty} \alpha_K^2 \right)^{-1/2} \quad \text{where} \quad \alpha_o = 1,$$

$$\alpha_K = \frac{\int \psi_o \mathcal{H}' \psi_K \, d\tau}{\varepsilon_K - \varepsilon_o} \quad \text{for} \quad \varepsilon_K \neq \varepsilon_o, \tag{39}$$

and $\mathcal{H}'$ is the interaction Hamiltonian. Except for the simplest molecules, these matrix elements are usually very difficult to evaluate. We proceed to eliminate most of the ψ_K's from the expression for ψ_m by assuming that their coefficients a_K are small. The infrared intensities and dipole moments are then calculated for arbitrary values of the remaining a_K's. An attempt will be made finally to determine whether or not all of the available experimental data may be fitted for reasonable values of these remaining a_K's.

In the general case the separated system is degenerate so that

there is more than one unperturbed wave function for the lowest energy level. The function φ_o must be that particular linear combination of these degenerate wave functions to which the actual molecular ground state wave function reduces as the interaction energy is allowed to approach zero. For highly excited states the difference $\epsilon_K - \epsilon_o$ is large and, therefore, a_K is probably small.[31] We shall assume that the energies ϵ_K corresponding to levels above the s and p orbitals of the valence shell of the halogen are sufficiently large to make the corresponding contributions to ψ_m negligibly small.

If h(i) denotes the 1s wave function of the i'th electron centered on the hydrogen nucleus and $p_x(i)$, $p_y(i)$, $p_z(i)$, and s(i) denote the p and s wave functions of the halogen valence shell for the i'th electron, then the ground state wave function of the interacting system will be a linear combination of the following wave functions:

1. $p_x(1)\, p_x(2)\, p_y(3)\, p_y(4)\, p_z(5)\, p_z(6)\, s(7)\, h(8)\, S(1,\ldots,8)$,
2. $p_x(1)\, p_x(2)\, p_y(3)\, p_y(4)\, p_z(5)\, p_z(6)\, h(7)\, s(8)\, S(1,\ldots,8)$,
3. $p_x(1)\, p_x(2)\, p_y(3)\, p_y(4)\, s(5)\, s(6)\, p_z(7)\, h(8)\, S(1,\ldots,8)$,
4. $p_x(1)\, p_x(2)\, p_y(3)\, p_y(4)\, s(5)\, s(6)\, h(7)\, p_z(8)\, S(1,\ldots,8)$,
5. $p_x(1)\, p_x(2)\, p_y(3)\, p_y(4)\, p_z(5)\, p_z(6)\, s(7)\, s(8)\, S(1,\ldots,8)$,
6. $p_x(1)\, p_x(2)\, p_y(3)\, p_y(4)\, p_z(5)\, p_z(6)\, h(7)\, h(8)\, S(1,\ldots,8)$,
7. $p_x(1)\, p_x(2)\, p_y(3)\, p_y(4)\, s(5)\, s(6)\, h(7)\, h(8)\, S(1,\ldots,8)$,

8. $p_x(1)\, p_x(2)\, p_y(3)\, p_y(4)\, h(5)\, h(6)\, p_z(7)\, s(8)\, S(1,\ldots,8)$,

9. $p_x(1)\, p_x(2)\, p_y(3)\, p_y(4)\, h(5)\, h(6)\, s(7)\, p_z(8)\, S(1,\ldots,8)$.

Here $S(1,\ldots,8)$ is the spin function $\alpha(1)\,\beta(2)\,\alpha(3)\,\beta(4)\,\alpha(5)\,\beta(6)\,\alpha(7)\,\beta(8)$ where $\alpha(i)$ represents the spin wave function (of the i'th electron) for which the z-component of the electron spin momentum is $+(1/2)(h/2\pi)$ and $\beta(i)$ is the wave function for which the z-component of the spin momentum is $-(1/2)(h/2\pi)$. In writing down the preceding nine wave functions, we have considered only products of one-electron wave functions which satisfy the following restrictions: (a) there must be two pairs of indistinguishable electrons in the p_x and p_y orbitals; (b) excited states outside the valence s and p orbitals do not contribute.

The first condition is derived from the fact that neither the p_x nor the p_y states can contribute to the binding because $\mathcal{H}'$ must be symmetric about the internuclear axis. Since the p_x and p_y orbitals are filled in the unperturbed ground state, the matrix element of the interaction hamiltonian $\mathcal{H}'$ between the unperturbed ground state and a state in which the p_x and p_y states are not completely filled vanishes because there will always be a factor of the form

$$\int p_x(1)\ \mathcal{H}' \left\{ p_z(1) \text{ or } s(1) \text{ or } h(1) \right\} d\tau_1,$$

which is zero on account of the symmetry of the interaction hamiltonian about the internuclear axis.* From the preceding argument it is clear

* p_x and p_y are odd functions with respect to the azimuthal coordinate whereas $\mathcal{H}'$, p_z, s, and h are even functions.

that, since there is always the same number of electrons in the p_x states as in the p_y states, the electronic angular momentum must be perpendicular to the internuclear axis for all the hydrogen halides (i.e., $\Lambda=0$), a fact which is well-known from experimental studies.

The wave function 1 is necessarily degenerate with wave function 2 in the separated molecule, as are also 3 with 4 and 8 with 9. As the interaction between the hydrogen and halogen atoms is decreased to zero, the electronic ground state wave function of the HX molecule approaches a unique wave function of the separated molecule. This unique function is a suitable linear combination of all the degenerate wave functions of the separated molecule which have the same lowest energy. For example, if the wave functions 1 and 2 have lower energies than any of the remaining wave functions, it may be shown quite generally that the limiting ground state wave function must be

$$\psi_{1,2} = p_x(1)\, p_x(2)\, p_y(3)\, p_y(4)\, p_z(5)\, p_z(6) \left[s(7)\, h(8) + s(8)\, h(7) \right] S(1,\ldots,8).$$

Actually, the preceding expression is not quite correct. According to the Pauli exclusion principle the wave function must be antisymmetric with respect to an interchange of the coordinates of any two electrons. However, this added complication can be allowed for later on and will therefore be ignored for the present. Any wave functions other than $\psi_{1,2}$ formed from 1 and 2 will yield a smaller binding energy than this particular one. Using a similar argument, we may then list the wave functions which we expect to give large binding energies and, therefore,

contribute appreciably to the actual molecular wave function. The quantities in question are

$$\phi^u = p_x(1)\, p_x(2)\, p_y(3)\, p_y(4)\, p_z(5)\, p_z(6) \left[s(7)h(8) + s(8)h(7) \right] S(1,\ldots,8),$$

$$\psi^u = p_x(1)\, p_x(2)\, p_y(3)\, p_y(4)\, s(5)\, s(6) \left[p_z(7)h(8) + p_z(8)h(7) \right] S(1,\ldots,8),$$

$$I^u = p_x(1)\, p_x(2)\, p_y(3)\, p_y(4)\, p_z(5)\, p_z(6)\, s(7)\, s(8)\, S(1,\ldots,8),$$

$$I_p' = p_x(1)\, p_x(2)\, p_y(3)\, p_y(4)\, p_z(5)\, p_z(6)\, h(7)\, h(8)\, S(1,\ldots,8),$$

$$I_s' = p_x(1)\, p_x(2)\, p_y(3)\, p_y(4)\, s(5)\, s(6)\, h(7)\, h(8)\, S(1,\ldots,8),$$

and

$$I_{sp}' = p_x(1)\, p_x(2) p_y(3)\, p_y(4)\, h(5)\, h(6) \left[p_z(7)s(8) + p_z(8)s(7) \right] S(1,\ldots,8).$$

The wave function ϕ^u is commonly called s-covalent, ψ^u is p-covalent, I^u is positive ionic (all electrons centered on the halogen) and I'_p, I'_s, and I'_{sp} are negative ionic (two electrons centered on the hydrogen nucleus). The relative magnitudes of the binding energies of the positive ionic bonds and the negative ionic bonds may be estimated from the measured values of ionization potentials and electron affinities. Since the electron affinity of a hydrogen atom is only 0.75 ev as compared, for example, with 3.72 ev for Cl, it is not unreasonable to expect that the negative ionic wave functions contribute little to the bonding and we shall therefore ignore them. Introducing now the restrictions imposed by the Pauli exclusion principle, we use only the following completely antisymmetrized functions:

$$\phi = \frac{1}{\sqrt{8!}} \sum_P (-1)^P \phi^u, \tag{40}$$

$$\psi = \frac{1}{\sqrt{8!}} \sum_{P} (-1)^{P} \psi^{u}, \tag{41}$$

$$I = \frac{1}{\sqrt{8!}} \sum_{P} (-1)^{P} I^{u}, \tag{42}$$

where the sums are taken over all permutations P of the electronic coordinates and P is even or odd as the number of electron interchanges is even or odd. The total molecular wave function is then given by the expression

$$\psi_{T} = I + \lambda \psi + \mathcal{K} \phi \tag{43}$$

where λ and $\mathcal{K}$ are adjustable parameters.

C. Dipole Moments and Effective Charges

The dipole moment μ and the effective charge $(\partial \mu / \partial r)_{r_e}$ have been calculated (see Section D for details) from the relation

$$\mu = e r_e - e \frac{\left(\psi_T \left| \sum_{i=1}^{N} z_i \right| \psi_T \right)}{\left(\psi_T | \psi_T \right)}. \tag{44}$$

In Figs. 2 to 7 we have plotted μ and $(1/e)\partial \mu / \partial r_e$ as functions of the percentage of s-p hybridization α and of the percentage of ionic character β. For these calculations the electronic wave functions were approximated by products of Slater-type wave functions. The quantities α and β are given in terms of λ and $\mathcal{K}$ by the expressions (see Part e of Section E)

$$\alpha = 100\, \mathcal{K}^2 / (\lambda^2 + \mathcal{K}^2) \tag{45}$$

and

$$\beta = 100/(1 + \lambda^2 + \kappa^2). \tag{46}$$

In the calculations of the effective charge $\partial\mu/\partial r_e$ the questionable assumptions were made that the extent of the s-p hybridisation and the amount of ionic character are not appreciably affected by small changes in the internuclear distance r_e, i.e.,

$$\frac{\partial\alpha}{\partial r_e} = \frac{\partial\beta}{\partial r_e} = 0.$$

D. Outline of Calculations

The dipole moment μ is given by Eq. (44) which may be re-written as

$$\frac{\mu}{e} = r_e - \frac{\left(\psi_T \middle| \sum_{i=1}^{N} z_i \middle| \psi_T\right)}{\left(\psi_T \middle| \psi_T\right)}. \tag{47}$$

The reduced effective charge $(1/e)(\partial\mu/\partial r_e)$ is then determined by

$$\frac{1}{e}\frac{\partial\mu}{\partial r_e} = 1 - \frac{\left(\psi_T \middle| \sum_{i=1}^{N} z_i \middle| \psi_T\right)'}{\left(\psi_T \middle| \psi_T\right)} + \frac{\left(\psi_T \middle| \sum_{i=1}^{N} z_i \middle| \psi_T\right)\left(\psi_T \middle| \psi_T\right)'}{\left(\psi_T \middle| \psi_T\right)^2} \tag{48}$$

where the primes denote differentiation with respect to r_e.

Assuming that λ and κ are not affected by small changes in r_e, the matrix elements appearing in Eqs. (47) and (48) may be written as

$$\left(\psi_T \middle| \sum_{i=1}^{N} z_i \middle| \psi_T\right) = \lambda^2\left(\psi \middle| \sum_{i=1}^{N} z_i \middle| \psi\right) + \kappa^2\left(\varphi \middle| \sum_{i=1}^{N} z_i \middle| \varphi\right) + 2\lambda\left(i \middle| \sum_{i=1}^{N} z_i \middle| \psi\right)$$

$$+ 2\kappa\left(i \middle| \sum_{i=1}^{N} z_i \middle| \varphi\right) + 2\lambda\kappa\left(\psi \middle| \sum_{i=1}^{N} z_i \middle| \varphi\right), \tag{49}$$

$$\left(\psi_T \middle| \psi_T\right) = 1 + \lambda^2 + \kappa^2 + 2\lambda\left(i \middle| \psi\right) + 2\kappa\left(i \middle| \varphi\right) + 2\lambda\kappa\left(\psi \middle| \varphi\right), \qquad (50)$$

$$\left(\psi_T \middle| \sum_{i=1}^{N} z_u \middle| \psi_T\right)' = \lambda^2\left(\psi \middle| \sum_{i=1}^{N} z_i \middle| \psi\right)' + \mu^2\left(\varphi \middle| \sum_{i=1}^{N} z_i \middle| \varphi\right)' + 2\lambda\left(i \middle| \sum_{i=1}^{N} z_i \middle| \psi\right)'$$

$$+ 2\kappa\left(i \middle| \sum_{i=1}^{N} z_i \middle| \varphi\right)' + 2\lambda\kappa\left(\psi \middle| \sum_{i=1}^{N} z_i \middle| \varphi\right)', \qquad (51)$$

and

$$\left(\psi_T \middle| \psi_T\right)' = 2\lambda\left(i \middle| \psi\right)' + 2\kappa\left(i \middle| \varphi\right)' + 2\lambda\kappa\left(\psi \middle| \varphi\right)'. \qquad (52)$$

Here ψ denotes $\psi/\sqrt{(\psi|\psi)}$, φ denotes $\phi/\sqrt{(\phi|\phi)}$ and i denotes $I/\sqrt{(I|I)}$. The multi-electron matrix elements appearing in Eqs. (49) and (50) have been evaluated by Kastler in terms of one-electron matrix elements (see Section F for details), viz.,

$$(i \mid \psi) = \sqrt{2}\,(p_z \mid h)\left[1-(s \mid h)^2 + (p_z \mid h)^2\right]^{-1/2}, \qquad (53)$$

$$(i \mid \varphi) = \sqrt{2}\,(s \mid h)\left[1+(s \mid h)^2 - (p_z \mid h)^2\right]^{-1/2}, \qquad (54)$$

$$(\psi \mid \varphi) = (i \mid \psi)(i \mid \varphi), \qquad (55)$$

$$\left(\psi \middle| \sum_{i=1}^{N} z_i \middle| \psi\right) = 2\left[\frac{r_e}{2} - (s \mid h)(s \mid z \mid h) + (p_z \mid h)(p_z \mid z \mid h)\right.$$

$$\left. -(s \mid h)(p_z \mid h)(s \mid z \mid p_z)\right]\left[1-(s \mid h)^2 + (p_z \mid h)^2\right]^{-1}, \qquad (56)$$

$$\left(\varphi \middle| \sum_{i=1}^{N} z_i \middle| \varphi\right) = 2\left[\frac{r_e}{2} + (s \mid h)(s \mid z \mid h) - (p_z \mid h)(p_z \mid z \mid h)\right.$$

$$\left. + (s \mid h)(p_z \mid h)(s \mid z \mid p_z)\right]\left[1+(s \mid h)^2 - (p_z \mid h)^2\right]^{-1}, \qquad (57)$$

$$\left\langle \psi \left| \sum_{i=1}^{N} z_i \right| \varphi \right\rangle = \left[2(p_z \mid h)(s \mid z \mid h) + 2(s \mid h)(p_z \mid z \mid h) \right.$$

$$\left. -(s \mid z \mid p_z)\left\{ 1 + (s \mid h)^2 + (p_z \mid h)^2 \right\} \right] \left[1 - \left\{ (s \mid h)^2 - (p_z \mid h)^2 \right\}^2 \right]^{-1/2} , \tag{58}$$

$$\left\langle i \left| \sum_{i=1}^{N} z_i \right| \psi \right\rangle = \sqrt{2} \left[(p_z \mid z \mid h) - (s \mid z \mid p_z)(s \mid h) \right] \left[1 - (s \mid h)^2 + (p_z \mid h)^2 \right]^{-1/2} , \tag{59}$$

$$\left\langle i \left| \sum_{i=1}^{N} z_i \right| \varphi \right\rangle = \sqrt{2} \left[(s \mid z \mid h) - (s \mid z \mid p_z)(p_z \mid h) \right] \left[1 + (s \mid h)^2 - (p_z \mid h)^2 \right]^{-1/2} . \tag{60}$$

Corresponding relations are easily obtained for the derivatives of these matrix elements. The one-electron matrix elements appearing in Eqs. (53) to (60) have been evaluated by Mulliken and collaborators[32] using Slater-type wave functions. These one-electron matrix elements are

$$(p_z \mid h) = \int u(Z, np_z; \vec{r}_1)\, u(1, 1s; \vec{r}_2) d\tau , \tag{61}$$

$$(s \mid h) = \int u(Z, ns; \vec{r}_1)\, u(1, 1s; \vec{r}_2) d\tau , \tag{62}$$

$$(p_z \mid z \mid h) = \int u(Z, np_z; \vec{r}_1)\, r_1 \cos\theta\, u(1, 1s; \vec{r}_2) d\tau , \tag{63}$$

$$(s \mid z \mid h) = \int u(Z, ns; \vec{r}_1)\, r_1 \cos\theta\, u(1, 1s; \vec{r}_2) d\tau , \tag{64}$$

$$(s \mid z \mid p) = \int u(Z, ns; \vec{r}_1)\, r_1 \cos\theta\, u(Z, np_z; \vec{r}_1) d\tau , \tag{65}$$

where $\vec{r}_1$ represents the radius vector of the electron measured from the halogen nucleus and $\vec{r}_2$ represents the radius vector from the hydrogen nucleus (see Fig. 1). The quantities Z and n represent, respectively, the atomic number and valence shell quantum number of the halogen.

The Slater wave functions $u(Z,ns;\vec{r})$, $u(Z,np_z;\vec{r})$, and $u(1,1s;\vec{r})$ are given by the expressions[33]

$$u(Z,ns;\vec{r}) = \frac{r^{n^*-1}\, e^{-Z^* r/n^* a_H}}{\sqrt{2\pi\,\Gamma(2n^*+1)}\,(n^* a_H/Z^*)^{n^*+1/2}}, \tag{66}$$

$$u(Z,np_z;\vec{r}) = \frac{r^{n^*-1}\, e^{-Z^* r/n^* a_H}\cos\theta}{\sqrt{\frac{2\pi}{3}\,\Gamma(2n^*+1)}\,(n^* a_H/Z^*)^{n^*+1/2}}, \tag{67}$$

$$u(1,1s;\vec{r}) = \frac{e^{-r/a_H}}{2\sqrt{2\pi a_H^{\,3}}}. \tag{68}$$

Here Z^* and n^* are the effective nuclear charge and effective radial quantum number, respectively, as given by Slater (see Table I).[33] Also a_H represents the Bohr radius which is equal to 0.529×10^{-8} cm).

Mulliken has tabulated[32] the values of the overlap integrals defined by Eqs. (61) to (65) for various effective nuclear charges Z^* and internuclear distances r_e for $n^* = 1, 2, 3$, and 4. The values for HF($n^* = 2$, $Z^* = 5.20$, $r_e = 1.73 a_H$) and HCl ($n^* = 3$, $Z^* = 6.10$, $r_e = 2.40\ a_H$) obtained by interpolating between his data are listed in Table II. For HBr, Z^* is 7.60, n^* is 3.7 and r_e is $2.66 a_H$. Since the values of the overlap integrals for $n^* = 3.7$ are not directly available, an approximate method was used to obtain results for HBr. Thus the 4s wave function of the Br atom was approximated by a linear combination of the 3s and 5s Slater functions. Similarly, the 4p wave function

was approximated by a combination of the 3p and 5p wave functions. For example, the 4s wave function of Br

$$u(4s, Z^* = 7.60, n^* = 3.7) = \frac{r^{2.7} e^{-\frac{7.60}{3.7}\frac{r}{a_H}}}{\left(\frac{3.7}{7.6} a_H\right)^{4.2} \sqrt{2\pi \Gamma(8.4)}} \qquad (69)$$

was approximated by

$$0.272u(3s, Z^* = 7.60, n^* = 3) + 0.742u(5s, Z^* = 7.60, n^* = 4). \qquad (70)$$

The coefficients, 0.272 and 0.742, were obtained to minimize the root mean square difference between this approximate wave function and the actual Slater function. In Table II we have also listed the values of $(\psi | \varphi)$, $\left(\psi \left| \sum_{i=1}^{N} z_i \right| \varphi\right)$, etc.

In Figs. 2 to 7 we have plotted the dipole moment μ and the effective charge $(\partial\mu/\partial r_e)$ as functions of the percentage ionicity β and the percentage s-p hybridization α for positive values of λ and κ. Negative values of λ and κ have not been considered since they correspond to a smaller bond energy. In Fig. 8 the effective charge has been plotted as a function of the percentage s-p hybridization when the ratio α/β is chosen so as to give agreement with the measured values of the dipole moment. Reference to Figs. 2, 4, 6, 8 shows that, in order to obtain agreement between the calculated and observed values of the dipole moment for HCl and HBr, the percentage s-p hybridization and percentage ionicity must be small. In Table III we have listed the values of the percentage ionicity which give agreement with the measured

dipole moments when the s-p hybridization is set equal to zero. Non-zero values of α correspond to smaller values of the ionicity than are indicated in Table III. The resulting values of β are considerably smaller than the estimates of percentage ionicity given by Pauling.*(34) Reference to Fig. 8 shows that the effective charges of HCl and HBr are insensitive to the amount of s-p hybridization when the ratio α/β is chosen to give the measured dipole moments; furthermore the value predicted for HBr agrees with the measured value whereas the calculated result for HCl does not.(35) This failure to predict the measured effective charge for HCl correctly may be attributed to the failure of one or more of the following assumptions.

a. The variation of extent of ionicity and s-p hybridization with small changes of r_e is negligible.

b. The polarizability of the inner core of the halogen is zero.

c. The excited states outside the s and p valence shells do not contribute to the bonding (i.e., the polarizability of the valence shell electrons may be neglected).

d. Slater wave functions constitute an adequate description of the atomic orbitals.

The high sensitivity of the dipole moment and effective charge to the extent of s-p hybridization and ionicity (see Figs. 2 to 7) indicates that

* Kastler obtained approximately the same values as we do but was able to reconcile his results with Pauling's estimates by defining the percentage ionicity as $\frac{100}{1+\lambda}$ (see Part e of Section E).

a really accurate description of the electronic structure of the molecule is necessary in order to make significant theoretical estimates for these quantities. In the following Section E we amplify this remark and consider the validity of these four assumptions in detail.

E. Discussion

a. Change of Ionicity with r_e

A coarse estimate of the error introduced into the effective charge calculations by the assumption that α and β remain constant during a vibration can be obtained in the following manner.

The effective charge may be written as

$$\frac{1}{e}\frac{\partial \mu}{\partial r} = \frac{1}{e}\left(\frac{\partial \mu}{\partial r}\right)_{\alpha,\beta} + \frac{1}{e}\left(\frac{\partial \mu}{\partial \alpha}\right)_{r,\beta}\alpha' + \frac{1}{e}\left(\frac{\partial \mu}{\partial \beta}\right)_{r,\alpha}\beta' \qquad (71)$$

where α' denotes $\frac{\partial \alpha}{\partial r}$ and β' denotes $\frac{\partial \beta}{\partial r}$. The derivatives α' and β' attain such values as to maintain the electronic energy at a minimum as the internuclear separation changes. The extent of ionicity α and s-p hybridization β enter the binding energy multiplied by the terms $(i\,|\,\mathcal{H}'\,|\,\psi)$, $(i\,|\,\mathcal{H}'\,|\,\varphi)$ and $(\varphi\,|\,\mathcal{H}'\,|\,\psi)$. As a result the values of α and β that give the largest binding energy will be functions of these resonance energies and of the overlap integrals. Since the overlap integrals $(i\,|\,\psi)$, $(i\,|\,\varphi)$, $(\varphi\,|\,\psi)$ and the resonance energies depend strongly on the internuclear separation, a rough estimate of the order of magnitude of the fractional rates of change of α and β is the fractional rate of change of the overlap integrals $(i\,|\,\psi)$, $(i\,|\,\varphi)$ and $(\varphi\,|\,\psi)$. Thus if β (or α) could be approximated by the relation

$$\beta = (\text{slowly varying function of } r_e)\, S^n,$$

where S represents an overlap integral $(i \mid \psi)$, $(i \mid \varphi)$, or $(\varphi \mid \psi)$, then

$$r_e \frac{\beta'}{\beta} \sim n\, r_e \frac{S'}{S}; \text{ etc. Hence, in general,}$$

$$\frac{r_e \alpha'}{\alpha} \sim \frac{r_e \beta'}{\beta} \sim r_e \frac{(i \mid \varphi)'}{(i \mid \varphi)}, \; r_e \frac{(i \mid \psi)'}{(i \mid \psi)} \text{ and } r_e \frac{(\varphi \mid \psi)'}{(\varphi \mid \psi)} . \tag{72}$$

Reference to Table II shows that a representative value of $r_e S'/S$ is -1.

The derivatives $\left(\frac{\partial \mu}{\partial \alpha}\right)_{r,\beta}$ and $\left(\frac{\partial \mu}{\partial \beta}\right)_{r,\alpha}$ may be obtained by differentiating Eq. (47) at constant r_e. A result for $\alpha = 0$ and small β is

$$100\, \frac{1}{e} \left(\frac{\partial \mu}{\partial \alpha}\right)_{r_e,\alpha} = \frac{\left(1 - \frac{\mu}{e r_e}\right) r_e}{1 + 0.4\sqrt{\beta}\,(i \mid \psi)} . \tag{73}$$

For HCl and HBr the resulting contributions to the effective charge are:

$$\frac{1}{e} \left(\frac{\partial \mu}{\partial \beta}\right)_{r_e,\alpha} \beta' = + \frac{0.0083\,\beta}{1 + 0.26\sqrt{\beta}} \left(\frac{\beta' r_e}{\beta}\right) \simeq - 0.022n \text{ for HCl with } \beta = 4\%$$

and

$$\frac{1}{e} \left(\frac{\partial \mu}{\partial \beta}\right)_{r_e,\alpha} \beta' = - \frac{0.00884\,\beta}{1 + 0.26\sqrt{\beta}} \left(\frac{\beta' r_e}{\beta}\right) \simeq -0.0053n \text{ for HBr with } \beta = 1\%$$

where $\left(\frac{\beta' r_e}{\beta}\right)$ has been equated to -n.

Reference to Table IV shows that the calculated value of the effective charge for HBr is relatively insensitive to the value of n. The

value of $\left(\frac{\partial \mu}{\partial r_e}\right)_{r=r_e}$ for HCl, on the other hand, is quite sensitive to n although fairly large values of n ($\simeq 8$) are required in order to obtain agreement with the measured data.

b. Polarization of the Inner Core of the Halogen

The polarizability P of the inner closed shell core of the halogen atom may be estimated from the relation[36]

$$P = \frac{4}{9a_H} \sum_i \left(\overline{r_i^2}\right)^2 \tag{74}$$

where the sum is over all the electrons under consideration and r_i is the radial distance of the i'th electron from the halogen nucleus. The quantity $\overline{r_i^2}$ may be estimated from the Slater screening constants[33] by the relation[36]

$$\overline{r_i^2} = \left[\frac{N_i^*}{2Z_i^*}\right]^2 \left[(2N_i^* + 1)(2N_i^* + 2)a_H^2\right] \tag{75}$$

where Z_i^* is the effective nuclear charge and N_i^* is the effective radial quantum number as given by Slater.[33] For example, the electron configuration of the inner core of Cl is $1s^2\ 2s^2\ 2p^6$. Thus, according to Eqs. (74) and (75), the polarizability of the inner core of Cl is

$$P_{inner} = 0.09 \text{ (Bohr radii)}^3.$$

The dipole moment induced in the core by a proton at a radius r_e=2.40 Bohr radii is given by the approximate relation

$$\frac{\mu_{ind}}{er_e} \simeq \frac{P_{inner}}{r_e^3} = 0.0065.$$

Thus, we may conclude that the inner core of Cl is virtually undeformed by the electrostatic field of the hydrogen nucleus.

c. Polarization of the Valence Shell Electrons

The effect of polarization of the valence shell electrons or, what is an equivalent statement, the effect of the contributions to the molecular orbital from the excited states of the halogen, is difficult to estimate. However, a rough estimate may be obtained for the ionic configuration $H^+ X^-$ from the values of the atomic polarizabilities of ions with closed valence shells (see Table V).

The dipole moment induced in the chlorine ion by the hydrogen nucleus is, very roughly,

$$\mu_{ind} = -\left(\alpha_{Cl^-}\right)(e/r_e^2) = -3.78ea_H$$

as compared to the dipole moment of the non-polarized ionic molecule $H^+ Cl^-$ given by

$$\mu = er_e = +2.40\ ea_H.$$

Of course, since the internuclear distance ($2.40a_H$) is less than the ionic radius[34] ($3.42a_H$) no quantitative significance should be attached to this calculation. However, it does suggest that the polarization of the halogen by the hydrogen nucleus is probably important and, consequently, that atomic states outside the valence ns and np shell must be considered in the description of the chemical bond. Thus it appears that the representation of the ionic state by the valence shell states alone is probably not accurate. Because of the more efficient shielding of the hydrogen nucleus in the covalent state the effect of polarization on the covalent wave functions will be less than that on the ionic wave functions. However, since the values of the dipole moment and effective

charge are fairly sensitive to changes of the electronic structure, it is evident that confident predictions of these quantities must await a considerably more accurate description of electronic wave functions in diatomic molecules than is available at present.

d. The Slater Wave Functions

Mulliken and collaborators have shown[32] that, for the molecule C_2, the overlap integrals computed by utilizing the Slater atomic wave functions differ somewhat from those computed with the free-atom self-consistent field wave functions given by Jucys.[38] However, as Mulliken points out, there is no reason a priori to assume that the self-consistent field wave functions computed for a free atom represent the atomic orbitals in the molecule any better than do the Slater wave functions. Nevertheless it may be reasonable to examine also the validity of the Slater wave functions.

e. The Percentage Ionicity and Percentage s-p Hybridization

The percentage ionicity β and the percentage s-p hybridization α are not well-defined concepts for the hydrogen halides because the wave functions i, φ and ψ are not mutually orthogonal. For orthogonal wave functions α and β are related to the coefficients λ and κ by the relations given in Eqs. (45) and (46). In the present report we follow the usual convention and define α and β to be given by Eqs. (45) and (46) even when the wave functions are not orthogonal. Other definitions of percentage ionicity have been used by different authors. For example,

Pauling defines the percentage ionicity as $100\mu_{obs}/er_e$ where μ_{obs} is the measured value of the dipole moment, [since μ_{cov}, the dipole moment of the covalent state, is non-zero an alternate definition of ionicity would be $100(\mu_{obs} - \mu_{cov})/er_e$].

F. Reduction of Molecular Matrix Elements to Functions of One-Electron Matrix Elements

The 8-electron matrix elements appearing in Eqs. (49) to (52) may be reduced to expressions involving only one-electron matrix elements in a straightforward manner. We reproduce here the calculation for $(\psi | \psi)$; the remaining matrix elements may be calculated in an analogous manner. The p-covalent wave function ψ is given by

$$\psi = \frac{1}{\sqrt{8!}} \sum_P (-1)^P s(1)\, s(2)\, p_x(3)\, p_x(4)\, p_y(5)\, p_y(6) \left[p_z(7)\, h(8) + p_z(8)\, h(7)\right] S(1,\ldots,8). \tag{76}$$

The matrix element $(\psi | \psi)$ may be written as

$$\left(\frac{1}{\sqrt{8!}} \sum_P (-1)^P s(1)\, s(2)\, p_x(3)\, p_x(4)\, p_y(5)\, p_y(6) \left[p_z(7)\, h(8) + p_z(8)\, h(7)\right] S(1,\ldots,8) \middle| \psi \right).$$

This expression can be written as the sum of the 8!/2 terms corresponding to an even number of permutations of the electronic coordinates plus the 8!/2 terms corresponding to an odd number of permutations, viz.,

$$(\psi | \psi) = \frac{1}{\sqrt{8!}} \sum_{\text{even } P} (\psi^u | \psi) - \frac{1}{\sqrt{8!}} \sum_{\text{odd } P} (\psi^u | \psi). \tag{77}$$

The terms in the summation over the even permutations differ only in

the labeling of the electrons; therefore, these terms have all the same value. A similar statement holds for the sum over the odd permutations. Thus $(\psi \mid \psi)$ may be written

$$(\psi \mid \psi) = \frac{\sqrt{8!}}{2}(\psi^{u}_{even} \mid \psi) - \frac{\sqrt{8!}}{2}(\psi^{u}_{odd} \mid \psi). \tag{78}$$

By an appropriate relabeling of the integration variables this expression may be reduced to

$$(\psi \mid \psi) = \frac{\sqrt{8!}}{2}\Big(s(1)\, s(2)\, p_x(3)\, p_x(4)\, p_y(5)\, p_y(6)\Big[p_z(7)\, h(8) + p_z(8)\, h(7)\Big] S(1,\ldots,8) \mid \psi\Big)$$

$$- \frac{\sqrt{8!}}{2}\Big(s(1)\, s(2)\, p_x(3)\, p_x(4)\, p_y(5)\, p_y(6)\Big[p_z(7)\, h(8) + p_z(8)\, h(7)\Big] S(1,\ldots,8) \mid -\psi\Big)$$

or

$$(\psi \mid \psi) = \sqrt{8!}\Big(s(1)\, s(2)\, p_x(3)\, p_x(4)\, p_y(5)\, p_y(6)\Big[p_z(7)\, h(8) + p_z(8)\, h(7)\Big] S(1,\ldots,8) \mid \psi\Big). \tag{79}$$

In order to evaluate this expression, we list below only those terms of ψ which give a non-zero matrix element with

$$s(1)\, s(2)\, p_x(3)\, p_x(4)\, p_y(5)\, p_y(6)\Big[p_z(7)\, h(8) + p_z(8)\, h(7)\Big]\, S(1,\ldots,8).$$

Type of Permutation	Contribution	Term
even	$2+2(p_z \mid h)^2$	$\Big[p_z(7)h(8) + p_z(8)h(7)\Big]\, \alpha(1)\beta(2)\ldots\alpha(7)\beta(8)$
odd	$-(s \mid h)^2$	$\Big[p_z(7)h(2) + p_z(2)h(7)\Big]\, \alpha(1)\beta(2)\ldots\alpha(7)\beta(2)$
odd	$-(s \mid h)^2$	$\Big[p_z(1)h(8) + p_z(8)h(1)\Big]\, \alpha(7)\beta(2)\ldots\alpha(1)\beta(8)$

The remaining matrix elements vanish because one (or several) of the following one-electron matrix elements appears:

$$\left(s(i)\left|p_z(i)\right.\right) = \left(\alpha(i)\left|\beta(i)\right.\right) = 0,$$

$$\left(p_x(i)\left|p_y(i)\right.\right) = \left(p_x(i)\left|p_z(i)\right.\right) = \left(p_x(i)\left|h(i)\right.\right) = \left(p_x(i)\left|s(i)\right.\right) = 0, \tag{80}$$

$$\left(p_y(i)\left|p_z(i)\right.\right) = \left(p_y(i)\left|s(i)\right.\right) = \left(p_y(i)\left|h(i)\right.\right) = 0.$$

Thus, the result for $(\psi \mid \psi)$ is

$$(\psi \mid \psi) = 2\left[1 + (p_z \mid h)^2 - (s \mid h)^2\right]. \tag{81}$$

III. EMISSIVITIES AND ABSORPTIVITIES

A. Introduction

Approximate infrared emissivity calculations for diatomic and linear polyatomic molecules were carried out some years ago for (a) elevated pressures where extensive overlapping occurs between the rotational lines of the vibration-rotation bands[54,64-67] and (b) low pressures and low optical densities where the rotational lines may be considered to be completely separated.[68,69] In this section we extend these ideas and obtain approximate analytic expressions for the engineering emissivity. In part B we utilize a statistical model of an absorption band to obtain analytic expressions for the emissivity of

molecules having complex spectra. In part C we discuss the "regular" band approximation and in part D we obtain explicit expressions for the total band radiancy. Part E is concerned with the calculation of absorptivity of a gas for radiation emitted by the same gas at a different temperature, and Part F with the validity of the procedure. Semi-empirical correlations of the emissivity of water vapor are presented in part G and in part H we estimate the emissivity of NO at high temperatures on the basis of the statistical model.

For diatomic molecules without Q branch the line intensities are in proportion to

$$j \exp(-E(v,j)/kT)$$

where we refer to the transition $j \rightarrow j-1$. Our calculations refer to the R branch; a similar analysis applies to the P branch. Here j and v denote, respectively, the rotational and vibrational quantum numbers of the initial state, $E(v,j)$ is the corresponding energy, k equals the Boltzmann constant and T is the absolute temperature. In the notation used by Mayer and Mayer,[39] $E(v,j)/kT$ may be shown to be given by the expression

$$E(v,j)/kT = u_e(v+\tfrac{1}{2})\left[1-x_e(v+\tfrac{1}{2})\right] + \gamma u_e j(j+1)\left[1-(v+\tfrac{1}{2})\delta^* - 4\gamma^2 j(j+1)\right]. \tag{82}$$

The value of $j = j^*$ for which $j \exp(-E(n,j)/kT)$ attains a maximum is, approximately,

$$j^* \simeq (2\gamma u_e)^{-1/2} \tag{83}$$

where $4\gamma^2 j(j+1)$, which accounts for band-head formation, and $(v+\frac{1}{2})\delta^*$.

have been assumed negligibly small. More accurate results may be obtained by replacing γu_e everywhere by $\gamma u_e(1-(v+\frac{1}{2})\delta^*)$. This causes a slow variation of j^* with vibrational quantum number. In this approximation the individual rotational lines are equally spaced by a separation δ given by

$$\delta = 2kT\,\gamma u_e/hc. \tag{84}$$

The wavenumber displacement, $\omega - \omega_o$, of the jth line from the band center at ω_o is given by

$$\omega - \omega_o = j\delta \tag{85}$$

For values of $j^* \gg 1$ the local mean absorption coefficient at the wavenumber ω, defined as the ratio of the local line intensity to the line spacing, is given by

$$\bar{P} = \frac{\alpha}{2}\frac{(\omega-\omega_o)}{(\omega^*-\omega_o)^2}\exp\left[-\frac{1}{2}\left(\frac{\omega-\omega_o}{\omega^*-\omega_o}\right)^2\right] \tag{86}$$

where

$$\omega^* - \omega_o = j^*\delta \tag{87}$$

and α represents the integrated intensity of the entire band.

We shall define a reduced wavenumber ξ and a characteristic absorption coefficient P^* by the relations

$$\xi = (\omega-\omega_o)/(\omega^*-\omega_o)$$

and

$$P^* = \alpha/2(\omega^*-\omega_o). \tag{88}$$

Then the mean absorption coefficient becomes

$$\bar{P} = \frac{P^*}{\bar{X}} \xi \exp(-\xi^2/2). \tag{89}$$

We now define a dimensionless band radiancy α' by the expression

$$\alpha' = \int_{-\infty}^{\infty} \left[1-\exp(-PX)\right] d\omega/(\omega^* - \omega_0)$$

$$= 2 \int_{0}^{\infty} \left[1-\exp(-PX)\right] d\xi \ . \tag{90}$$

Here P represents the true absorption coefficient. Usually the spectrum of a molecule is much too rapidly varying to allow a direct integration of Eq. (90) to be carried out without tremendous effort. Approximation procedures have been developed to allow an evaluation of α' without undue labor. Four cases are amenable to analysis: 1) overlapping lines - here the pressure or temperature is assumed high enough so that the line widths are comparable to the line spacing. For dispersion lines it is found that a ratio of line width to line spacing greater than 0.3 is sufficient to reduce the amplitude of the oscillations of the absorption coefficient to less than 5% of the mean value. 2) Non-overlapping lines - here the line width is assumed small compared to the line spacing so that each line radiates independently and the total radiancy is simply the sum of the radiancies from each isolated line. 3) Regularly spaced lines - Elsasser[40] has computed the absorption coefficient in a band of equally intense equally spaced dispersion lines.

4) Statistically distributed lines - Mayer[41] and Goody[42,43] have evaluated the mean absorption coefficient in a band in which the centers of the spectral lines are distributed randomly. Since cases 1) and 2) are included in cases 3) and 4), we shall only consider explicitly regularly spaced lines and statistically distributed lines in the following discussion.

B. The Statistical Model

Mayer[41] and Goody[43] have developed a method for calculating the mean emissivity of a group of randomly distributed spectral lines. Consider a group of N spectral lines in a wave number interval of width $N\delta$ whose centers are randomly distributed with a mean separation $\delta\,(\mathrm{cm}^{-1})$. Also, suppose that the probability that a line has an integrated intensity between S and S + dS is $\mathcal{P}\left[S, \bar{S}(\omega)\right]dS$ where $\bar{S}(\omega)$ is the mean intensity at the wave number ω. Both $\mathcal{P}$ and $\bar{S}$ are determined by the N spectral lines. The probability that the r'th line has its center between ω_r and $\omega_r + d\omega_r$ and an intensity between S_r and $S_r + dS_r$ is

$$\frac{1}{N\delta}\,\mathcal{P}(S_r, \bar{S})dS_r d\omega_r .$$

For a given arrangement of lines and a given distribution of intensities the spectral emissivity at the wave number ω is given by

$$\varepsilon_\omega = 1 - \prod_{r=1}^{N} \exp\left[-S_r X s(\omega-\omega_r)\right] \qquad (91)$$

where X is the optical density (in cm-atmos) and $s(\omega-\omega_r)$ represents the line contour for the r'th line ($\int_{-\infty}^{\infty} s(\omega')d\omega' = 1$). Hence the mean,

or expected, value of the emissivity at the wave number ω is

$$\bar{\varepsilon}(\omega) = \frac{1}{(N\delta)^N} \int_{\frac{-N\delta}{2}}^{\frac{N\delta}{2}} \cdots \int_{\frac{-N\delta}{2}}^{\frac{N\delta}{2}} \int_{0}^{\infty} \cdots \int_{0}^{\infty} \prod_{r=1}^{N} \left[1-\exp\left[-S_r X s(\omega-\omega_r)\right]\right] \cdot \mathcal{P}(S_r, \bar{S}) d\omega_r dS_r \qquad (92)$$

or

$$\bar{\varepsilon}(\omega) = 1-\left[1-\frac{1}{N\delta}\int_{\frac{-N\delta}{2}}^{\frac{N\delta}{2}}\int_{0}^{\infty} \mathcal{P}(S,\bar{S})\left[1-\exp(-SXs(\omega-\omega')\right] d\omega' dS\right]^N . \qquad (93)$$

For large values of $N\delta$, Eq. (93) may be approximated by

$$\bar{\varepsilon}(\omega) = 1-\exp\left[-\frac{1}{\delta}\int_{-\infty}^{\infty}\int_{0}^{\infty} \mathcal{P}(S,\bar{S})\left[1-\exp(-SXs(\omega-\omega')\right] dSd\omega'\right] . \qquad (94)$$

In terms of the total absorption A of an isolated line, defined by

$$A = \int_{-\infty}^{\infty}\left[1-\exp(-SXs(\omega-\omega')\right] d\omega', \qquad (95)$$

the mean emissivity is

$$\bar{\varepsilon}(\omega) = 1-\exp\left[-\frac{1}{\delta}\int_{0}^{\infty} \mathcal{P}(S,\bar{S})AdS\right] = 1-\exp\left[-\frac{\bar{A}}{\delta}\right] \qquad (96)$$

where $\bar{A}$ denotes the mean value of the total absorption of an isolated line averaged over all possible intensities. Note that $\bar{A}/\delta$ is the mean emissivity that results when the lines are assumed to be non-overlapping.

The result expressed in Eq. (96) may be extended to include the case of a superposition of several independent groups of randomly distributed lines each with different mean line spacings and different intensity distributions (e.g., the γ- and β-systems of NO). For a given arrangement of lines the transmission is

$$T = T_1 \cdot T_2 \cdots = \prod_{r_1} \exp\left[-S_{r_1} X s(\omega-\omega_{r_1})\right] \prod_{r_2} \exp\left[-S_{r_2} X s(\omega-\omega_{r_2})\right] \cdots \tag{97}$$

where ω_{r_i} is the wave number at the center of the r'th line of the i'th group and S_{r_i} is the corresponding integrated intensity. If the line positions and intensities in the different groups are distributed independently, the total mean transmission is the product of the individual mean transmissions, i.e.,

$$\bar{T} = \bar{T}_1 \cdot \bar{T}_2 \cdots \quad . \tag{98}$$

Now $\bar{T}_i$ is given by

$$\bar{T}_i = 1 - \bar{\varepsilon}_i = \exp\left\{-\frac{1}{\delta_i} \int_0^\infty \rho_i\left[S_i(\omega), S\right] A_i(S) dS\right\} \tag{99}$$

where the subscript i refers to the i'th group of lines and the other symbols have their previously defined meanings. Hence the mean emissivity for a superposition of several groups of randomly distributed lines is given by

$$\bar{\varepsilon} = 1 - \bar{T} = 1 - \exp\left[-\sum_i \frac{\bar{A}_i}{\delta_i}\right] . \tag{100}$$

The preceding expressions apply also to the mean emissivity of

groups of randomly distributed vibration-rotation bands if the shape factor $s(\omega-\omega')$ represents the band contour rather than an individual line contour and if S is replaced by the total integrated intensity α of the band. Explicitly, the band contour is

$$s_b(\omega-\omega_o) = \frac{1}{\alpha} \sum_j S_j s_l(\omega-\omega_j) \tag{101}$$

where the subscripts b and l denote "band" and "line", respectively, S_j and ω_j are, respectively, the intensity and wave number of the j'th line in the band, ω_o is the wave number of the band center and α is the total integrated intensity of the band. Thus

$$\int_{-\infty}^{\infty} s_b(\omega-\omega_o)d\omega = 1. \tag{102}$$

C. The Regularly Spaced Model

Elsasser[40] has evaluated the absorption coefficient for a series of equally spaced and equally intense spectral lines having a dispersion contour, viz.,

$$P = \frac{\bar{P} \tanh a'}{1 - \dfrac{\cos\left[2\pi(\omega-\omega')/\delta\right]}{\cosh a'}} \tag{103}$$

where

$\bar{P} = S/\delta$,

S = line intensity,

δ = line spacing,

$a' = 2\pi b/\delta$,

b = dispersion (semi) half-width of the lines,

and ω' = the wavenumber of the center of one of the lines.

The average value of the spectral emissivity $\bar{\varepsilon}$ is given by

$$\bar{\varepsilon} = \int_{\omega'}^{\omega'+\delta} (1-e^{-\bar{P}X})d\omega . \tag{104}$$

Asymptotic forms of $\bar{\varepsilon}$ are

$$\bar{\varepsilon} \sim 1-\exp\left(-\frac{A}{\delta}\right) \qquad \text{for } a' \gg 1 \tag{105}$$

and

$$\bar{\varepsilon} \sim \operatorname{erf}\left(\frac{\sqrt{\pi}}{2}\frac{A}{\delta}\right) \qquad \text{for } \bar{P}X/a' \gg 1. \tag{106}$$

Here A is the radiancy of an isolated dispersion line, given by the expression

$$A = \int_{-\infty}^{\infty} \left\{ 1-\exp\left[\frac{-SX\, b/\pi}{b^2+(\omega-\omega')^2}\right]\right\} d\omega$$

$$= 2\pi b f(SX/2\pi b) = a'\delta f(\bar{P}X/a') \tag{107}$$

where $f(x)$ is given by

$$f(x) = xe^{-x}\left[J_0(ix) - iJ_1(ix)\right] \tag{108}$$

and J_0 and J_1 represent Bessel functions of order zero and one, respectively. For intermediate values of a' and $\bar{P}X/a'$ the mean emissivity lies between that given by Eq. (105) and Eq. (106). Since these two limiting emissivity expressions differ by, at most, 25% it is sufficient for many engineering purposes merely to realize that the average emissivity lies between these limiting values.

D. Approximate Expressions for Vibration-Rotation Band Radiancies

We shall now obtain an approximate value for the dimensionless band radiancy $\mathcal{A}'$ for the simple band described by Eq. (86). We shall assume that the spectral lines are distributed statistically, although the expression in Eq. (86) refers to a band of regularly spaced lines. As was

indicated previously, the band radiancy for a band having equally spaced lines will be larger than that for statistically distributed lines although the difference will certainly be less than 25%. For statistically distributed lines the mean spectral emissivity is

$$\bar{\varepsilon} = 1-\exp\left[-a'f\left(\frac{\bar{P}x}{a'}\right)\right] . \tag{109}$$

For $a' \ll 1$ and $a' \gg 1$ we shall evaluate the dimensionless radiancy α', defined by

$$\alpha' = \int_{\text{band}} \varepsilon d\xi = 2\int_0^\infty \bar{\varepsilon} d\xi \tag{110}$$

utilizing the statistical expression given by Eq. (109) for $\bar{\varepsilon}$. For dispersion lines the mean spectral emissivity may be written in the form

$$\bar{\varepsilon} = 1-\exp\left[-P^*X\xi e^{-\xi^2/2}\right] \qquad \text{for } P^*X/a' \ll 1 \tag{111}$$

and

$$\bar{\varepsilon} = 1-\exp\left[-\sqrt{\frac{2}{\pi}P^*a'X}\,\xi^{1/2}e^{-\xi^2/4}\right] \quad \text{for } P^*X/a' \gg 1. \tag{112}$$

The reduced radiancy α' may be expressed, within 5%, in terms of an effective band width, viz.,

$$\alpha' = \Delta\xi'\left[1-\exp(-2P^*X/\Delta\xi')\right] \tag{113}$$

where

$$\Delta\xi' = 2\sqrt{2\ln(e^{8/\pi} + 2CP^*X\Delta\xi')} \quad \text{for } P^*X/a' \ll 1 \tag{114}$$

and C = Euler's constant $\simeq 1.780172$, or

$$\alpha' = \Delta\xi''\left[1-\exp\left(-4\Gamma(3/4)\sqrt{P^*a'X/\pi}\,/\Delta\xi''\right)\right] \quad \text{for } P^*X/a' \gg 1 \tag{115}$$

where

$$\Delta\xi'' = 2\sqrt{2\ln\left(e^{2\left[\Gamma(3/4)\right]^4} + \frac{4C^2}{\pi}P^*a'X\Delta\xi''\right)} . \tag{116}$$

These forms of $\Delta\xi'$ and $\Delta\xi''$ are so chosen that the first and second terms in the asymptotic expansions of a' for both large and small values of P^*X agree with those obtained by expanding the approximate forms for a' given by Eqs. (113) and (115). For example, for small values of P^*X, Eq. (110) may be expanded, utilizing Eq. (111), to give

$$a' = 2P^*X - \frac{\sqrt{\pi}}{4}(P^*X)^2 + O\left\{(P^*X)^3\right\} \quad \text{for } P^*X \ll 1 \tag{117}$$

and, for large values of P^*X, Eq. (110) may be expanded to give the (iterative) relation

$$a' = 2\sqrt{2\ln(2CP^*X\,a')} + O\left\{(\ln P^*X)^{-3/2}\right\} \quad \text{for } P^*X \gg 1 . \tag{118}$$

The approximate expressions for a' given by Eqs. (113) and (114) agrees with Eqs. (117) and (118) to the degree indicated.

In terms of the function f(u) we may write a' in a similar form for both $P^*X/a' \ll 1$ and $P^*X/a' \gg 1$, viz.,

$$a' = \Delta\xi\left[1-\exp\left\{-\frac{2\sqrt{2}\,a'}{\Delta\xi}f\left(\frac{P^*X}{\sqrt{2}a'}\right)\right\}\right] . \tag{119}$$

In analogy with the expression for the absorption coefficient for equally spaced lines [Eq. (103)] we expect tanh a' to be a suitable interpolation parameter for $\Delta\xi$. Thus, if we define $\Delta\xi$ by

$$\Delta\xi = 2\sqrt{2\ln\left\{e^{2\left[\Gamma(3/4)\right]^4} - \left[e^{2\left[\Gamma(3/4)\right]^4} - e^{8/\pi}\right]\tanh a' + 2C\left(1+\frac{2C}{\pi}\tanh a'\right)P^*X\Delta\xi\right\}} \tag{120}$$

then the expression for the reduced band width $\Delta\xi$ agrees with that given by Eq. (116) for $P^*X/a' \gg 1$ and that given by Eq. (114) for $P^*X/a' \ll 1$.

where the integration is over a single line of intensity S having a dispersion contour.

We expect, from the form of Eqs. (119) and (120), that they give useful answers for lines with other than dispersion contours except when the spectral lines are both well separated and strongly self-absorbing at their centers. In section III-H we consider the evaluation of the band radiancy for separated lines having a Doppler contour. Equation (119) may be interpreted in the following manner.

Rewriting Eq. (119) we have

$$\mathcal{A}' = \Delta\xi \left[1-\exp\left\{ -\bar{a}' f\left(\frac{\bar{\bar{P}}x}{\bar{a}'} \right) \right\} \right] \tag{121}$$

where

$$\bar{\bar{P}} = 2P^*/\Delta\xi \tag{122}$$

and

$$\bar{a}' = a' / \left[\Delta\xi / 2\sqrt{2} \right] . \tag{123}$$

Now for a band of width $\Delta\xi$ containing statistically distributed lines of uniform intensity $S' = \bar{P}\delta$

$$\mathcal{A}' = \Delta\xi \left[1-\exp\left\{ -a' f\left(\frac{\bar{\bar{P}}x}{a'} \right) \right\} \right] . \tag{124}$$

This $\bar{\bar{P}}$ represents an effective mean absorption coefficient and $\bar{a}'$ an effective mean value of the line width to line spacing ratio a'.

E. Absorptivity of Molecular Vibration-Rotation Bands for Radiation Emitted by Molecular Vibration-Rotation Bands

In this section we wish to evaluate the absorptivity of a gas for radiation emitted by a volume of the same type of gas but having a different temperature. The following analysis utilizes the concept of

an average absorption coefficient for an entire vibration-rotation band. For this reason, the results are applicable only at elevated pressures and moderate or large optical densities where extensive overlapping occurs between rotational lines.

Consider two isothermal parallel layers of the same gas at temperatures T_{G1} and T_{G2} with optical densities (in cm atmos) $X_1 = p_1 L_1$ and $X_2 = p_2 L_2$, respectively. Here p_1 and p_2 denote the partial pressures of absorber and emitter, respectively, whereas L_1 and L_2 represent the corresponding geometric pathlengths throughout which the gas molecules are distributed.

The total energy emitted by region 2 in unit time from unit area, at the interface between regions 1 and 2, toward region 1 is

$$I_{2\longrightarrow 1} = \int_0^\infty \left[1-e^{-P(\omega, T_{G2})X_2}\right] R^0(\omega, T_{G2})\,d\omega \tag{125}$$

where $P(\omega, T_{G2})$ is the absorption coefficient (in cm^{-1}-$atmos^{-1}$) in region 2 at the wave number ω and temperature T_{G2} and $R^0(\omega, T_{G2})$ equals the Planck radiation function evaluated at the wave number ω and temperature T_{G2}. The fraction of the energy $I_{2\longrightarrow 1}$ which is absorbed in region 1, i.e., the absorptivity $\alpha(2\longrightarrow 1)$ of the gases in region 1 for radiation emitted from region 2, is

$$\alpha(2\longrightarrow 1) = \frac{\int_0^\infty \left[1-e^{-P(\omega, T_{G1})X_1}\right]\left[1-e^{-P(\omega, T_{G2})X_2}\right] R^0(\omega, T_{G2})\,d\omega}{\int_0^\infty \left[1-e^{-P(\omega, T_{G2})X_2}\right] R^0(\omega, T_{G2})\,d\omega}. \tag{126}$$

We now assume[45] that the i'th vibration-rotation band may be described by an average absorption coefficient $\bar{P}_i(T)$ over the effective band-width $\Delta\omega_i(T)$ of the band whose center lies at $\bar{\omega}_i$. It has been shown previously[45] that, for the calculation of overall emissivities (i.e., for evaluation of the denominator of Eq. (126),

$$\bar{P}_i(T) = \frac{1}{\Delta\omega_i}\int P(\omega, T)d\omega \tag{127}$$

represents a good approximation for vibration-rotation bands at pressures which are sufficiently high to smear out the rotational fine structure in such a way that the spectral absorption coefficient $P(\omega, T)$ is no longer a rapidly varying function of ω. The integral in Eq. (127) extends over the i'th vibration-rotation band. Exact evaluation of the numerator of Eq. (126), using reasonable representations of $P(\omega, T_{Gi})$, shows again that, for moderate values of T_{G2}/T_{G1}, Eq. (127) is a good approximation.

Introduction of average absorption coefficients for each vibration-rotation band in the numerator of Eq. (126) reduces this relation to

$$\alpha(2\rightarrow 1) = \sum_i \frac{\left[1-e^{-\bar{P}_i(T_{G1})X_1}\right]\left[1-e^{-\bar{P}_i(T_{G2})X_2}\right] R^0(\bar{\omega}_i, T_{G2})\Delta\omega^*_i}{\int_0^\infty \left[1-e^{-P(\omega, T_{G2})X_2}\right] R^0(\omega, T_{G2})d\omega} \tag{128}$$

where the approximation has been made of using the value of the Planck function at temperature T_{G2} evaluated at the band center for each vibration-rotation band. The quantity $\Delta\omega^*_i$ in Eq. (128) denotes the effective width of the narrower vibration-rotation band. Thus,

$\Delta\omega^*_i = \Delta\omega_i(T_{G2})$ for $T_{G2} \leq T_{G1}$ and $\Delta\omega^*_i = \Delta\omega_i(T_{G1})$ for $T_{G1} \leq T_{G2}$.

In the present calculations we ignore the weak dependence of the effective band width on the optical density.

From Eq. (127) and the relation $\int k(\omega, T)d\omega \sim T^{-1}$ it is apparent that

$$\frac{\bar{P}_i(T_{G1})}{\bar{P}_i(T_{G2})} = \frac{T_{G2}}{T_{G1}} \frac{\Delta\omega_i(T_{G2})}{\Delta\omega_i(T_{G1})} . \tag{129}$$

The first factor in Eq. (129) arises because the number density of absorbers is inversely proportional to the temperature. The value of $\Delta\omega_i$ may be derived from Eqs. (83), (84), (87), (88) and (117). For small optical densities, $\Delta\omega_i$ is given by

$$\Delta\omega_i = 3.78\sqrt{C\,kT\,\omega_e/hc} \tag{130}$$

where we have used the relation

$$u_e = hc\,\omega_e/kT. \tag{131}$$

Thus

$$\frac{\bar{P}_i(T_{G1})}{\bar{P}_i(T_{G2})} = \left(\frac{T_{G2}}{T_{G1}}\right)^{3/2} . \tag{132}$$

In view of Eq. (131) we find that

$$\Delta\omega^*_i(T) = \Delta\omega_i(T_{G1}) = \left(\frac{T_{G1}}{T_{G2}}\right)^{1/2} \Delta\omega_i(T_{G2}) \text{ for } T_{G2} \geq T_{G1} \tag{133}$$

and

$$\Delta\omega^*_i(T) = \Delta\omega_i(T_{G2}) \text{ for } T_{G1} \geq T_{G2}. \tag{134}$$

Hence Eq. (128) becomes

$$\alpha(2\rightarrow 1) =$$

$$\sum_i \left(\frac{T_{G1}}{T_{G2}}\right)^{\frac{1}{2}} \frac{\left[1-e^{-\bar{P}_i(T_{G2})X_1(T_{G2}/T_{G1})}\right]^{\frac{3}{2}}\left[1-e^{-\bar{P}_i(T_{G2})X_2}\right] R^0(\bar{\omega}_i, T_{G2})\Delta\omega_i(T_{G2})}{\int_0^\infty \left[1-e^{-P(\omega, T_{G2})X_2}\right] R^0(\omega, T_{G2})d\omega}$$

$$\text{for } T_{G2} \geq T_{G1} \tag{135}$$

and

$$\alpha(2\rightarrow 1) =$$

$$\sum_i \frac{\left[1-e^{-\bar{P}_i(T_{G2})X_1(T_{G2}/T_{G1})}\right]^{\frac{3}{2}}\left[1-e^{-\bar{P}_i(T_{G2})X_2}\right] R^0(\omega_i, T_{G2})\Delta\omega_i(T_{G2})}{\int_0^\infty \left[1-e^{-P(\omega, T_{G2})X_2}\right] R^0(\omega, T_{G2})d\omega}$$

$$\text{for } T_{G1} \geq T_{G2}. \tag{136}$$

It is now convenient to transform the summation over individual vibration-rotation bands back to an integration over wave numbers. Thus

$$\alpha(2\rightarrow 1) =$$

$$\left(\frac{T_{G1}}{T_{G2}}\right)^{\frac{1}{2}} \frac{\int_0^\infty \left[1-e^{-P(\omega, T_{G2})X_1(T_{G2}/T_{G1})}\right]^{\frac{3}{2}}\left[1-e^{-P(\omega, T_{G2})X_2}\right] R^0(\omega, T_{G2})d\omega}{\int_0^\infty \left[1-e^{-P(\omega, T_{G2})X_2}\right] R^0(\omega, T_{G2})d\omega}$$

$$\text{for } T_{G1} \leq T_{G2}, \tag{137}$$

$$\alpha(2\rightarrow 1) = \frac{\int_0^\infty \left[1-e^{-P(\omega, T_{G2})X_1(T_{G2}/T_{G1})^{\frac{3}{2}}}\right]\left[1-e^{-P(\omega, T_{G2})X_2}\right] R^0(\omega, T_{G2})\,d\omega}{\int_0^\infty \left[1-e^{-P(\omega, T_{G2})X_2}\right] R^0(\omega, T_{G2})\,d\omega}$$

for $T_{G1} \geq T_{G2}$.

In terms of tabulated isothermal emissivities, $E(T,X)$, Eq. (137) may be rewritten in the form

$$\alpha(2\rightarrow 1) = \begin{cases} \left(\frac{T_{G1}}{T_{G2}}\right)^{\frac{1}{2}} \left\{1 - \frac{E\left[T_{G2}, X_2 + X_1(T_{G2}/T_{G1})^{\frac{3}{2}}\right] - E\left[T_{G2}, X_1(T_{G2}/T_{G1})^{\frac{3}{2}}\right]}{E(T_{G2}, X_2)}\right\} \\ \qquad \text{for } T_{G1} \leq T_{G2} \\ \left\{1 - \frac{E\left[T_{G2}, X_2 + X_1(T_{G2}/T_{G1})^{\frac{3}{2}}\right] - E\left[T_{G2}, X_1(T_{G2}/T_{G1})^{\frac{3}{2}}\right]}{E(T_{G2}, X_2)}\right\} \\ \qquad \text{for } T_{G1} \geq T_{G2}. \end{cases} \tag{138}$$

Equation (138) represents the desired relation for the absorptivity at temperature T_{G1} of a gas characterized by vibration-rotation bands for radiation emitted by the same gas at a temperature T_{G2}. The procedure presented in this section has been extended to include the case of arbitrarily varying temperature distributions. Expressions

have been obtained for the radiant emission from a gas in which the temperature varies with position. For details see Ref. (47).

a. Absorptivities of Water Vapor for Blackbody Radiation

Using measured values for the absorptivity of water vapor for blackbody radiation, Hottel[46] obtained the following empirical formula for the absorptivity

$$\alpha_H = \left(\frac{T_g}{T_s}\right)^{.45} E\left[T_s, X(T_s/T_g)\right]. \tag{139}$$

Here α_H is the absorptivity of a layer of water vapor at temperature T_g and mean optical density X for radiation emitted by a blackbody at temperature T_s, and $E\left[T_s, X(T_s/T_g)\right]$ is the tabulated isothermal emissivity corresponding to a temperature T_s and a mean optical density $X(T_s/T_g)$. For blackbody radiation, Eq. (138) reduces to the expression (noting that $E(T, X_2) = 1$ and that the first of the relations given in Eq. (138) applies now for $T_{G2} \leq T_{G1}$ as well as for $T_{G2} \geq T_{G1}$),

$$\alpha = \left(\frac{T_g}{T_s}\right)^{\frac{1}{2}} E\left[T_s, X(T_s/T_g)^{\frac{3}{2}}\right]. \tag{140}$$

Here T_{G2} has been replaced by T_s, T_{G1} by T_g and X_1 by X.

In Figs. 9 to 11 we have plotted the ratios of the calculated to the observed[46] absorptivities, using both Eqs. (139) and (140), for various values of the gas temperature T_g and blackbody temperature T_s. Reference to Figs. 9 to 11 shows that Eqs. (139) and (140) represent the experimental data about equally well. In this connection it is of

interest to note that the measured absorptivities were obtained at a total pressure of one atmosphere for partial pressures of water vapor varying from zero to one atmosphere. Since Eq. (140) was derived for overlapping rotational lines, it is not expected to apply at very low pressures and optical densities. It is apparent from Figs. 9 to 11 that significant deviations from Eq. (140) occur only at the lowest optical densities, a conclusion which is evidently in accord with expectations.

b. Absorptivities of Carbon Dioxide Vapor for Blackbody Radiation

Using measured values of the absorptivity of carbon dioxide vapor for blackbody radiation, Hottel and Mangelsdorf[46] obtained the following empirical formula for the absorptivity

$$\alpha_H = \left(\frac{T_g}{T_s}\right)^{.65} E\left[T_s, X(T_s/T_g)\right]. \qquad (141)$$

For the absorption of blackbody radiation by carbon dioxide, Eq. (140) does not yield a satisfactory correlation of observed results. The reason for this discrepancy becomes apparent if it is noted that the effective band-width estimates obtained in Section D are invalid for carbon dioxide because of the presence of the exceedingly strong ν_3-fundamental. In this case the tails of the intense rotational lines near the band center make appreciable contributions at wavelengths outside of the "effective band-width". Limiting conditions for failure of the theoretical band limit estimates are easily derived from this physical picture and are considered in greater detail in Section F.

c. Improved Representation of the Absorptivity

Equation (140) for the absorptivity of a gas volume for blackbody radiation emitted at a temperature different from that of the gas represents the experimental data obtained at a total pressure of 1 atmos within 10% for optical densities greater than 0.5 ft-atmos and also for very small optical densities. Equation (140) was derived on the assumption that the rotational fine structure was smeared out. It is known experimentally that at pressures below about four atmospheres total pressure the emissivity of water vapor is sensitive to pressure, indicating that the rotational fine structure is significant below four atmospheres. In this section we shall consider the evaluation of the absorptivity when the rotational line structure is important.

First we consider the case of very low optical densities. For very small values of X the hemispherical absorptivity of a gas at temperature T_g for radiation emitted by a blackbody at temperature T_s is given by

$$\alpha = \frac{1}{\sigma T_s^4} \int_0^\infty \left[1-\exp(-P_\omega(T_g)X)\right] R^o_\omega(T_s)\,d\omega$$

$$\simeq \frac{1}{\sigma T_s^4} \sum_{\text{bands}} \overline{R^o_\omega}(T_s) X \int P_\omega(T_g)\,d\omega$$

$$= \frac{1}{\sigma T_s^4} \sum_{\text{bands}} \overline{R^o_\omega}(T_s)\, \alpha_i(T_g) X \qquad (142)$$

where α_i is the integrated intensity of the i'th band. Now $\alpha_i(T_g)$ is

related to $\alpha_i(T_s)$ by the approximate expression

$$\alpha_i(T_g) = \frac{T_s}{T_g}\,\alpha_i(T_s). \tag{143}$$

Thus the absorptivity α is given in good approximation by

$$\alpha = \frac{T_s}{T_g}\,E(T_g, X) \tag{144}$$

for X sufficiently small. Equation (144) is valid for any pressure. Since, for very small values of X (when $E(T,X)$ depends linearly on X), Eq. (140) also reduces to Eq. (144), we expect the absorptivities computed for an overlapping line model to be useful at both very large and very small optical densities.

We shall now evaluate the hemispherical absorptivity of a gas at a temperature T_g for radiation emitted by a blackbody at the temperature T_s when the gas pressure is so low that the rotational lines may be considered to be non-overlapping. For a collision-broadened line centered at a wavenumber ω_o and having an integrated intensity $S = S(T_g)$ at the temperature T_g, the absorption coefficient is given by

$$P_\omega(T_g) = S(T_g) \frac{b(T_g)/\pi}{(\omega-\omega_o)^2 + [b(T_g)]^2} . \tag{146}$$

The reduced radiancy A is given by

$$A = 2\pi b\, f\left(\frac{SX}{2\pi b}\right) \tag{147}$$

where

$$f(u) = ue^{-u}\left[J_o(iu) - iJ_1(iu)\right] .$$

For a spectrum in which the lines may be assumed to be non-overlapping, the absorptivity α is given by

$$\alpha_{N.O.} = \frac{1}{\sigma T_s^4} \sum_{\text{bands}} \left\{ \sum_{\text{lines}} A_g \right\} \overline{R^o_\omega}(T_s) \tag{148}$$

where the subscripts g and s denote, respectively, values obtained at the gas temperature T_g and at the source temperature T_s. For a band with P and R branches of the type discussed in Section III-A, the line intensity S is given, approximately, by

$$S_g = \alpha_g J \frac{hcB_e}{kT_g} e^{-hcB_eJ^2/kT_g} \tag{149}$$

for large values of J. Then the absorptivity α may be written, approximately, as a sum over bands, viz.,

$$\alpha_{N.O.} = \frac{1}{\sigma T_s^4} \sum_{\text{bands}} \overline{R}^{\circ}_{\omega} \left\{ 2 \int_0^{\infty} 2\pi b_g \, f(S_g X / 2\pi b_g) \, dJ \right\} . \tag{150}$$

Here the summation over lines within each band has been replaced by an integral over J. According to Eq. (149) the line intensity S_g for the simple bands described in Section III-A had the form

$$S_g = \alpha \sqrt{\frac{hcBe}{kT_g}} \, g\left(\sqrt{\frac{hcBe}{kT_g}} \, J \right) \tag{151}$$

where

$$g(x) = x e^{-x^2} .$$

We shall consider the absorptivity of a gas whose spectrum satisfies Eq. (151) when g(x) represents any arbitrary function of x. In this case Eq. (150) may be rewritten in the form

$$\alpha_{N.O.} = \frac{1}{\sigma T_s^4} \sum_{\text{bands}} \overline{R}^{\circ}_{\omega} \left\{ 2 \int_0^{\infty} 2\pi b_g \sqrt{\frac{kT_g}{hcBe}} \, f\left(\frac{\alpha_g X}{2\pi b_g} \sqrt{\frac{hcBe}{kT_g}} \, g(u) \right) \right\} du$$

$$= \frac{1}{\sigma T_s^4} \sum_{\text{bands}} \overline{R}^{\circ}_{\omega} \left\{ 2 \int_0^{\infty} 2\pi b_s \sqrt{\frac{kT_s}{hcBe}} \, f\left(\frac{\alpha_s}{2\pi b_s} \sqrt{\frac{hcBe}{kT_s}} \, X \left(\frac{T_s}{T_g} \right) \, g(u) \right) \right\} du \tag{152}$$

where we have assumed that

$$b_g(T_g) = \sqrt{\frac{T_s}{T_g}} \, b_s(T_s) . \tag{153}$$

Equation (152) may be written in terms of the equilibrium emissivities E(T,X), viz.,

$$\alpha_{N.O.} = E\left(T_s, \frac{T_s}{T_g} X\right). \tag{154}$$

For more complicated spectra than that corresponding to the simple P and R branches discussed in Section III-A, the derivation of Eq. (154) is invalid. An empirical fit[55] of the empirical emissivity data for water

vapor (which has a rather complex spectrum) indicates that a useful representation of a water vapor band is one in which the lines are equally intense and in which the effective line spacing varies as a power of the temperature. We shall show that the absorptivity computed for such a representation reduces to that given by Eq. (154) in the special case that the effective line spacing is independent of temperature. The absorptivity is given by

$$\alpha_{N.O.} = \frac{1}{\sigma T_s^4} \sum_{\text{bands}} \overline{R}^{o}_{\omega}(T_s)\, N_g\, 2\pi b_g\, f\left(\frac{S_g X}{2\pi b_g}\right)$$

$$= \frac{1}{\sigma T_s^4} \sum_{\text{bands}} \overline{R}^{o}_{\omega}(T_s)\, N_s\, 2\pi b_s \left(\frac{T_g}{T_s}\right)^{\eta} f\left[\frac{S_s X}{2\pi b_s}\left(\frac{T_s}{T_g}\right)^{\eta}\right] . \qquad (155)$$

In terms of the isothermal engineering emissivities Eq. (155) may be written

$$\alpha_{N.O.} = \left[\frac{T_g}{T_s}\right]^{\eta-1} \varepsilon\left(T_s, X\left(\frac{T_s}{T_g}\right)^{\eta}\right) \qquad (156)$$

where we have introduced the temperature dependences

$$N_g = \left(\frac{T_g}{T_s}\right)^{\eta-1/2} N_s \qquad (157)$$

and

$$S_g = \left(\frac{T_s}{T_g}\right)^{\eta+1/2} S_s . \qquad (158)$$

For a fixed line spacing ($\eta = 1$), Eq. (156) reduces to Eq. (154). However, if the effective line spacing varies inversely with the temperature, as is indicated for water vapor from a semi-empirical fit of the emissivity data to a statistical model of the spectrum,[55] then $\eta = 2$. For $\eta = 2$, Eq. (156) becomes

$$\alpha_{N.O.} = \frac{T_g}{T_s} \quad E\left[T_s, \left(\frac{T_s}{T_g}\right)^2 X\right]. \tag{159}$$

For the overlapping line model of the spectrum the absorptivity is, according to Eq. (140),

$$\alpha_{N.O.} = \left(\frac{T_g}{T_s}\right)^{1/2} E\left[T_s, \left(\frac{T_s}{T_g}\right)^{3/2} X\right]. \tag{160}$$

These two expressions for α do not differ greatly. The percentage deviation may be estimated by the following argument. For small values of X,

$$E \sim X.$$

For moderate values of X at low total pressures

$$E \sim X^{1/2}.$$

Now in the intermediate region we may set $E \sim X^{\epsilon}$, where ϵ ranges between 1/2 and 1. For constant values of ϵ the non-overlapping approximation to the absorptivity gives

$$\alpha_{N.O.} = \left(\frac{T_s}{T_g}\right)^{2\epsilon - 1} E(T_s, X) \tag{161}$$

and the overlapping approximation gives

$$\alpha_{O.} = \left(\frac{T_s}{T_g}\right)^{(3/2)\epsilon - (1/2)} E(T_s, X). \tag{162}$$

Thus

$$\alpha_{N.O.} \simeq \left(\frac{T_g}{T_s}\right)^{1/2(1-\epsilon)} \alpha_{O.}. \tag{163}$$

For the optical densities for which the non-overlapping line model may be expected to be useful

$$\frac{1}{2} \leq \varepsilon \leq 1$$

or

$$0 \leq \frac{1}{2}(1-\varepsilon) \leq \frac{1}{4}$$

so that, for T_g not too different from T_s, $\alpha_{N.O.} \sim \alpha_{O.}$. For $T_g = \frac{1}{2} T_s$ the error induced by neglecting the fine structure is less than 20%. For $T_g = \frac{1}{10} T_s$ the error is less than 80%.

Reference to Figs. 9, 10 and 11 shows that, at one atmosphere total pressure, for water vapor temperatures between 700°R and 1300°R the overlapping line model is useful for optical densities greater than 0.4 ft-atmos. As X is decreased below 0.4 ft-atmos the absorptivity decreases towards that given by the non-overlapping line model. Except for the linear molecules, polyatomic molecules generally have spectra with a rather complex rotational fine structure. A vibration-rotation band cannot usually be characterized by smoothly varying line intensity and a uniform line spacing. As was indicated previously a statistical model of water vapor bands in which a uniform line intensity was assigned to all the lines within a well-defined spectral region and in which the mean line spacing

decreased inversely with the temperature was found useful for correlating empirical emissivity data. For diatomic and linear polyatomic molecules for which band head formation is unimportant, the line spacing is independent of temperature (i.e., $\eta = 1/2$). For such molecules in the non-overlapping line region the absorptivity is given by

$$\alpha = E(T_s, \frac{T_s}{T_g} X). \tag{165}$$

In Table VII we have summarized the absorptivity expressions.

For rough calculations the absorptivity expression for $\eta = 1$ gives reasonable results (less than 20% error) for values of T_g/T_s not too different from unity (i.e., within a factor of 2).

F. Limits of Validity of the Effective Band-Width Approximation

The effective band-width approximation described in Section D fails to apply at very high pressures and optical densities because the intense rotational lines near the band center make appreciable contributions at wavelengths outside the "effective band-width". In the following discussion we shall obtain the large optical density limit of the approximate calculations.

Many detailed theoretical and experimental studies of spectral line shapes have appeared in the recent literature.[48] It is known that, even for impact broadening, the spectral absorption coefficients

$P_{j\to j+1}(\omega)$ and $P_{j\to j-1}(\omega)$ of the j'th rotational lines in the P and R branches, respectively, are complicated functions of the wave number ω.[48] However, for the present purposes it is sufficient to obtain an approximate estimate of the spectral absorption coefficient near the band limit by using the Lorentz distribution

$$P_{j\to j\pm1}(\omega) = \frac{S_{j\to j\pm1}\ b/\pi}{(\omega-\omega^{o}_{j\to j\pm1})^2 + b^2} \tag{166}$$

where $S_{j\to j+1}$ and $S_{j\to j-1}$ are the integrated intensities for the lines centered at $\omega^{o}_{j\to j+1}$ and $\omega^{o}_{j\to j-1}$, in the P and R branches, respectively, and b equals the collision (semi) half-width, which is assumed to be uniform for the entire vibration-rotation band.

If the anharmonicity terms in the energy expression are neglected, then the spectral absorption coefficient at a wave number ω for the rotational transition $j\to j-1$ is, for large values of j,

$$P_{j\to j-1}(\omega) \simeq \frac{\alpha\gamma u_e j\, e^{-\gamma u_e j^2}\ (b/\pi)}{(\omega-\omega^{o}_{j\to j-1})^2 + b^2} \tag{167}$$

where the line strength $S_{j\to j-1}$ has been approximated by

$$S_{j\to j-1} \simeq \alpha\gamma u_e j\, e^{-\gamma u_e j^2} \tag{168}$$

with α representing the integrated intensity for the entire vibration-rotation band. Similarly

$$P_{j\to j+1} = \frac{\alpha\gamma u_{ej}\, e^{-\gamma u_{ej}^2}\,(b/\pi)}{(\omega-\omega^{o}_{j\to j+1})^2 + b^2} \tag{169}$$

represents the spectral absorption coefficient for the transition $j\to j+1$ whose line strength is also

$$S_{j\to j+1} \simeq \alpha\gamma u_{ej}\, e^{-\gamma u_{ej}^2}. \tag{170}$$

Evidently

$$\sum_{j=0}^{\infty} (S_{j\to j-1} + S_{j\to j+1}) = \alpha. \tag{171}$$

Let the wave number at the center of the vibration-rotation band, corresponding to the (forbidden) transition $j=0\to j=0$, be identified by ω_o. If the centers of the rotational lines are uniformly spaced with a wave-number difference δ then

$$(\omega-\omega^{o}_{j\to j-1})^2 = (\omega-\omega_o-\delta j)^2$$

and

$$(\omega-\omega^{o}_{j\to j+1})^2 = (\omega-\omega_o+\delta j)^2.$$

The total spectral absorption coefficient at the wave number ω is

$$P(\omega) = \sum_{j=0}^{\infty} \left[P_{j\to j-1}(\omega) + P_{j\to j+1}(\omega)\right] \tag{172}$$

or, explicitly,

$$P(\omega) = \alpha\gamma u_e \frac{b}{\pi} \sum_{j=0}^{\infty} j e^{-\gamma u_{ej}^2} \left\{ \frac{1}{(\omega-\omega_o-\delta j)^2 + b^2} + \frac{1}{(\omega-\omega_o+\delta j)^2 + b^2} \right\}. \tag{173}$$

The quantity $\left|P_{j\to j-1}(\omega) + P_{j\to j+1}(\omega)\right|$ has been evaluated numerically and is plotted in Fig. 13 as a function of j for $\omega = \omega_o + 100\delta$, $\frac{b}{\delta} = 2.5$ and $(2\gamma u_e)^{-1/2} = 25$. These values apply approximately for the ν_3-fundamental of CO_2 at a temperature of 820°K and a pressure of 31 atmos. The peak at $j \simeq (\omega-\omega_o)/\delta$ represents the contributions of the central portions of the rotational lines whose centers lie close to $j = (\omega-\omega_o)/\delta$. The broad maximum centered at $j \simeq 35$ represents the contribution of the tails of the intense rotational lines to the absorption at the wave number ω. This latter contribution may be roughly estimated by replacing, in Eq. (173), the term in braces by its value when $j = j^*$, i.e., when $j\, e^{-\gamma u_e j^2}$ attains its maximum. Replacing the sum by an integral then results in an explicit expression for $P'(\omega)$, the contribution to $P(\omega)$ of the tails of the intense lines, viz.,

$$P'(\omega) = \frac{b}{2\pi(\omega-\omega_o)^2}\left\{\frac{1}{\left[1-\frac{\delta}{(\omega-\omega_o)\sqrt{2\gamma u_e}}\right]^2} + \frac{1}{\left[1+\frac{\delta}{(\omega-\omega_o)\sqrt{2\gamma u_e}}\right]^2}\right\}$$

$$= \frac{\alpha b \eta'}{\pi(\omega-\omega_o)^2} \qquad (174)$$

where, for $j^*\delta/(\omega-\omega_o) = 4$, $\eta' = 1.2$. This approximate calculation underestimates the value of $P'(\omega)$. For a more lengthy discussion of the evaluation of $P(\omega)$ see Ref. (44) where η' is found to have the value 1.7 when $j^* = 25$ and $\omega-\omega_o/\delta = 100$.

We shall assume that the limiting optical density obtains when the tails of the intense rotational lines near the center of the band

contribute appreciably to the absorption near the edges of the band. A convenient definition of the band edge is that used previously[44] to define a fixed mean value of the band-width useful for a large range of optical densities. According to this definition the band edge occurs where the absorption coefficient is reduced to 1/1000 of its maximum value. For a band having simple P and R branches the resulting band width $\Delta\omega'$ is given by

$$\Delta\omega' = 11.9\sqrt{\gamma kT\omega_e/hc}.$$

The limiting value of the optical density X_u, for which our effective band-width estimate applies, may then be defined by

$$X_u = 0.2/P'(\omega_o + \Delta\omega'/2) \tag{175}$$

since $P'(\omega_o + \Delta\omega'/2)$ is a slowly varying function of $\Delta\omega'$. Evidently $P'(\omega_o + \Delta\omega'/2)$ is the contribution to $P(\omega)$ of the tails of the intense rotational lines at the limit of the effective band-width. For $\eta = 1.7$, Eq. (175) becomes

$$X_u \simeq \frac{0.1\pi(\Delta\omega')^2}{4\alpha b} \quad . \tag{176}$$

Relevant spectroscopic data for CO, HCl, and CO_2 are given in Table VIII for the most intense vibration-rotation bands. In Table IX the values of X_u are listed for various temperatures and pressures.

G. Semi-Empirical Correlation of Infrared Emissivities for Heated Water Vapor

Penner[54] has shown that, at the present time, it is practically

impossible to perform a priori emissivity calculations as a function of temperature even for the simple linear triatomic molecule CO_2. Considering the enormous complication associated with the spectral details of asymmetric top triatomic molecules such as water, it therefore appears preferable to abandon attempts at calculations from first principles altogether and consider only an intelligent semi-empirical correlation of data.

Goody has justified the applicability of the statistical model to water vapor. We shall utilize the statistical model and the concept of an effective band width to correlate the empirical emissivity data for water vapor listed by Hottel. The mean emissivity $\bar{\varepsilon}(\omega)$ and the mean transmission $\bar{\tau}(\omega) = 1-\bar{\varepsilon}(\omega)$ are given in terms of the line contour $s(\omega-\omega', b)$ and the intensity distribution function $P(\bar{S}, S)$ by Eq. (96).

In order to evaluate $\bar{\varepsilon}(\omega)$ or $\bar{\tau}(\omega)$ explicitly, the distribution $P(\bar{S}, S)$ and the line shape $s(\omega-\omega', b)$ must be known. In the present analysis, only the dispersion distribution

$$s(\omega-\omega', b) = (b/\pi)/\left[(\omega-\omega')^2 + b^2\right] \qquad (177)$$

will be considered. We proceed now to evaluate $\bar{\varepsilon}(\omega)$ for the distributions $P^{(1)}(\bar{S}, S) = (1/\bar{S})\exp(-S/\bar{S})$ and $P^{(2)}(\bar{S}, S) = \delta(S-\bar{S})$ where $\delta(x)$ denotes the Dirac delta function of argument x.

a. Mean Emissivity $\bar{\varepsilon}^{(1)}$ for the Distribution $P^{(1)}(\bar{S}, S)=(1/\bar{S})\exp(-S/\bar{S})$

For the distribution $P^{(1)}(\bar{S}, S) = (1/\bar{S})\exp(-S/\bar{S})$, Eq. (96) reduces to

$$\bar{\varepsilon}^{(1)} = 1-\exp\left\{-(1/\delta)\int_{-\infty}^{\infty}(1+\bar{S}sX)^{-1}\,\bar{S}sX\,d\omega\right\} \tag{178}$$

after the integration over S has been performed. For a dispersion line shape $s = (b/\pi)\left[(\omega-\omega_o)^2 + b^2\right]^{-1}$ and Eq. (178) becomes

$$\bar{\varepsilon}^{(1)} = 1-\exp\left\{-(SX/\pi\delta)(1+SX/\pi b)^{-1/2}\int_{-\infty}^{\infty}(1+u^2)^{-1}\,du\right\}$$

$$= 1-\exp\left\{-(SX/\delta)(1+SX/\pi b)^{-1/2}\right\}. \tag{179}$$

b. Mean Emissivity $\bar{\varepsilon}^{(2)}$ for the Distribution $P^{(2)}(\bar{S},S)=\delta(S-\bar{S})$

For the distribution $P^{(2)}(\bar{S},S) = \delta(S-\bar{S})$, Eq. (96) reduces to

$$\bar{\varepsilon}^{(2)} = 1-\exp\left\{-(1/\delta)\int_{-\infty}^{\infty}\left[1-\exp(-SsX)\right]\,d\omega\right\} \tag{180}$$

after the integration over S has been performed. The integral appearing in Eq. (180) is equal to the total absorption of a single isolated spectral line and may be obtained for spectral lines having combined collision and Doppler broadening from the curves of growth.

The total absorption of a single line with dispersion contour has been obtained previously. The result is

$$\int_{-\infty}^{\infty}\left[1-\exp(-\bar{S}sX)\right]\,d\omega = \bar{S}X\left[\exp(-\bar{S}X/2\pi b)\right]\left\{J_o(i\bar{S}X/2\pi b) - iJ_1(i\bar{S}X/2\pi b)\right\}. \tag{181}$$

Hence the mean emissivity for a spectral line with dispersion contour is

$$\bar{\varepsilon}^{(2)} = 1-\exp\left\{-(\bar{S}X/\delta)\left[\exp(-\bar{S}X/2\pi b)\right]\left[J_o(i\bar{S}X/2\pi b) - iJ_1(i\bar{S}X/2\pi b)\right]\right\}. \tag{182}$$

If we define the function $g(u, b/\delta)$ by the relation

$$g(u, b/\delta) = 1-\exp\left\{-(2\pi b/\delta)u\left[\exp(-u)\right]\left[J_o(iu)-iJ_1(iu)\right]\right\} \tag{183}$$

then it follows that

$$\bar{\varepsilon}^{(2)} = g(u, b/\delta) \tag{184}$$

where

$$u = \bar{S}X/2\pi b. \tag{185}$$

c. The Engineering Emissivity for Water Vapor[55]

The applicability of the disordered absorption band to water vapor at low temperatures has been justified by Goody[43] on the basis of a detailed comparison with exact numerical calculations performed by Cowling.[56] Goody has also shown[42] that the mean transmissions $\bar{\tau}(\omega)$ are not significantly different when either the distribution function $P^{(1)}(\bar{S}, S) = (1/\bar{S})\exp(-S/\bar{S})$ or the function $P^{(2)}(\bar{S}, S) = \delta(S-\bar{S})$ is used. In the following analysis only the distribution function $P^{(2)}(\bar{S}, S)$ and the emissivity $\bar{\varepsilon}^{(2)}$ will be used for the correlation of data.

The overall (engineering) emissivity is defined, as usual, by the relation

$$\varepsilon = (1/\sigma T^4)\int_0^\infty \bar{\varepsilon}(\omega)R^o(\omega, T)d\omega. \tag{186}$$

We are unable to utilize Eq. (186) without further approximation because the values of $\bar{S}$ for groups of lines are not known. In order to obtain a tractable procedure, we therefore introduce an important simplification, which follows the procedures for emissivity calculations

described in the preceding sections. Thus we shall use an average value

$$\bar{\delta}_i = \alpha_i/(\Delta\omega_i/\delta) \tag{187}$$

for an effective band-width $\Delta\omega_i$ for the entire i'th vibration-rotation band whose integrated absorption is α_i. In the present calculations we shall assume that the effective band width is independent of the optical density. The approximation expressed by Eq. (185) should become better as the temperature is raised. Equation (186) now reduces to

$$\mathcal{E} = (1/\sigma T^4) \sum_i \bar{\mathcal{E}}_i R^\circ_{\omega_i} \Delta\omega_i \tag{188}$$

where $\bar{\mathcal{E}}_i$ is computed either from Eqs. (179) and (187) or from Eqs. (183) and (187), $R^\circ_{\omega_i}$ represents the mean value of $R^\circ(\omega, T)$ for the i'th band, which is conveniently evaluated at the band center $\omega = \omega_i$. In the following calculations we shall assume that δ and b are independent of ω.

d. Outline of Emissivity Calculations for Water Vapor

The vibration-rotation bands of water vapor which contribute to the emissivity in the temperature range between 600°R and 5000°R are assumed to be centered at 20μ, 6.3μ, 2.7μ, 1.87μ, 1.38μ, and 1.1μ. Assuming that all of the $\Delta\omega_i$ are equal to $\Delta\omega$, a six-term sum is obtained for $\mathcal{E}$. Thus the use of $\bar{\mathcal{E}}_i^{(2)}$ leads to the result

$$\mathcal{E}^{(2)} = \frac{\Delta\omega}{\sigma T^4} \sum_{i=1}^{6} R^\circ_{\omega_i} g(u_i, b/\delta)$$

with

$$u_i = \alpha_i \delta X / 2\pi b \Delta\omega. \tag{189}$$

Here the subscripts i=1, 2,..., and 6 identify appropriate values for the vibration-rotation bands centered at 20μ, 6.3μ, ..., and 1.1μ, respectively.

No reliable values are available for all of the integrated intensities α_i for water vapor. The relative intensities of the 6.3μ, 2.7μ, 1.87μ, 1.38μ, 1.1μ band may, however, be estimated from the data of Howard, Burch, and Williams[57] who have plotted the optical depth $X \equiv X_o$ for which the mean transmission is 0.5 as a function of ω. For $\bar{\varepsilon}_i^{(2)} = 1 - \bar{T}_i^{(2)} = 0.5$, Eq. (184) becomes

$$\bar{\varepsilon}_i^{(2)} = 0.5 = g(u_o = \bar{S}_i X_{o,i}/2\pi b,\ b/\delta) \tag{190}$$

and, for any given vibration-rotation band at fixed temperature,

$$S_i = \text{constant } (2\pi b / X_{o,i}).$$

According to Eq. (187) and the preceding relation, we now find that

$$\alpha_i = \bar{S}_i \Delta\omega/\delta \sim 2\pi b \Delta\omega / X_{o,i}\delta \tag{191}$$

whence the integrated intensities, as estimated from the data of Burch, Howard and Williams[57] are listed in reference (55). The relative integrated intensity of the 20μ band is not known.

In order to utilize the emissivity relation given in Eq. (189) at different temperatures it is necessary to know the dependence on temperature of the parameters α_i, $\Delta\omega$, b and δ. For collision-broadened lines the rotational half-width b varies linearly with pressure

and inversely as the square root of the temperature. The effective band-widths are assumed to be proportional to the square root of the temperature, i.e.,

$$\Delta\omega_i = \Delta\omega = \Delta\omega^\circ (T/T^\circ)^{1/2}. \tag{193}$$

The temperature dependence of the integrated intensity of the fundamental vibration-rotation bands is

$$\alpha_i(T) = \alpha_i(T^\circ)\,(T^\circ/T). \tag{194}$$

Equation (194) actually applies only for the fundamental bands at moderate temperatures (below 3000°R). Unfortunately, a rigorous expression for the temperature dependence of the integrated intensities for an asymmetric top molecule such as H_2O does not appear to exist at the present time. However, since the fundamental bands are the dominant contributors to the emissivity in the temperature range (600 to 3000°R) considered in the present calculations, and since any decrease in the population of the ground state is offset by a corresponding increase in the population of the excited states, it seems reasonable to expect that the approximation contained in Eq. (194) will not involve large errors.

The temperature dependence of the mean line spacing δ is assumed to be of the form

$$\delta(T) = (T^\circ/T)^\eta \;\delta(T^\circ) \tag{195}$$

where the exponent η is to be chosen so as to give "best" agreement with the experimentally determined emissivity data.

The emissivity expression given in Eq. (189) has been fitted to

Hottel's data[58] by varying the following five adjustable parameters: $\Delta\omega(T^\circ)$, $2\pi b(T^\circ)/\delta(T^\circ)$, $b(T^\circ)\Delta\omega(T^\circ)/\alpha_{6.3\mu}(T^\circ)\delta(T^\circ)$, $\alpha_{20\mu}(T^\circ)/\alpha_{6.3\mu}(T^\circ)$ and η. The reference temperature T° was chosen to be $600^\circ R$.

For the selection of suitable numerical values of the adjustable parameters according to the emissivity expression given in Eq. (189), it proved to be convenient to plot the logarithm of the emissivity as a function of the logarithm of the optical density for different temperatures. In such a plot, variations of the parameters $\Delta\omega(T^\circ)$ and of $X/u_{6.3}\Big|_{T=T^\circ}$ induce only rigid translations of the emissivity curves, the magnitude of the translations being independent of temperature. A variation of η similarly induces a rigid translation which does, however, depend on the temperature. Thus the form of the emissivity curves depends only on the two parameters $2\pi b/\delta$ at T° and $\alpha_{20\mu}(T^\circ)/\alpha_{6.3\mu}(T^\circ)$. When the empirical emissivity data for a given temperature were plotted in this manner, it was observed that they could be represented reasonably well by an expression of the form

$$\varepsilon \simeq \mathcal{K} g(\bar{u}, b/\delta).$$

The parameters $\mathcal{K}$, $X/\bar{u}$, and b/δ vary, of course, with the temperature. The values of $2\pi b/\delta$ and $X/\bar{u}$, which gave the best fit at each of the temperatures for which experimental data were available, were then plotted as a function of temperature. Since the temperature dependence of

$$X/\bar{u} = 2\pi b(T)\Delta\omega(T)/\bar{\alpha}(T)\delta(T)$$

is known except for that of $\delta(T)$, two independent estimates may be obtained for the variation of δ with temperature. It has been found that δ varies roughly inversely with the temperature. A decrease in the mean line spacing δ with increasing temperature is reasonable in view of the fact that an increasing number of spectral lines must make an important contribution to ε at elevated temperatures.

Numerical calculations have been carried out[55] using $\delta \sim T^{-1.0}$, i.e., $\eta = 1.0$. For $\eta = 1.0$ the "best" value of $2\pi b/\delta$ at T^o was chosen to be 0.165 for $T^o = 600^oR$. The emissivity was then evaluated according to Eq. (189) for different values of $\alpha_{20\mu}(T^o)/\alpha_{6.3\mu}(T^o)$. The ratio giving the best fit to the measured data was found to be

$$\alpha_{20\mu}(T^o)/\alpha_{6.3\mu}(T^o) = 0.33 \text{ for } T^o = 600^oR.$$

Finally, the "best" scale factors $\Delta\omega(T^o)$ and $X/u_{6.3\mu}$ at T^o were found to be 609 cm^{-1} and 0.0188 ft-atmos, respectively. The resulting correlation of emissivity data for water vapor is shown in Fig. 14.

H. Emissivity Estimates for Heated NO

a. Introduction

The total hemispherical* emissivity E is given by

$$E = \int_0^\infty \frac{R_\omega^o}{\sigma T^4}\, \varepsilon_\omega\, d\omega \qquad (196)$$

* The hemispherical emissivity is defined as the ratio of power emitted by a hemisphere of radiator through a unit area at the center of its base to that emitted per unit area by a blackbody. We shall use the words "hemispherical emissivity" and "emissivity" interchangeably.

where $R^{o}_{\omega} = c_1\omega^3 / \left[\exp(c_2\omega/T)-1\right]$ is the Planck radiation function, ω is the wave number (cm^{-1}), T is the absolute temperature (^{o}K), ε_{ω} is the spectral hemispherical emissivity, $c_1 = 2\pi hc^2 \simeq 3.471 \times 10^{-5}$ erg-cm^2-sec^{-1}, $c_2 = hc/k \simeq 1.439$ cm-^{o}K, and $\sigma = 2\pi^5 k^4/15h^3c^2 \simeq 5.662\times10^{-5}$ erg-sec^{-1}-cm^{-2}-$(^{o}K)^{-4}$ is the Stefan-Boltzmann constant.

The spectral emissivity ε_{ω} is given by

$$\varepsilon_{\omega} = 1 - \exp\left[-P_{\omega} X\right] \tag{197}$$

where X is the optical density (the product of the effective pathlength in cm and of the partial pressure of emitter in atmospheres) and P_{ω} is the spectral absorption coefficient (in cm^{-1}-$atmos^{-1}$). In the temperature range between 4000°K and 8000°K and γ- and β-band systems contribute most of the radiant energy emission of NO. Thus

$$P_{\omega} = (P_{\omega})_{\gamma} + (P_{\omega})_{\beta} \tag{198}$$

where

$$(P_{\omega})_{\gamma,\beta} = \left(\sum_{v'',v'} \alpha_{v''v'}\, s(\omega-\omega_{v''v'}) \right)_{\gamma,\beta}. \tag{199}$$

Here $\alpha_{v''v'}$ is the integrated intensity (in cm^{-2}-$atmos^{-1}$) of the vibration-rotation band corresponding to the transition ($v' \longrightarrow v''$), v' and v'' are the vibrational quantum numbers of the upper and lower state, respectively, and $s(\omega-\omega_{v''v'})$ represents the contribution to the absorption coefficient from the ($v' \longrightarrow v''$) band normalized to unit intensity $\left(\int_{-\infty}^{\infty} s(\omega-\omega_{v''v'})d\omega = 1 \right)$. The integrated intensity $\alpha_{v''v'}$ of the ($v' \longrightarrow v''$) band is given[59] by the approximate relation

$$\alpha_{v''v'} = 2.38\,(10^7)\,\frac{273.1}{T}\,\frac{N_{v''}}{N_T}\,f_{elec}\,\frac{\omega_{v''v'}}{\omega_{oo}}\,q^2_{v''v'}. \tag{200}$$

Here $N_{v''}$ is the number density of NO molecules in the v'' (lower) state (in cm^{-3}), N_T is the total number density of NO molecules, $\omega_{v''v'}$ is the wave number of the ($v' \longrightarrow v''$) band for rotationless transitions, ω_{oo} is the origin of the $v' = 0 \longrightarrow v'' = 0$ band, $q^2_{v''v'}$ is the vibrational matrix element for the transition and f_{elec} is the electronic f-number for the band system. Because of the large number of vibration-rotation bands in each band system, and because of considerable overlapping of bands, an exact calculation of the spectral emissivity is exceedingly tedious and, indeed, impossible on the basis of presently available information. It is the purpose of this section to obtain a simplified representation for the spectral emissivity ε_ω utilizing the statistical model. The present work is related to that of Kivel, Mayer and Bethe[26] but the analytic procedure is quite different.

Several difficulties arise in the calculation of the emissivity of NO at high temperatures. The f-numbers of the γ- and β-band systems are not well established. Weber and Penner[60,61] have measured the integrated intensities of some of the low-lying bands of the two systems in absorption at room temperature. They found the electronic f-numbers to be $f_{elec_\gamma} \simeq 0.0025$ and $f_{elec_\beta} \simeq 0.008$. In the present paper we assume the electronic f-number to be independent of the vibrational quantum number. The accuracy of the available values of the vibration overlap integrals $q^2_{v''v'}$ is also uncertain. Kivel, Mayer and Bethe, in their paper on the emissivity of NO, give extensive tables of the overlap

integrals of the β- and γ-systems. Their values should be accurate at low values of the vibrational quantum number where the wave-functions are well-known. For high vibrational quantum numbers their values may be in error. Also, at 8000°K there is considerable emission from transitions not included in their tables. It is evident that there is a need for an extensive experimental study of these band systems.

b. Outline of the Calculations

Because, at high temperatures, the number of bands that have appreciable intensity is large the spectrum of NO has an irregular appearance (see Fig. 22). In order to obtain a tractable procedure for estimating the emissivity we shall introduce two simplifying approximations. First, we shall assume that the origins of the vibration-rotation bands are randomly distributed. Second, we assume that, at the wave number ω, the probability that a band has an integrated intensity between α and $\alpha + d\alpha$ is $P_\gamma[\alpha, \bar{\alpha}_\gamma(\omega)]\, d\alpha$ for a band belonging to the γ-system and $P_\beta[\alpha, \bar{\alpha}_\beta(\omega)]\, d\alpha$ for a band belonging to the β-system. Here $\bar{\alpha}_\gamma(\omega)$ and $\bar{\alpha}_\beta(\omega)$ are the mean integrated band intensities at the wavenumber ω. The choice of the probability distribution functions $P_\gamma[\alpha, \bar{\alpha}_\gamma(\omega)]$ and $P_\beta[\alpha, \bar{\alpha}_\beta(\omega)]$ will be made by reference to the calculated values of the vibration overlap integrals $q^2_{v''v'}$ of the γ- and β-band systems. Goody has calculated the mean, or expected, spectral emissivity of a group of spectral lines whose

centers are distributed randomly and whose intensities are distributed statistically. Using Goody's method as applied to a distribution of bands (rather than of lines) we are able to calculate the mean spectral emissivity $\bar{\varepsilon}_\omega$ as a function of wave number. Using the resulting expression for ε_ω we integrate Eq. (196) numerically to obtain the total emissivity of nitric oxide.

Section c deals with the structure of the ultraviolet spectrum of NO. In Section d we calculate the total emissivity of a single isolated band and in Section e we utilize the results of Section d to calculate the spectral emissivity of a group of randomly distributed bands. In Section f we apply the results of the previous sections to the NO γ- and β-band systems. The resulting emissivity is presented (see Fig. 21) for the β-band system alone and for the γ- and β-band systems together both for low pressure (pure Doppler broadening) and for high pressure (rotational fine structure smeared out).

For the γ- and β-band systems of NO the mean emissivity at the wave number ω is given, according to Eq. (100), by the expression

$$\bar{\varepsilon} = 1 - \exp\left[-\frac{\bar{A}_\beta}{\delta_\beta} - \frac{\bar{A}_\gamma}{\delta_\gamma}\right] \tag{201}$$

where

$$\bar{A}_\beta = \int_0^\infty \rho_\beta\left[\alpha, \bar{\alpha}_\beta(\omega)\right]\left\{\int_{-\infty}^{\infty}\left\{1-\exp\left[-P_\beta(\alpha;\omega')X\right]\right\}d\omega'\right\}d\alpha \tag{202}$$

represents the mean total absorption of a band in the β-system at the

wave number ω. Here $P_\beta(\alpha;\omega')$ is the spectral absorption coefficient at the wave number ω' of a band belonging to the β-system and having an intensity α. A relation similar to Eq. (202) obtains for the γ-system.

The statistical approach to the calculation of the emissivity is not as useful for the γ-system as for the β-system because the γ-system has a relatively small number of bands of appreciable intensity. However, since the γ-system is weaker and contributes considerably less to the emissivity than does the β-system, the resultant error in the total emissivity will not be large.

c. Structure of the Spectrum

1. Line Widths

The Doppler (semi) half-width b_D is given by

$$b_D = \omega \sqrt{2(\ell n 2)RT/Mc^2} \tag{203}$$

where R = gas constant $\simeq 8.31436 \times 10^7$ ergs/$^\circ$K-mole, M = molecular weight of NO $\simeq 30.015$ gm, and c = velocity of light $\simeq 3 \times 10^{10}$ cm/sec. For NO, b_D is

$$b_D = 6.52\,(10^{-8})\,\omega\sqrt{T}\ \text{cm}^{-1}. \tag{203a}$$

The collision half-width b_C of NO at high temperatures is not known. An order of magnitude estimate is 0.10 cm^{-1} at T = 300°K and 1 atmos pressure or

$$b_C \sim \frac{0.10\,p}{\sqrt{T/300}}\ \text{cm}^{-1} \tag{204}$$

where p is the pressure in atmospheres. In Table XII some representative

values of b_D and b_C are listed.

2. Electronic Structure

The $v' = 0 \longrightarrow v'' = 0$ band of the β-system has its origin at approximately $\omega_{oo} = 45,440\ cm^{-1}$. Actually, because of spin splitting, there are two $v' = 0 \longrightarrow v'' = 0$ bands, one arising at $45,395\ cm^{-1}$ and the other at $45,486\ cm^{-1}$; the mean of these two wavenumbers is $45,440\ cm^{-1}$. The $v' = 0 \longrightarrow v'' = 0$ band of the γ-system has its (mean) origin at $\omega_{oo} = 44,138\ cm^{-1}$. In the temperature range $4000^{\circ}K$ to $8000^{\circ}K$ there is appreciable emission from both systems for $\omega \sim 20,000\ cm^{-1}$ to about $70,000\ cm^{-1}$.

3. Vibrational Structure

In the notation used by Herzberg,[62] the wave number $\omega_{v''v'}$ of the origin of the $v' \longrightarrow v''$ band is given by

$$\omega_{v''v'} = \omega_{oo} - (\omega''_e - \omega''_e x''_e + \tfrac{3}{4}\omega''_e y''_e)v'' + (\omega''_e x''_e - \tfrac{3}{2}\omega''_e y''_e)v''^2 - \omega''_e y''_e v''^3 + (\omega'_e - \omega'_e x'_e + \tfrac{3}{4}\omega'_e y'_e)v' - (\omega'_e x'_e - \tfrac{3}{2}\omega'_e y'_e)v'^2 + \omega'_e y'_e v'^3. \quad (205)$$

For the β-band system of NO, $\omega_{v''v'}$ denotes the mean of the wavenumbers of the $B^2\Pi_{1/2} \longrightarrow X^2\Pi_{1/2}$ and the $B^2\Pi_{3/2} \longrightarrow X^2\Pi_{3/2}$ transitions*, viz.,

$$\omega_{v''v'} = 45440 - 1889.9v'' + 14v''^2 + 0.001v''^3 + 1030.3v' - 7.45v'^2 - 0.10v'^3 \ cm^{-1} \quad (205a)$$

---

* The transitions in which the spin flips are very weak and contribute little to the emissivity.

and for the γ-system

$$\omega_{v''v'} = 44138 - 1889.9v'' + 14v''^2 + 0.001v''^3 + 2356.6v' + 14.7v'^2 - 0.28v'^3 \quad \text{cm}^{-1}. \tag{205b}$$

In the temperature range 4000°K to 8000°K a large number of bands emit appreciably so that the apparent regularity of the vibrational structure is suppressed. As stated previously, we make the approximation that the wave numbers of the band origins are distributed at random (see Fig. 22).

4. Rotational Structure

In the bands of the β-system the intensity of the Q-branches decreases rapidly (compared to that of the P- and R-branches) with increasing values of the rotational quantum number.* For this reason we shall include only the P- and R-branches, which exhibit a fourfold splitting (a two-fold splitting because of Λ-doubling and a two-fold splitting because the spin assumes two values. Thus there are eight branches of roughly equal intensity in each band of the β-system in the present emissivity computations.

In the bands of the γ-system the Q-branches have roughly twice the intensity of the P- or R-branches. These P-, Q- and R-branches exhibit only a two-fold splitting (because of the two values of spin; Λ-doubling does not produce additional splitting in the γ-system). It

* For a discussion of the structure and intensity distribution of the γ- and β-band systems see Chapter V, Section 3 of reference (62).

is convenient for the purposes of calculation (and will not introduce large errors) to consider a band of the γ-system to consist of six equally intense branches.

The wave number for the $J' \longrightarrow J''$ transition is (neglecting the centrifugal stretching terms and the vibration terms)

$$\omega = \omega_{v''v'} - B''_e J''(J''+1) + B'_e J'(J'+1) \tag{206}$$

or

$$\omega = \omega_{v''v'} - (B''_e - B'_e)J''^2 - \left[(2\Delta J - 1)B'_e + B''_e\right] J'' + B'_e \Delta J(\Delta J - 1) \tag{207}$$

where $\Delta J = J'' - J' = \pm 1, 0$. The band head is located near

$$J'' = J''_{BH} \simeq - \frac{\left[(2\Delta J - 1)B'_e + B''_e\right]}{2(B''_e - B'_e)} . \tag{208}$$

For $B''_e > B'_e$ (γ-system of NO) the band head forms in the P-branch ($\Delta J = -1$) at

$$J''_{BH} \simeq \frac{(B'_e + B''_e)}{2\Delta B} - 1 \tag{209}$$

and the band is shaded to the blue. Here we write ΔB for $\left|B'_e - B''_e\right|$. For $B''_e < B'_e$ (β-system of NO), the band head forms in the R-branch ($\Delta J = +1$) at

$$J''_{BH} \simeq \frac{(B'_e + B''_e)}{2\Delta B} \tag{210}$$

and the band is shaded to the red. For the NO β-system $J_{BH} \sim 3$ and for the γ-system $J_{BH} \sim 5$. In the temperature range 4000°K to 8000°K many rotational lines are excited. Roughly, the largest value of $J'' = J''_m$ which needs to be considered in the emissivity computations is given by

$$hcB''_e J''_m (J''_m + 1)/kT \sim 2 \tag{211}$$

or

$$J''_m \sim \sqrt{2kT/hcB''_e}\,. \tag{211a}$$

At $4000^{\circ}K$, $J''_m \sim 57$. Thus, for most practical purposes, the band head may be considered to occur at the band origin.

In each branch the line arising from a transition to the J'' level has an integrated intensity given approximately (for large J) by

$$S_{J''} \simeq (2\alpha_{v''v'} hcB''_e J''/nkT) \exp\left[-hcB''_e J''^2/kT\right] \tag{212}$$

where n is the number of branches, B''_e is the rotational constant in the lower state and J'' is the rotational quantum number in the lower state.

The wave number displacement from the band origin of the J''th line is, approximately,

$$\omega - \omega_{v''v'} = (B''_e - B'_e)J''^2 \tag{213}$$

and, therefore, the line spacing $q_{J''} = q(\omega)$ is, approximately,

$$q_{J''} = 2\Delta B J''. \tag{214}$$

Thus, at the wave number ω, the average absorption coefficient $\bar{P}(\omega)$ is

$$P(\omega) \equiv S_{J''}/q_{J''} = (\alpha_{v''v'} hcB''_e/nkT\Delta B) \exp\left[-hcB''_e \left|\omega - \omega_{v''v'}\right|/\Delta B kT\right]$$

$$= (\alpha_{v''v'}/n\Delta\omega) \exp\left[-\left|\omega - \omega_{v''v'}\right|/\Delta\omega\right] \tag{215}$$

where $\Delta\omega = \Delta B kT/hcB''_e$. Equation (215) applies for $(\omega - \omega_{v''v'})/(B''_e - B'_e) > 0$. For $(\omega - \omega_{v''v'})/(B''_e - B'_e) < 0$, $\bar{P}(\omega)$ vanishes.

The line spacing q is given as a function of ω by

$$q = q_o \sqrt{|\omega - \omega_{v''v'}| / \Delta\omega} \tag{216}$$

where $q_o = 2\Delta B \sqrt{kT/hcB''_e}$.

In Table XII we have listed representative values of the band-width $\Delta\omega$ and mean line spacing q_o. Reference to Table XII shows that for an isolated branch at low pressure the lines are widely separated. Even for a band with eight overlapping branches the overlapping of individual lines at low pressures is negligible except at very large optical densities. Thus we may obtain the total absorption, A_{band}, of an isolated band by summing the absorptions of the individual lines computed on the assumption that no overlapping occurs.

d. The Total Absorption of an Isolated Band of Non-Overlapping Spectral Lines having Combined Doppler and Collision Broadening

In Section III-D we obtained an approximate expression for the radiancy of a band having simple P and R branches and composed of spectral lines having a dispersion contour. The results are useful for vibration-rotation spectra when the formation of band heads may be neglected. In the ultraviolet region of the spectrum where we are generally concerned with electronic transitions we may no longer overlook the band head formation so that the results of Section III-D are useful only where the lines are non-overlapping. Also, at the temperatures that the electronic transitions contribute dominantly to the emissivity, the Doppler broadening of the spectral lines is usually more important than the collision broadening. In the present section we obtain

an expression for the radiancy of band of Doppler-broadened lines 1) when the lines are non-overlapping and 2) when the lines are overlapping and the band head occurs near the band origin. We shall find that we may make an approximate interpolation between the two expressions and thus obtain, as was previously done for dispersion lines, an expression for the band radiancy for any value of the overlapping parameter $2\pi b/\delta$.

The intensity, S_J, of the Jth line of one of the equally intense branches of a band whose intensity is α is, approximately,

$$S_J \simeq (2B''_e hc\alpha J/nkT) \exp\left[-hcB''_e J^2/kT\right] . \qquad (217)$$

Here

$$\alpha = \sum_{J=0}^{\infty} S_J \simeq n \int_0^{\infty} S_J dJ$$

and n denotes the number of branches. If the lines do not overlap the total absorption of the band is given by

$$A_{band} = \int_{band} \left[1-\exp(-P_\omega X)\right] d\omega = n \sum_{J=0}^{\infty} A_J \simeq n \int_0^{\infty} A_J dJ \qquad (218)$$

where

$$A_J = \int_{Jth\ line} \left[1-\exp(-P_J(\omega)X)\right] d\omega$$

and

$$S_J = \int_{Jth\ line} P_J(\omega) d\omega .$$

For an isolated spectral line with combined dispersion and Doppler contour the absorption coefficient $P_J(\omega)$ is given by

$$P_J(\omega) = P'_J \frac{a}{\pi} \int_{-\infty}^{\infty} \frac{\exp(-y^2)}{a^2 + (\xi - y)^2} \, dy \qquad (219)$$

where

$$P'_J = \left[S_J \sqrt{(\ell n 2)/\pi} \right] / b_D,$$

$$a = (b_C / b_D) \sqrt{\ell n 2},$$

$$\xi = (\omega - \omega_J) \sqrt{\ell n 2} / b_D,$$

ω_J = wave number of the Jth line center,

and

$$b_D = \omega_J \sqrt{\ell n 2} / \sqrt{mc^2/2kT}.$$

If the fractional change of b_D (i.e., of ω_J) is small across the band, the total absorption of the band becomes

$$A_{band} = 2 b_D n (kT/hcB''_e \ell n 2)^{1/2} \int_0^{\infty} \frac{\sqrt{\ell n 2}}{2 b_D} A_{J(u)} du \qquad (220)$$

where $A_{J(u)}$ is the value of A_J at $J = (kT/hcB''_e)^{1/2} u$. The integrand of Eq. (220) may be evaluated as a function of u by utilizing the well-known curves of growth. For example, in reference (63), $\sqrt{\ell n 2} A_J / 2 b_D$ is plotted as a function of $\log(10.6 P'_J X)$ for different values of the parameter a. Now, if we define the parameter γ by the expression

$$\gamma = 0.212 \sqrt{\ln 2}\ (\alpha X/nb_D)(hcB''_e/wkT)^{1/2} \tag{221}$$

then

$$0.106\ P'_J X = \gamma u \exp(-u^2). \tag{222}$$

Thus, we may write

$$\int_0^\infty \frac{\sqrt{\ln 2}\, A_{J(u)}\, du}{2b_D} = H(\gamma, a), \tag{223}$$

where the function $H(\gamma, a)$ is defined by

$$H(\gamma, a) = \frac{1}{2} \int_0^\infty du \int_{-\infty}^{\infty} d\xi \left\{ 1 - \exp\left[- \frac{u e^{-u^2}}{0.106} \frac{a}{\pi} \int_{-\infty}^{\infty} \frac{\exp(-y^2)\, dy}{a^2 + (\xi - y)^2} \right] \right\}, \tag{224}$$

$H(\gamma, a)$ has been computed by numerical integrations according to Eq. (223) from the curves of growth utilizing Eq. (222) to relate the value of u to the abscissa of the curves of growth. In Fig. 19 we have plotted $H(\gamma, a)$ as a function of γ for various values of a. For very large or very small values of γ, asymptotic expressions for $H(\gamma, a)$ may be obtained. For a = 0 the asymptotic forms of $H(\gamma, a)$ are

$$H(\gamma, 0) \sim (\sqrt{\pi}/0.424)\gamma = 4.17\gamma \qquad \text{for} \quad \gamma \ll 1 \tag{225}$$

and

$$H(\gamma, 0) \sim (\pi/4) \ln \gamma \qquad \text{for} \quad \gamma \gg 1\ . \tag{226}$$

Hence we obtain for the total absorption of a band of intensity a the expression

$$A_{\text{band}} = 2b_D n (kT/hcB''_e \ln 2)^{1/2} H(\gamma, a) \tag{227}$$

where γ has been defined in Eq. (221).

e. Approximation Procedures

In this section useful approximate analytic expressions will be obtained for the total absorption of a band of Doppler broadened lines. We first derive an approximation of the function $H(\gamma, 0)$. $H(\gamma, 0)$ is defined by the expression

$$H(\gamma,0) = \frac{1}{2}\int_0^\infty du \int_{-\infty}^{\infty} d\xi \left[1-\exp\left(-\frac{\gamma u}{0.106}\exp\left[-(u^2+\xi^2)\right]\right)\right] \qquad (228)$$

or, expanding the exponential,

$$H(\gamma,0) = \frac{1}{2}\int_0^\infty du \int_{-\infty}^{\infty} d\xi \left[\sum_{\nu=1}^{\infty} \frac{(-1)^{\nu+1}}{\nu!}\left(\frac{\gamma}{0.106}\right)^{\nu} u^{\nu}\exp\left[-(\nu u^2+\nu\xi^2)\right]\right]$$

$$= \frac{\sqrt{\pi}}{4}\sum_{\nu=1}^{\infty} \frac{(-1)^{\nu+1}(\gamma/0.106)}{\nu!\ \nu^{(\nu/2)+1}}\Gamma\left(\frac{\nu+1}{2}\right) \qquad (229)$$

where $\Gamma(n)$ represents the gamma-function of argument n. The series in Eq. (229) may be rewritten in a form which converges appreciably faster, viz.,

$$H(\gamma,0) = \frac{\sqrt{\pi}}{4}\, h\left(\frac{\gamma}{0.106\sqrt{2e}}\right) - \frac{\sqrt{2\pi}}{4}\sum_{\nu=1}^{\infty} \frac{(-1)^{\nu+1}}{\nu\,\nu!}\left(\frac{\gamma}{0.106\sqrt{2e}}\right)^{\nu}\left[1-\frac{\Gamma\left(\frac{\nu+1}{2}\right)}{\sqrt{2\pi}\left(\frac{\nu}{2e}\right)^{\nu/2}}\right] \qquad (230)$$

where $h(x) = \ln Cx - Ei(-x)$ and C = Euler's constant $\simeq 1.781072$. The first term in Eq. (230) results when Stirling's approximation is used to replace the term $\Gamma\left((\nu+1)/2\right)$ in Eq. (229), viz.,

$$\Gamma\left(\frac{\nu+1}{2}\right) \simeq \sqrt{2\pi}\left(\frac{\nu}{2e}\right)^{\nu/2} . \qquad (231)$$

The second term in Eq. (230) is the necessary correction. Another form in which Eq. (229) may be written which is sometimes useful for quick calculations is

$$H(\gamma,0) = \frac{\pi}{4} h\left(\frac{\gamma}{0.106\sqrt{\pi}}\right) - \frac{\pi}{4}\sum_{\nu=1}^{\infty} \frac{(-1)^{\nu+1}}{\nu\,\nu!}\left(\frac{\gamma}{0.106\sqrt{\pi}}\right)^{\nu}\left[1 - \frac{\Gamma\left(\frac{\nu+1}{2}\right)}{\sqrt{\pi}\left(\frac{\nu}{\pi}\right)^{\nu/2}}\right]. \quad (232)$$

This form has the advantage that the first term gives the correct asymptotic values of $H(\gamma,0)$ for both large and small γ, viz.,

$$H(\gamma,0) \longrightarrow \frac{\sqrt{\pi}}{4}(\gamma/0.106) \quad \text{for } \gamma << 1$$

and

$$H(\gamma,0) \longrightarrow \frac{\pi}{4}(\ln \gamma) \qquad \text{for } \gamma >> 1.$$

In fact, the error induced by neglecting the second term entirely is less than 7% for all values of γ (see Table X).

Let this approximate form of $H(\gamma,0)$ be denoted by $H_a(\gamma,0)$, viz.,

$$H_a(\gamma,0) = \frac{\pi}{4} h(\gamma/0.106\sqrt{\pi}). \quad (233)$$

The total absorption $A_{N.O.}$ of a branch of non-overlapping lines may be expressed, approximately, in terms of $H_a(\gamma,0)$, viz.,

$$A_{N.O} \simeq (kT/hcB''_e)^{1/2}(2b_D/\sqrt{\ln 2})\, H_a(\gamma,0). \quad (234)$$

For a branch whose head forms at the origin, Eq. (234) may be written as

$$A_{N.O} \simeq \frac{\Delta\omega}{q_o}\,\frac{4b_D}{\sqrt{\ln 2}}\, H_a(\gamma,0) \quad (235)$$

or

$$A_{N.O.} = \frac{\Delta\omega}{q_o}\,\frac{\pi b_D}{\sqrt{\ln 2}}\, h\left(\frac{\sqrt{\ln 2}}{\pi}\,\frac{\alpha X}{\Delta\omega}\,\frac{q_o}{b_D}\right) \quad (236)$$

where we have introduced the notation

$$\Delta\omega = \Delta B kT/hcB''_e \tag{237}$$

and

$$q_o = 2\Delta B \sqrt{kT/hcB''_e} \ . \tag{238}$$

Equation (236) may be rewritten as

$$A_{N.C.} = a''\Delta\omega h(\alpha X/a''\Delta\omega) \tag{239}$$

where we have defined a parameter a'' by

$$a'' = \frac{\pi}{\sqrt{\ln 2}} \frac{b_D}{q_o} = 0.601\ (2\pi b_D/q_o). \tag{240}$$

The parameter a'' measures the degree of overlapping of adjacent lines and is, for the case considered here, small compared to unity.

It is of interest to calculate the total absorption of a branch when the lines are well overlapped and the band head forms at the branch origin. In this case the absorption coefficient is

$$P(\omega) = (\alpha/\Delta\omega) \exp(-|\omega-\omega_o|/\Delta\omega) \tag{241}$$

and the total absorption becomes

$$A_O = \int_{\omega_o}^{\infty} \left\{ 1-\exp\left[(\alpha X/\Delta\omega)e^{-|\omega-\omega_o|/\Delta\omega}\right] \right\} d\omega \tag{242}$$

or

$$A_O = \Delta\omega h(\alpha X/\Delta\omega). \tag{243}$$

Elsasser[40] has calculated the spectral absorption coefficient for a series of equally spaced equally intense spectral lines with dispersion contour, viz.,

$$P(\omega) = \frac{(S/q)\tanh(2\pi b_c/q)}{1 - \dfrac{\cos(2\pi\omega/q)}{\cosh(2\pi b_c/q)}} \quad . \tag{244}$$

Here S is the intensity per line, q the line spacing and b_c is the collision (semi) half width. Reference to Eq. (244) shows that the dependence on line width occurs only through the terms $\tanh(2\pi b_c/q)$ and $\cosh 2\pi b_c/q$. In analogy with this result we may postulate an expression for the total absorption of a branch with band head at the origin for arbitrary values of a" which agrees with Eq. (239) for $a'' \ll 1$ and with Eq. (243) for $a'' \gg 1$, viz.,

$$A = \Delta\omega \tanh a'' \left[h(\alpha X/\Delta\omega \tanh a'') \right] . \tag{245}$$

Utilizing this analytic expression for A the mean value of $A = \bar{A}$ for an exponential distribution of intensities may be calculated. The result is

$$\bar{A} = \int_0^\infty \frac{\exp(-\alpha/\bar{\alpha})}{\bar{\alpha}} A\, d\alpha$$

$$= \frac{\Delta\omega \tanh a''}{\bar{\alpha}} \int_0^\infty \exp\left[-\alpha/\bar{\alpha}\right] h(\alpha X/\Delta\omega \tanh a'')\, d\alpha \tag{246}$$

or

$$A = \Delta\omega \tanh a'' \ln\left[1 + (\bar{\alpha} X/\Delta\omega \tanh a'')\right] \tag{247}$$

The mean emissivity $\bar{\varepsilon}$ for a random distribution of branches with mean spacing δ is given by

$$\bar{\varepsilon} = 1 - \exp\left[-\frac{\bar{A}}{\delta}\right] \tag{248}$$

or, for an exponential intensity distribution,

$$\bar{\varepsilon} = 1 - \left[1 + (\bar{\alpha}X/\Delta\omega \tanh a'')\right]^{-\Delta\omega(\tanh a'')/\delta} . \qquad (249)$$

f. The Total Emissivity of a Band System in Which the Bands are Distributed Statistically

The mean spectral emissivity $\bar{\varepsilon}_\omega$ for a random distribution of bands with a mean separation δ is given by the expression

$$\bar{\varepsilon}_\omega = 1 - \exp\left\{-\frac{\bar{A}_{band}}{\delta}\right\} . \qquad (250)$$

Here $\bar{A}_{band}$ is the mean value of the total absorption of an isolated band averaged over the possible intensities, i.e.,

$$\bar{A}_{band} = \int_0^\infty \mathcal{P}(\alpha, \bar{\alpha}) A_{band} d\alpha \qquad (251)$$

where $\mathcal{P}(\alpha, \bar{\alpha})d\alpha$ is the probability that a band has an intensity between α and $\alpha + d\alpha$ and $\bar{\alpha}$ is the mean intensity. In terms of the function $H(\gamma, a)$, $\bar{A}_{band}$ becomes

$$\bar{A}_{band} = 2b_D n(kT/hcB''_e \ln 2)^{1/2} \int_0^\infty \mathcal{P}(\gamma, \bar{\gamma}) H(\gamma, a) d\gamma \qquad (252)$$

where

$$\bar{\gamma} = (0.212\bar{\alpha}X/nb_D)(hcB''_e \ln 2/\pi kT)^{1/2} .$$

The integral appearing in Eq. (252) had been evaluated numerically for the special case a = 0 and $\mathcal{P}(\alpha, \bar{\alpha}) = (1/\bar{\alpha}) \exp(-\alpha/\bar{\alpha})$. The mean emissivity for a = 0 is then given by

$$\bar{\mathcal{E}}_{\omega} = 1-\exp\left\{-\frac{2nb_D}{\delta}(kT/hcB''_e\ln 2)^{1/2}\left[1-\mathcal{E}(\bar{\gamma})\right]H(\bar{\gamma},0)\right\} \tag{253}$$

where

$$1-\mathcal{E}(\bar{\gamma}) = H(\bar{\gamma},0)^{-1}\int_0^{\infty}\exp(-\gamma/\bar{\gamma})H(\gamma,0)\,d\gamma/\bar{\gamma}).$$

The function $1-\mathcal{E}(\bar{\gamma})$ is plotted in Fig. 20.

The choice of the appropriate distribution function $\rho(\alpha,\bar{\alpha})$, and of the values of $\bar{\alpha}$ and δ to be used in the emissivity computations must be made with reference to the vibrational matrix elements of the particular band system in question.

g. The Total Emissivity of the NO β- and γ-Band Systems (at 8000°K)

In this section we apply the results of the preceding sections to the NO β- and γ-band systems. We first outline the determination of the distribution function $\rho(\alpha,\bar{\alpha})$, the mean intensity $\bar{\alpha}(\omega)$ and the mean band spacing δ.

Utilizing the approximate relation

$$\frac{N_{v''}}{N_T} = \frac{\exp(-hcF''/kT)}{Q_v} \tag{254}$$

where

$$F'' = (\omega''_e-\omega''_e x''_e+\tfrac{3}{4}\omega''_e y''_e)v''+(\omega''_e x''_e-\tfrac{3}{2}\omega''_e y''_e v''^2-\omega''_e y''_e v''^3,$$

and

$$Q_v = \sum_{v''=0}^{\infty}\exp(-hcF''/kT),$$

the emission intensity $\alpha_{v''v'}$ may be written as[59]

$$\alpha_{v''v'} = 2.38(10^7)\,\frac{273.1}{T}\; f_{elec}(\omega/\omega_{oo})\,q^2_{v''v'}\left[\exp(-hcF''/kT)\right](Q_v)^{-1}. \tag{255}$$

The wave number ω is related to the term values of the upper and lower states by the expression

$$\omega = F' - F'' \tag{256}$$

where the term value F' of the upper state is given by

$$F' = \omega_{oo} + (\omega'_e - \omega'_e x'_e + \tfrac{3}{4}\omega'_e y'_e)v' + (\omega'_e x'_e - \tfrac{3}{2}\omega'_e y'_e)v'^2 - \omega'_e y'_e v'^3.$$

Thus, at the wave number ω, $\alpha_{v''v'}$ is given by

$$\alpha_{v''v'} = 2.38(10^7)\,\frac{273.1}{T}\; f_{elec}(\omega/\omega_{oo})(Q_v)^{-1}\beta_{v''v'} \tag{257}$$

with

$$\beta_{v''v'} = q^2_{v''v'} \exp\left[-hc(\omega_{oo}-\omega)/kT\right] \exp\left[-hc(F'-\omega_{oo})/kT\right]. \tag{257a}$$

For the β-bands of NO we have evaluated the parameter $\beta_{v''v'}$ for each value of v'' and v' from the tables of $q^2_{v''v'}$ given by Bethe, Kivel and Mayer[26] (see Table XIII). For several different values of ω, the values of $\beta_{v''v'}$ at 8000°K for $v'' = v''_o(\omega, v') \pm 0,1$ and $v' = 0,1,\ldots,6$ have been ordered in terms of decreasing magnitude and plotted against N, where N is the ordering parameter, i.e., $N=1,\ldots,21$ (see Figs. 15 to 18). Here $v''_o(\omega, v')$ is the value of the vibrational quantum number of the lower state of the transition whose wavenumber is ω and whose upper vibrational state is v'. Reference to Figs. 15 to 18 shows that, for moderate values of β,

$$N \sim N_o \exp(-\beta/\bar{\beta}_{v' \leq 6}) \tag{258}$$

where $\bar{\beta}_{v' \leq 6}$ denotes the mean value of $\beta_{v''v'}$ at the wave number ω for $0 \leq v' \leq 6$. Thus, at the wavenumber ω the intensities of the bands for which $v' \leq 6$ may be considered to be distributed according to the probability function

$$\mathcal{P}(\beta, \bar{\beta}_{v' \leq 6}) \equiv N_o^{-1}(dN/d\beta) \simeq (1/\bar{\beta}_{v' \leq 6}) \exp(-\beta/\bar{\beta}_{v' \leq 6}). \tag{259}$$

In Fig. 18, $\bar{\beta}_{v' \leq 6}$ is plotted as a function of ω. Reference to Fig. 18 shows that, approximately,

$$\bar{\beta}_{v' \leq 6} \simeq 0.031 \exp\left[-hc(\omega_{oo} - \omega)/k(8000)\right]. \tag{260}$$

In terms of the matrix elements $q^2_{v''v'}$, the mean value of $\beta_{v''v'}$ for the N-bands for which $v' \leq N-1$ is given by the approximate expression

$$\bar{\beta}_{v' \leq N-1} = (N)^{-1} \exp\left[-hc(\omega_{oo} - \omega)/kT\right] \sum_{v'=0,\, v''=v''_o(\omega, v')}^{v'=N-1} q^2_{v''v'}$$

$$\exp\left[-hc(\omega'_e v'/kT\right]. \tag{261}$$

Comparison of Eqs. (260) and (261) shows that, at $T = 8000^{\circ}K$,

$$\frac{1}{7} \sum_{v'=0,\, v''=v''_o(\omega, v')}^{v'=6} q^2_{v''v'} \exp\left[-hc(\omega'_e v'/kT\right] \simeq 0.031 \tag{262}$$

for values of $\omega > 15000$ cm^{-1}. In Eqs. (261) and (262) we have made the approximation

$$F' = \omega_{oo} \sim \omega'_e v'. \qquad (263)$$

In order to obtain a tractable procedure for calculating the spectral emissivity we shall assume that in any small wavenumber interval, the band intensities $\alpha_{v''v'}$ (which are proportional to the parameters $\beta_{v''v'}$) are distributed statistically according to the distribution function $\beta\left[\alpha, \bar{\alpha}(\omega)\right] = \left[\bar{\alpha}(\omega)\right]^{-1} \exp\left[-\alpha/\bar{\alpha}(\omega)\right]$ where $\bar{\alpha}(\omega)$ is the mean intensity at the wavenumber ω. The choice of an exponential distribution of intensities implies that, within the given wavenumber interval, only a finite number of bands contribute to the emissivity, i.e., the very weak bands are ignored. However, for NO, these weak bands contribute negligibly to the emissivity since, for optical densities large enough for their contributions to be significant, the overlapping of neighbouring lines of the stronger bands is sufficient to blacken the spectrum.

The number of contributing bands per unit wavenumber (i.e., the reciprocal of the mean band spacing δ) may be estimated by reference to the values of the vibrational overlap integrals (see Table XIII). Reference to Table XIII shows that the "local mean value"* of the overlap integrals $q^2_{v''v'}$ of the β-bands is not a strong function of v'' or v' for $\omega_{v''v'} > 15000\ cm^{-1}$, at least within the limits of the table. Indeed, Eq. (262) indicates that the (weighted) mean value of $q^2_{v''v'}$ at the wave

* The "local mean value" of $q^2_{v''v'}$ at $v''=v_1''$ and $v'=v_1'$ may be (arbitrarily) defined as the arithmetic mean value of $q_{v''v'}$ for $v''=v_1'' \pm 0,1$ and $v'=v_1' \pm 0,1$.

number ω for $v' \leq 6$ is roughly independent of ω for wavenumbers greater than 15000 cm^{-1}. Thus we may obtain an approximate estimate of the mean band spacing by evaluating the distribution of intensities which obtains when a uniform value of $q^2_{v''v'} = \overline{q^2}$ is assigned to all transitions. By requiring that this distribution approximate an exponential distribution we obtain values for $\overline{\alpha}(\omega)$ and δ.

For a uniform value of $q^2_{v''v'} = \overline{q^2}$ the parameter $\beta_{v''v'}$ is given, approximately, by

$$\beta_{v''v'} = \beta = \overline{q^2} \exp\left[-hc(\omega_{oo} - \omega)/kT\right] \exp\left[-hc\omega'_e v'/kT\right]. \tag{264}$$

In the wavenumber interval of width ω''_e centered at ω, the number of bands with intensities between β and $\beta + d\beta$ is given by

$$dN = N_o \exp(-\beta/\overline{\beta}) d(\beta/\overline{\beta}) \tag{265}$$

for an exponential intensity distribution and

$$dN = (kT/hc\omega'_e \beta) d\beta \tag{266}$$

for the distribution corresponding to a uniform value of $q^2_{v''v'}$. Here N_o denotes the total number of bands in the interval ($N_o = \omega'_e/\delta$) and $\overline{\beta}$ the mean value of the parameter β for the N_o bands. Equation (266) may be written as

$$dN = \left[kT/Chc\omega'_e\right] C'(\beta/\overline{\beta})^{-1} d(\beta/\overline{\beta}) \ . \tag{266a}$$

The parameter C' is to be chosen so that the distribution $C(\beta/\overline{\beta})^{-1}$ approximates the exponential distribution $\exp(-\beta/\overline{\beta})$ as well as possible for a moderate range of β, say $\overline{\beta}/2 \lesssim \beta \lesssim 2\overline{\beta}$. A satisfactory value is $C' = 0.30$. Comparison of Eqs. (265) and (266a) shows that

$$N_o = kT/\acute{C}hc\omega'_e$$

or

$$\delta = \acute{C}hc\omega''_e\omega'_e/kT. \tag{267}$$

The mean band intensity $\overline{\alpha}(\omega)$ may now be estimated. For a uniform value of $q^2_{v''v'}$, Eq. (262) reduces to

$$0.031 = \frac{1}{7}\overline{q^2}\left[\frac{1-\exp(-7hc\omega'_e/k(8000)}{1-\exp(-hc\omega'_e/k(8000)}\right]$$

or

$$\overline{q^2} = 0.031/0.613 = 0.0506.^* \tag{268}$$

The mean value of the parameter β at the wavenumber ω for a uniform value of $q^2_{v''v'}$ is given by Eq. (262) when $N = N_o = kT/\acute{C}hc\omega'_e$, viz.,

$$\overline{\beta}(\omega) \simeq \acute{C}\left[1-\exp(-\acute{C}^{-1})\right]\overline{q^2}\exp\left[-hc(\omega_{oo}-\omega/kT\right] = 0.29\,\overline{q^2}\exp\left[-hc(\omega_{oo}-\omega)kT\right]. \tag{269}$$

The mean band intensity is given by

$$\overline{\alpha}(\omega) = 2.38(10^7)\,\frac{273.1}{T}\,f_{elec}(\omega/\omega_{oo})\,\Omega^{-1}_v\,\overline{\beta}(\omega). \tag{270}$$

If the concept of a uniform value of $q^2_{v''v'}$ is to be useful, then the inequality

$$\sum_{v'=0}^{N_o}\overline{q^2}_{v''v'} \simeq N_o\overline{q^2} < 1 \tag{271}$$

---

* For comparison, the arithmetic mean value of $q^2_{v''v'}$ for all transitions between 15400 cm^{-1} and 45440 cm^{-1} for which $v' \leq 6$ is 0.044.

must be satisfied. In other words, we may expect the exponential intensity distribution to be useful for emissivity calculations when the temperature is less than $hc\omega'_e/k\overline{q^2}$ (= 8900°K for the β-band system of NO).

Utilizing Eqs. (252), (269) and (270) we obtain for the mean value of $\overline{\gamma}$ for $\omega < \omega_{oo}$

$$\overline{\gamma} = (.29)(.212)(2.38)10^7 \,(hcB''_e \ell n 2/\pi kT)^{1/2} \omega \exp\left[-hc\omega_{oo} - \omega)/kT\right]$$

$$\frac{273.1}{T} f_{elec} \overline{q^2} X \left[1-\exp(-hc\omega''_e/kT\right] \qquad (272)$$

where we have evaluated the vibrational partition function by the harmonic oscillator approximation: $Q_v = \left[1-\exp(-hc\omega''_e/kT\right]^{-1}$. For $\omega > \omega_{oo}$, $\overline{\gamma}$ is given by Eq. (272) except that the exponential term $\exp\left[-hc(\omega_{oo}-\omega)/kT\right]$ is omitted.

For the β-bands of NO, $\overline{\gamma} = \overline{\gamma}_\beta$ becomes

$$\overline{\gamma}_\beta = 0.988(10^{11})(f_{elec_\beta} \overline{q^2_\beta} X/8T^2) \exp\left[-1.439(\omega_{oo}-\omega)/T\right]\left[1-\exp(-2720/T)\right]$$

$$\text{for } \omega < \omega_{oo} = 45440 \text{ cm}^{-1} \qquad (273)$$

and the mean total absorption at low pressure of an isolated band is given by from Eqs. (252) and (267)

$$(\overline{A}_{band}/\delta)_\beta = 0.951(10^{-12})\omega T^2\left[1-\varepsilon(\overline{\gamma}_\beta)\right] H(\overline{\gamma}_\beta, 0). \qquad (274)$$

For the γ-bands of NO

$$\overline{\gamma}_\gamma = 1.352(10^{11})(f_{elec_\gamma} \overline{q^2_\gamma} X/6T^2) \exp\left[-1.439(\omega_{oo}-\omega)/T\right]\left[1-\exp(-2720/T)\right]$$

$$\text{for } \omega < \omega_{oo} = 44,138 \text{ cm}^{-1}. \qquad (275)$$

Also

$$(\bar{A}_{band}/\delta)_\gamma = 0.312(10^{-12})\,\omega T^2\left[1-\varepsilon(\bar{\gamma}_\gamma)\right]H(\bar{\gamma}_\gamma, 0). \tag{276}$$

The mean emissivity for the superposition of the γ- and β-band systems is

$$\bar{\varepsilon}_\omega = 1-\exp\left[-\left(\frac{\bar{A}_{band}}{\delta}\right)_\gamma - \left(\frac{\bar{A}_{band}}{\delta}\right)_\beta\right]. \tag{277}$$

Finally, the overall hemispherical emissivity E at low pressure is given by

$$E = \frac{1}{6.4939}\int_0^\infty \frac{u^3}{e^u-1}\left[1-\exp\left\{-0.661(10^{-12})T^3u\left[\left[1-\varepsilon(\bar{\gamma}_\beta)\right]H(\bar{\gamma}_\beta, 0) + 0.33\left[1-\varepsilon(\bar{\gamma}_\gamma)\right]H(\bar{\gamma}_\gamma, 0)\right]\right\}\right]du \tag{278}$$

where $u = hc\omega/kT$. The total hemispherical emissivity E has been evaluated by numerical integration for various optical densities and various temperatures as a function of $\xi_\beta = 273.1\, f_{elec_\beta} X/2T$ (see Fig. 21). The emissivity E was also calculated for several cases assuming that the line structure was completely smeared out {in which case Eq. (278) applies with $\left[1-\varepsilon(\gamma)\right]H(\gamma, 0)$ replaced by 4.17γ}. At 8000°K the neglect of the line structure may introduce a 20% error, at 4000°K the error may be as much as 40%. The measurements of Weber and Penner [60,61] indicate that $f_{elec_\gamma} \simeq 0.025$ and $f_{elec_\beta} \simeq 0.008$. An appropriate estimate of $(\overline{q^2})_\gamma$ is 0.10. Thus it is expected that

$$(f_{elec}\overline{q^2})_\gamma \simeq 0.6(f_{elec}\overline{q^2})_\beta \tag{279}$$

(here equality would imply $\overline{\gamma}_\gamma = 1.08\overline{\gamma}_\rho$). In the calculations $\overline{\gamma}_\gamma$ was placed equal to $\overline{\gamma}_\rho$.

For small values of $\xi \equiv (273.1/T)K_{elec}X/2$, explicit expressions for the total emissivity E may be obtained. For ξ small, Eqs. (221), (227), (250) and (267) may be combined to yield the mean spectral emissivity of a single band system, viz.,

$$\overline{\varepsilon}_\omega = 2(2.38)(10^7)(\xi\overline{q^2}/\omega'_e)(\omega/\omega_{oo})\left[1-\exp(-1/\acute{C})\right]$$

$$\left\{\begin{array}{ll}\exp\left[-hc(\omega_{oo}-\omega)/kT\right] & \text{for } \omega<\omega_{oo}\\ 1 & \text{for } \omega>\omega_{oo}\end{array}\right\}\left\{\frac{1-\exp(-hc\omega''_e/kT)}{hc\omega''_e/kT}\right\}. \quad (280)$$

Thus, the overall hemispherical emissivity for a single band system is given, for $\xi \ll 1$ and $u_{oo} = hc\omega_{oo}/kT \gg 1$ by the approximate expression

$$E \simeq \frac{2\left[1-\exp(-1/\acute{C})\right](2.38)10^7}{6.4939}(\xi\overline{q^2}/\omega'_e)\left[\frac{1-\exp(-hc\omega''_e/kT}{hc\omega''_e/kT}\right]$$

$$\left\{\frac{e^{-u_{oo}}}{u_{oo}}\int_0^{u_{oo}} u^4du + \frac{1}{u_{oo}}\int_{u_{oo}}^{\infty} u^4e^{-u}\,du\right\}$$

$$\simeq \frac{2\left[1-\exp(-1/\acute{C})\right](2.38)10^7}{6.4939}(\xi\overline{q^2}/\omega'_e)\left[\frac{1-\exp(-hc\omega''_e/kT)}{hc\omega''_e/kT}\right]\exp(-u_{oo})$$

$$\left\{\frac{u_{oo}^4}{5} + u_{oo}^3 + 4u_{oo}^2 + 12u_{oo} + 24 + \frac{24}{u_{oo}}\right\}. \quad (281)$$

The total emissivity of the γ- and β-band systems may be obtained, for small values of ξ, by adding the individual contributions of the γ- and β-band systems, viz.,

$$E = E_\gamma + E_\beta$$

where E_γ and E_β are given by Eq. (281) when appropriate values of the parameters are substituted.

In Fig. 21 we have also plotted values of the emissivity of NO at 8000°K taken from the paper of Kivel, Mayer and Bethe.* Reference to Fig. 21 shows that their estimates of the emissivity of NO (when their electronic f-number of the β-system is normalized to the value used in this report) are about 50 percent higher than ours. This difference is in part due to our use of a relatively smaller value of the electronic f-number of the γ-system (0.0025 as compared to 0.008 for the β-system; Kivel et al used $f_{elec_\gamma} = f_{elec_\beta}$) and in part due to the different analytical procedure.

In Fig. 22 we have plotted the partial emission spectrum of the β-bands of NO at 8000°K which obtains at low optical densities when the rotational fine structure is smeared out (i.e., high pressure). Only transitions from the first six upper vibrational states are included. The

---

* When comparing the results of the present paper with those of Kivel et al, one must remember that Kivel presents the emissivity of a flat layer of NO whereas our hemispherical emissivity describes the radiant emission from a hemisphere. Kivel uses the value $1.8\,l$ as the effective mean hemispherical radius of a layer of NO of transverse thickness l cm. Thus our parameter ξ_β is related to Kivel's parameter η by the expression

$$\xi_\beta = 1.8\eta .$$

contribution to the spectral absorption coefficient from each band was computed according to Eq. (215) utilizing Eqs. (257) and (257a) to obtain the integrated intensities from the values of the vibrational overlap integrals listed by Kivel, Mayer and Bethe.[26] In Figs. 23 and 24 we have plotted the "smoothed" spectral radiancy of the β-bands of NO at 4000°K and 8000°K as a function of wavenumber corresponding to the mean spectral emissivity given by Eqs. (273), (274) and (277) when f_{elec_γ} is set equal to zero.

The procedure outlined in this report should be useful for estimating the ultraviolet emissivity of molecules whose spectra contains a large number of bands. Molecules whose equilibrium internuclear distance is appreciably different in the upper and lower states will usually generate such spectra. Typical examples of such band systems are the Vegard-Kaplan bands of N_2, the Schumann-Runge bands of O_2 and the second negative bands of O_2^+. For each molecule the appropriate distribution function $\mathcal{P}[\alpha, \alpha(\omega)]$ and the mean intensity $\bar{\alpha}(\omega)$ must be determined by specific reference to the relevant vibrational overlap integrals.

The emissivity of a mixture of gases whose spectra overlap may be computed by the method outlined in Section III for overlapping band systems. Thus, the total mean spectral emissivity $\bar{\varepsilon}_\omega$ of a mixture of N species is given by

$$\bar{\varepsilon}_\omega = 1 - \exp\left[- \sum_{i=1}^{N} \left[\varepsilon_{\omega_i} \right]_{\text{non-overlapping}} \right] \tag{282}$$

where $\left[\varepsilon_{\omega_i}\right]_{\text{non-overlapping}}$ is the emissivity of the i'th species computed assuming no overlapping occurs among the bands belonging to that species. Hence, the overall emissivity is

$$E = \int_0^\infty \left[R^o_\omega / \sigma T^4\right] \bar{\varepsilon}_\omega \, d\omega \, . \tag{283}$$

The integral appearing in Eq. (283) must generally be evaluated numerically.

REFERENCES

1. S. S. Penner and A. Thomson, "Determination of Equilibrium Infrared Emissivities from Spectroscopic Data", Technical Report No. 25 , Contract Nonr-220(03), NR 015 401, California Institute of Technology, Pasadena 1957.

2. M. Planck, The Theory of Heat Radiation, translated by M. Masius, P. Blakiston's Son and Co., Philadelphia 1914, Chapter II.

3. L. Page, Introduction to Theoretical Physics, D. Van Nostrand Co., New York 1935, pp. 546-550.

4. For a derivation of the Planck blackbody distribution law see, for example, J. E. Mayer and M. G. Mayer, Statistical Mechanics, John Wiley and Sons, New York 1940, pp. 363-372.

5. Planck Radiation Functions and Electronic Functions, Federal Works Agency, WPA, National Bureau of Standards (1941).

6. W. E. Forsythe, Chapter I on "Fundamental Concepts and Radiation Laws" in Measurements of Radiant Energy, McGraw-Hill Book Co., New York 1937.

7. A. Einstein, Physik. Z. 18, 121 (1917).

8. See, for example, A. Unsöld, Physik der Sternatmosphären, J. W. Edwards, Ann Arbor 1948, pp. 170-174.

9. V. Weisskopf and E. Wigner, Z. Physik 63, 54 (1930).

10. Unsöld, loc. cit., pp. 176-178.

11. H. A. Lorentz, Versl. Amsterd. Akad. 14, 518, 577 (1905).

12. W. Lenz, Z. Physik 25, 299 (1924); 80, 423 (1933).

13. V. Weisskopf, Z. Physik 85, 451 (1933).

14. V. Weisskopf, Observatory 56, 291 (1933).

15. P. W. Anderson, Phys. Rev. 76, 647 (1949).

16. J. H. Van Vleck and H. Margenau, Phys. Rev. 76, 1211 (1949).

17. L. H. Aller, Astrophysics, The Ronald Press Co., New York 1953, pp. 308-318.

18. A. C. Kolb, "Theory of Hydrogen Line Broadening in High-Temperature Partially Ionized Cases", Report 2189-3-T, University of Michigan, Engineering Research Institute, Ann Arbor 1957.

19. B. Kivel, S. Bloom, and H. Margenau, Rev. Mod. Phys. 8, 41 (1936).

20. See, for example, S. S. Penner and R. W. Kavanagh, J. Opt. Soc. Am. 43, 385 (1953).

21. A. C. G. Mitchell and M. W. Zemansky, Resonance Radiation and Excited Atoms, Cambridge University Press, Cambridge 1934, Appendix I.

22. E. M. F. van der Held, Z. Physik 70, 508 (1931).

23. A. Thomson, "Calculation of Dipole Moments and Absolute Intensities of HF, HCl, and HBr", Technical Report No. 24, Contract Nonr-220(03), NR 015 401, California Institute of Technology, Pasadena, April 1957.

24. B. L. Crawford, Jr., and H. L. Dinsmore, J. Chem. Phys. 18, 983, 1682 (1950).

25. W. R. Jarmain, P. A. Fraser and R. W. Nicholls, Astrophys. J. 118, 228 (1953); Astrophys. J. 122, 55 (1955).

26. B. Kivel, H. Mayer and H. Bethe, Annals of Phys. 2, 57 (1957).

27. G. Herzberg, Infrared and Raman Spectra, 2nd Ed., D. Van Nostrand Co., Inc., Princeton.

28. P. C. Cross, R. M. Hainer, and G. W. King, J. Chem. Phys. 12, 210 (1944).

29. S. S. Penner, J. Chem. Phys. 19, 272, 1434 (1951).

30. D. Kastler, Comptes Rendus, 232, 2324 (1951).

31. C. A. Coulson, Valence, The Clarendon Press (Oxford) 1952, p. 71.

32. R. S. Mulliken, C. A. Rieke, P. Orloff and H. Orloff, J. Chem. Phys. 17, 1248 (1949).

33. J. C. Slater, Phys. Rev. 36, 57 (1930).

34. L. Pauling, Nature of the Chemical Bond, Cornell University Press, Ithaca 1939, pp. 51, 338.

35. S. S. Penner and D. Weber, J. Chem. Phys. 21, 649 (1953).

36. J. O. Hirschfelder, C. F. Curtiss and R. B. Bird, Molecular Theory of Gases and Liquids, John Wiley and Sons, Inc., New York 1954, pp. 946-954.

37. P. Debye, Polar Molecules, Dover Publications, Inc., New York 1929, p. 61.

38. A. Jucys, Proc. Roy. Soc. 173A, 59 (1939).

39. J. E. Mayer and M. G. Mayer, Statistical Mechanics, John Wiley and Sons, New York 1940, Chapter 7.

40. W. M. Elsasser, Harvard Meteorological Studies No. 6, Milton, Mass, (1942).

41. H. Mayer, "Methods of Opacity Calculations", Los Alamos Scientific Laboratory, Technical Report No. LA-647, (1948).

42. R. M. Goody, Quart. J. Roy. Met. Soc. 78, 165 (1952).

43. R. M. Goody, The Physics of the Stratosphere, Cambridge University Press, Cambridge 1954, pp. 161-163.

44. S. S. Penner and A. Thomson, J. Appl. Phys. 28, 614 (1957).

45. (a) S. S. Penner, J. Appl. Phys. 21, 685 (1950); (b) J. Appl. Mech. 18, 53 (1951); (c) S. S. Penner and D. Weber, J. Appl. Phys. 22, 1164 (1951).

46. H. C. Hottel and R. B. Egbert, Trans. Am. Inst. Chem. Eng. 38, 531 (1942); H. C. Hottel and H. G. Mangelsdorf, Trans. Am. Inst. Chem. Eng. 31, 517 (1935).

47. A. Thomson, "Radiant Emission from Non-isothermal Water Atmospheres Computed from Isothermal Emissivity Data", Technical Note No. 2, Gruen Applied Science Labs., Pasadena (September 1956).

48. See, for example, H. A. Lorentz, Proc. Amst. Akad. Sci. 8, 59 (1906); W. Lenz, Z. Physik 80, 423 (1933); V. F. Weisskopf, Physik. Z. 34, 1 (1933); E. Lindholm, Arkiv. Mat. Astron. Fysik 32, 17 (1945); J. H. Van Vleck and V. F. Weisskopf, Revs. Modern Phys. 17, 227 (1945); J. H. Van Vleck and H. Margenau, Phys. Rev. 76, 1211 (1949); P. W. Anderson, Phys. Rev. 76, 647 (1949); H. Margenau, Phys. Rev. 82, 156 (1951);

49. S. S. Penner and D. Weber, J. Chem. Phys. 19, 807 (1951).

50. S. S. Penner and D. Weber, J. Chem. Phys. 21, 649 (1953).

51. D. Weber, R. J. Holm and S. S. Penner, J. Chem. Phys. 20, 1820 (1952).

52. D. Weber and S. S. Penner, J. Chem. Phys. 21, 1503 (1953).

53. (a) S. S. Penner, M. Ostrander, and H. S. Tsien, J. Appl. Phys. 23, 256 (1952); (b) S. S. Penner, J. Appl. Phys. 23, 825 (1952).

54. S. S. Penner, J. Appl. Phys. 25, 660 (1954).

55. A. Thomson, "An Approximate Analytic Expression for the Engineering Emissivity of Water Vapor", Technical Note No. 4, Gruen Applied Science Labs., Pasadena (April 1957).

56. T. G. Cowling, Phil. Mag. 41, 109 (1950).

57. J. N. Howard, D. L. Burch and D. Williams, Geophysical Research paper No. 40, AFRC-TR-55-213, Ohio State University, (Nov. 1955).

58. W. H. McAdams, Heat Transmission, Chapter III by H. C. Hottel, McGraw-Hill Book Co., New York 1952.

59. See, for example, S. S. Penner and E. K. Björnerud, J. Chem. Phys. 23, 143 (1955).

60. D. Weber and S. S. Penner, "Absolute Intensities for the Ultraviolet γ-bands of NO", Technical Report No. 18, Contract Nonr-220(03), NR 015 401, California Institute of Technology, Pasadena, April 1956.

61. D. Weber, "Approximate Estimates for Several Ultraviolet β-bands of NO", Technical Report No. 23, Contract No. Nonr-220(03), NR 015 401, California Institute of Technology, Pasadena, March 1957.

62. G. Herzberg, Spectra of Diatomic Molecules, 2nd ed., D. Van Nostrand Company, Inc., New York 1950.

63. R. W. Kavanagh and S. S. Penner, J. Opt. Soc. Am. 43, 383 (1953).

64. S. S. Penner, J. Appl. Phys. 21, 685 (1950).

65. S. S. Penner, J. Appl. Mech. 18, 53 (1951).

66. S. S. Penner and D. Weber, J. Appl. Phys. 22, 1164 (1951).

67. S. S. Penner, "Infrared Emissivity of Diatomic Gases" in National Bureau of Standards Circular No. 523 on Energy Transfer in Hot Gases, Washington (1954).

68. S. S. Penner, M. H. Ostrander and H. S. Tsien, J. Appl. Phys. 23, 256 (1952).

69. S. S. Penner, J. Appl. Phys. 23, 825 (1952).

70. S. S. Penner and A. Thomson, "Infrared Emissivities and Absorptivities of Gases", Technical Report No. 21, Contract Nonr-220(03), NR 015 401, California Institute of Technology, Pasadena, August 1956 (this report has been published in J. Appl. Phys. - see ref. 44).

71. A. Thomson, "Emissivity Estimates for Heated NO", Technical Report No. 6, Contract AF 18(603)-2, California Institute of Technology, Pasadena, November 1957.

TABLE I

Parameters occurring in the Slater wave functions for the hydrogen halides

	HF	HCl	HBr
Z	9	17	35
Z^*	5.20	6.10	7.60
n^*	2.0	3.0	3.7
r_e, cm	0.917×10^{-8}	1.275×10^{-8}	1.414×10^{-8}
r_e/a_H	1.73	2.40	2.66

TABLE II

Numerical values of various integrals for the hydrogen halides

	HF	HCl	HBr
$(i \mid \psi)$	.456	.659	.696
$(i \mid \varphi)$	.629	.693	.694
$(\psi \mid \varphi)$	.286	.457	.483
$(\psi \mid z \mid \psi) a_H^{-1}$*	1.863	2.33	2.51
$(\varphi \mid z \mid \varphi) a_H^{-1}$	1.350	1.609	1.70
$(\psi \mid z \mid \varphi) a_H^{-1}$	-.1107	+.044	+.0705
$(i \mid z \mid \psi) a_H^{-1}$	.340	.658	.782
$(i \mid z \mid \varphi) a_H^{-1}$	.1299	.191	.199
$(s \mid h)$	.474	.503	.490
$(p \mid h)$	.299	.460	.493
$(s \mid z \mid h) a_H^{-1}$	.264	.595	.723
$(p \mid z \mid h) a_H^{-1}$	.487	.960	1.133
$(s \mid z \mid p) a_H^{-1}$	.555	.995	1.182
$(i \mid \psi)' r_e$	-.417	-.630	-.682
$(i \mid \varphi)' r_e$	-.598	-.779	-.829
$(\psi \mid \varphi)' r_e$	-.545	-.960	-1.050
$(\psi \mid z \mid \psi)'$	-.862	1.068	1.143
$(\varphi \mid z \mid \varphi)'$	1.300	1.600	1.750
$(\psi \mid z \mid \varphi)'$	-.406	-.599	-.675

* z denotes $\sum_{i=1}^{N} z_i$.

TABLE II (continued)

	HF	HCl	HBr
$(i \mid z \mid \psi)'$	-.0870	+.0206	+.01311
$(i \mid z \mid \varphi)'$	-.00396	+.0790	+.1065
$(s \mid h)'r_e$	-.498	-.636	-.632
$(p \mid h)'r_e$	-.205	-.362	-.437
$(s \mid z \mid h)'$	-.0243	-.1018	-.1245
$(p \mid z \mid h)'$	-.204	-.219	-.252
$(s \mid z \mid p)'$	.000	.000	.000
$(i \mid \psi)'r_e/(i \mid \psi)$	-.915	-.957	-.980
$(i \mid \varphi)'r_e/(i \mid \varphi)$	-.951	-1.123	-1.192
$(\psi \mid \varphi)'r_e/(\psi \mid \varphi)$	-1.901	-2.10	-2.18

TABLE III

Percentage ionicities required to give agreement between calculated and observed values of the dipole moments for zero s-p hybridization (non-zero values of the s-p hybridization correspond to smaller ionicities).

Molecule	β (present study)	$\frac{100(\mu_{obs}-\mu_{cov})}{er_e}$ *	$\frac{100\,\mu_{obs}}{er_e}$ (Pauling)
HF	42%	51%	43%
HCl	4%	14%	17%
HBr	0.8%	5.4%	11%

* $\mu_{cov} = er_e - e\langle\psi\left|\sum_{i=1}^{N} z_i\right|\psi\rangle$

TABLE IV

The quantity $\frac{1}{e}\frac{\partial \mu}{\partial r_e}$ for different values of $(r_e\beta'/\beta)$ and for zero s-p hybridization ($\alpha=0$) when the ionic character (β) is chosen in such a way that the calculated dipole moments agree with the measured values.

$(r_e\beta'/\beta)=n$	$\left(\frac{1}{e}\frac{\partial \mu}{\partial r_e}\right)_{HCl}$	$\frac{1}{e}\left(\frac{\partial \mu}{\partial r_e}\right)_{HBr}$
0	-0.031	-0.122
-3	-0.10	-0.14
-5	-0.14	-0.15
-7	-0.18	-0.16
-9	-0.23	-0.17
Measured Values [12]	±0.198	±0.12

TABLE V

Atomic polarizabilities of various ions[37] (in Bohr radii).

O^- 10.5	F^- 5.67	N_e 2.60	N_a^+ 1.91	Mg^{++} 1.13
S^- 38.7	C 21.8	A 10.9	K^+ 7.35	C_a^{++} 5.14
	Br^- 30.5	K 16.6	R_b^+ 11.4	Sr^{++} 8.30
	I^- 47.6	Xe 27.2	C_s^+ 19.0	Ba^{++} 13.5

TABLE VI

Comparison of the functions g(u) and f(u)

u	f(u)	g(u)
0.0010	.0010	.0010
0.010	.0099	.00936
0.10	.0952	.0824
1.0	.674	.568
10.0	2.491	2.47

TABLE VII

Summary of absorptivity expressions

	Type of Molecule	Absorptivity (α)
1/2	Diatomic or linear molecule at low pressure	$E\left[T_s, \frac{T_s}{T_g} X\right]$
1	All molecules at high pressure	$\left(\frac{T_g}{T_s}\right)^{1/2} E\left[T_s, \left(\frac{T_s}{T_g}\right)^{3/2} X\right]$
3/2	Water vapor at low pressure	$\left(\frac{T_g}{T_s}\right) E\left[T_s, \left(\frac{T_s}{T_g}\right)^{2} X\right]$

TABLE VIII

Relevant spectroscopic constants for CO, HCl and CO_2

Molecule	α_F (cm^{-2}-atmos^{-1})	δ (cm^{-1})	$b_F^\dagger$ (cm^{-1})
CO (fundamental)[49]	$237\left(\frac{300}{T}\right)$	3.86	$0.1\,p(T/300)^{-1/2}$
HCl (fundamental)[50]	$160\left(\frac{300}{T}\right)$	21.2	$0.1\,p(T/300)^{-1/2}$
CO_2 (ν_3-fundamental)[51]	$2700\left(\frac{300}{T}\right)$	0.791	$0.1\,p(T/300)^{-1/2}$

† Representative experimental data suggest that $b_F \simeq 0.10\ cm^{-1}$ at 1 atmos and 300°K. See, for example, reference (52).

TABLE IX

Optical density limits X_u for CO, HCl and CO_2.

Molecule	T (^oK)	$\Delta\omega'$ (cm^{-1})	for $b/\delta = 0.1$ X_u (cm-atmos)	X_u at p=1 atmos (cm-atmos)
CO (fundamental)	300	239	74	370
	1000	436	820	7,700
	3000	756	7,400	114,000
HCl (fundamental)	300	560	35,000	700,000
	1000	1022	390,000	14,300,000
	3000	1722	3,500,000	220,000,000
CO_2 (ν_3-fundamental)	300	108	2.6	2.1
	1000	197	30	45
	3000	342	260	660

TABLE X

Comparison of the exact and approximate forms of $H(\gamma, 0)$

γ	$H(\gamma,0)_{approx.}$ *	$H(\gamma,0)_{exact}$ †	% error
0.01	0.041	0.041	0.0%
0.1	0.363	0.37	1.9%
1.0	1.89	1.97	4.1%
10	3.70	3.96	6.6%
100	5.52	5.83	5.3%

† Obtained by numerical integrations.

* $H(\gamma,0)_{approx.} \equiv \frac{\pi}{4} h(\gamma/0.106\sqrt{\pi})$

TABLE XI

The molecular constants of NO*

State	$\omega_{oo}(cm^{-1})$	$B_e(cm^{-1})$	$\Delta B^{\dagger}(cm^{-1})$	$\omega_e(cm^{-1})$	$\omega_e x_e(cm^{-1})$	$\omega_e y_e(cm^{-1})$
$X^2\Pi_r$	$\begin{Bmatrix}121\\0\end{Bmatrix}$	1.7046		1904	13.97	-.0012
$B^2\Pi_{1/2}$	45486	1.076	-.6286	1037	7.603	.0467
$B^2\Pi_{3/2}$	45394	1.177	-.5276	1038		
$A^2\Sigma$	43966	1.9952	.2906	2371	14.48	-.28

* All numerical values are taken from Herzberg.[62]

† $\Delta B \equiv B''_e - B'_e$

TABLE XIIa

Spectroscopic parameters of the β-band system of NO

T	b_D (cm^{-1}) at 25000 cm^{-1}	b_C (cm^{-1}) at 1 atmos*	$\Delta\omega$ (cm^{-1})		q_o (cm^{-1})	
			$\frac{1}{2}\ \frac{1}{2}$	$\frac{3}{2}\ \frac{3}{2}$	$\frac{1}{2}\ \frac{1}{2}$	$\frac{3}{2}\ \frac{3}{2}$
4000°K	0.103	0.027	1024	860	50.6	42.5
6000°K	0.126	0.022	1537	1290	62.0	52.0
8000°K	0.146	0.019	2028	1720	71.6	60.1

TABLE XIIb

Spectroscopic parameters of the γ-band system of NO

T	b_D (cm^{-1}) at 25000 cm^{-1}	b_C (cm^{-1}) at 1 atmos*	$\Delta\omega$ (cm^{-1})	q_o (cm^{-1})
4000°K	0.103	0.027	474	23.4
6000°K	0.126	0.022	711	28.8
8000°K	0.146	0.019	948	33.2

* These values of b_C correspond to the choice $b_C = 0.10\ cm^{-1}$ at 300°K and 1 atmos pressure.

TABLE XIIIa

Ovelap integrals $q^2_{v''v'}$ for the NO β-bands calculated by Kivel, Mayer and Bethe.[26]

v''	v''=0	1	2	3	4	5	6	7	8
0	0.0000	0.0002	0.0010	0.0032	0.0079	0.0161	0.0280	0.0429	0.0587
1	0.0003	0.0024	0.0087	0.0219	0.0414	0.0624	0.0778	0.0811	0.0707
2	0.0021	0.0119	0.0336	0.0619	0.0819	0.0803	0.0569	0.0257	0.0040
3	0.0086	0.0364	0.0735	0.0896	0.0680	0.0273	0.0016	0.0065	0.0286
4	0.0250	0.0750	0.0967	0.0607	0.0115	0.0025	0.0286	0.0471	0.0362
5	0.0554	0.1069	0.0693	0.0077	0.0100	0.0447	0.0448	0.0146	0.0001
6	0.0972	0.0120	0.0153	0.0121	0.0530	0.0371	0.0027	0.0097	0.0341
7	0.1380	0.0556	0.0041	0.0573	0.0363	0.0001	0.0231	0.0401	0.0170
8	0.1603	0.0075	0.0497	0.0489	0.0000	0.0317	0.0389	0.0055	0.0066
9	0.1522	0.0101	0.0756	0.0046	0.0629	0.0004	0.0567		
10	0.1276	0.0452	0.0391	0.0395	0.0286	0.0301	0.0299		
11	0.0964	0.0849	0.0059	0.0686	0.0006	0.0572	0.0003		
12	0.0657	0.1100	0.0033	0.0599	0.0158	0.0382	0.0198		
13	0.0405	0.1123	0.0318	0.0252	0.0515	0.0047	0.0506		
14	0.0226	0.0956	0.0704	0.0010	0.0619	0.0070	0.0399		
15	0.0113	0.0698	0.0962	0.0102	0.0363	0.0404	0.0070		
16	0.0051	0.0442	0.0985	0.0449	0.0057	0.0587	0.0046		
17	0.0021	0.0246	0.0816	0.0793	0.0036	0.0394	0.0361		
18	0.0007	0.0120	0.0565	0.0932	0.0329	0.0080	0.0557		
19	0.0002	0.0051	0.0334	0.0838	0.0693	0.0022	0.0374		
20	0.0001	0.0019	0.0169	0.0610	0.0881	0.0297	0.0068		
21		0.0006	0.0074	0.0369	0.0821	0.0663	0.0031		
22		0.0002	0.0028	0.0188	0.0603	0.0852	0.0326		
23			0.0009	0.0801	0.0361	0.0784	0.0685		

TABLE XIIIa (continued)

v''	v''=0	1	2	3	4	5	6	7	8
24				0.0030	0.0179	0.0559	0.0865		
25				0.0009	0.0074	0.0331	0.0727		
26					0.0026	0.0150	0.0486		
27					0.0007	0.0057	0.0258		
28						0.0018	0.0110		
29							0.0038		

	v'=9	10	11	12	13	14	15	16	17
v''=0	0.0731	0.0837	0.0892	0.0866	0.0841	0.0744	0.0601	0.0445	0.0303

	v'=18	19	20	21	22	23	24	25	26
v''=0	0.0190	0.0110	0.0059	0.0029	0.0013	0.0006	0.0002	0.0001	0.0000

TABLE XIIIb

Overlap integrals $q^2_{v''v'}$ for the NO γ-bands calculated by Kivel, Mayer and Bethe.[26]

v''	v'=0	1	2	3	4	5	6	7	8
0	0.1735	0.2555	0.2199	0.1426	0.0781	0.0390	0.0187	0.0090	0.0043
1	0.3170	0.0753	0.0465	0.0645	0.1070	0.0989	0.0700	0.0433	0.0253
2	0.2588	0.0659	0.0954	0.0340	0.0632	0.0464	0.0588	0.0625	0.0510
3	0.1247	0.1537	0.0589	0.0528	0.0414	0.0381	0.0735	0.0516	0.0349
4	0.0416	0.1601	0.1083	0.0298	0.0788	0.0310	0.0144	0.0532	0.0777
5	0.0147	0.0818	0.1117	0.1355	0.0155	0.0440	0.0717	0.0097	0.0149
6	0.0061	0.0351	0.0861	0.0992	0.0890	0.0528	0.0049	0.0703	0.0446
7	0.0017	0.0210	0.0437	0.0630	0.1704	0.0270	0.0792	0.0060	0.0351
8	0.0005	0.0071	0.0408	0.0368	0.0363	0.1899	0.0023	0.0631	0.0354
9	0.0001	0.0024	0.0176	0.0566	0.0218	0.0899	0.1543	0.0103	0.0271
10	0.0000	0.0007	0.0067	0.0314	0.0609	0.0075	0.1450	0.0942	0.0292

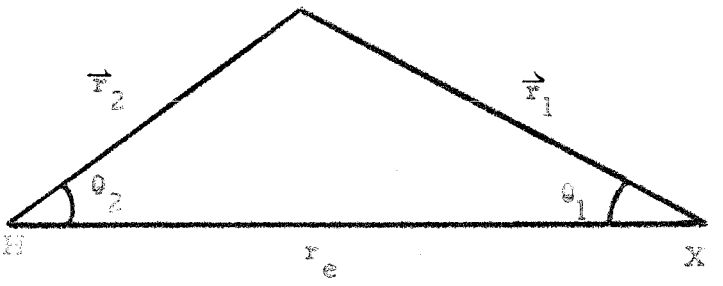

Fig. 1. Geometry of the molecule HX.

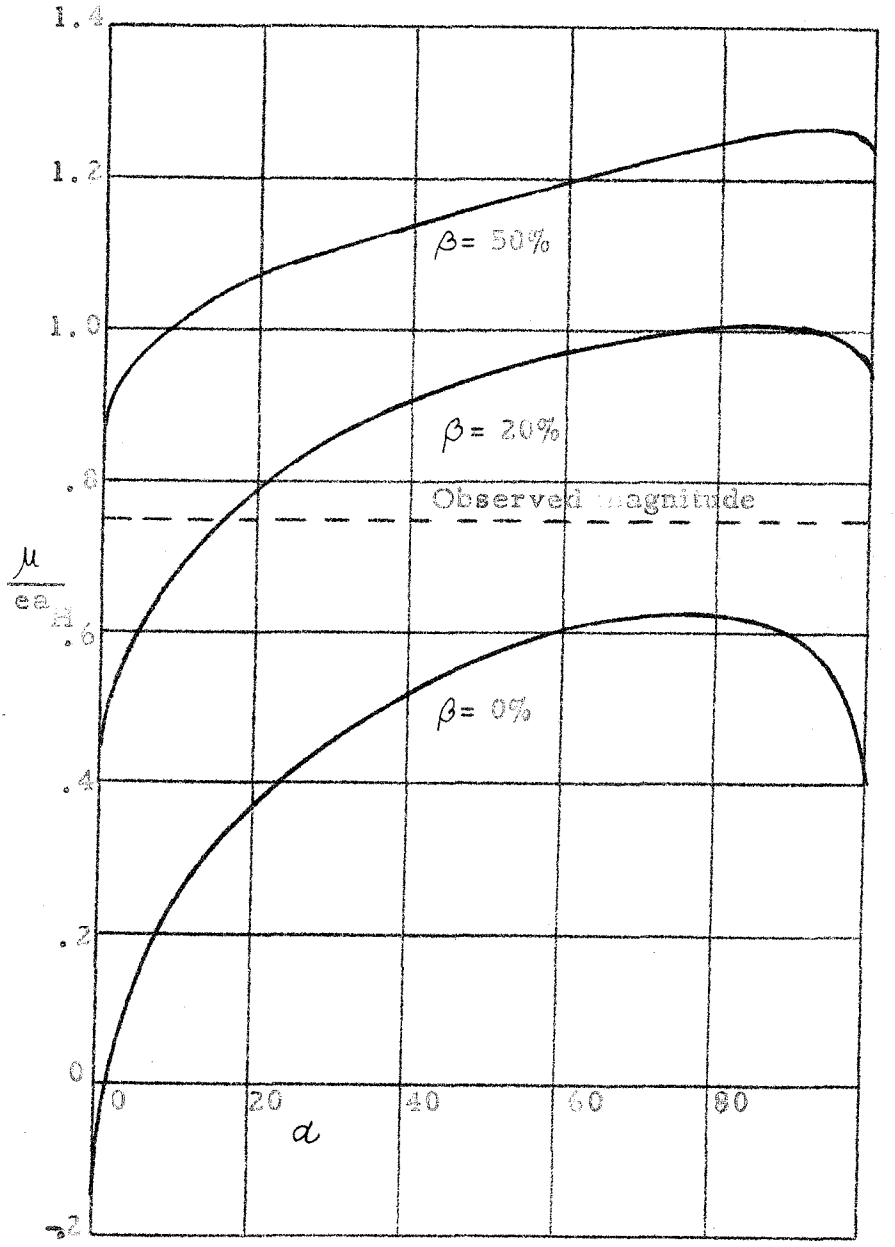

Fig. 2. The reduced dipole moment μ/ea_H of HF as a function of percentage s-p hybridization for different ionicities.

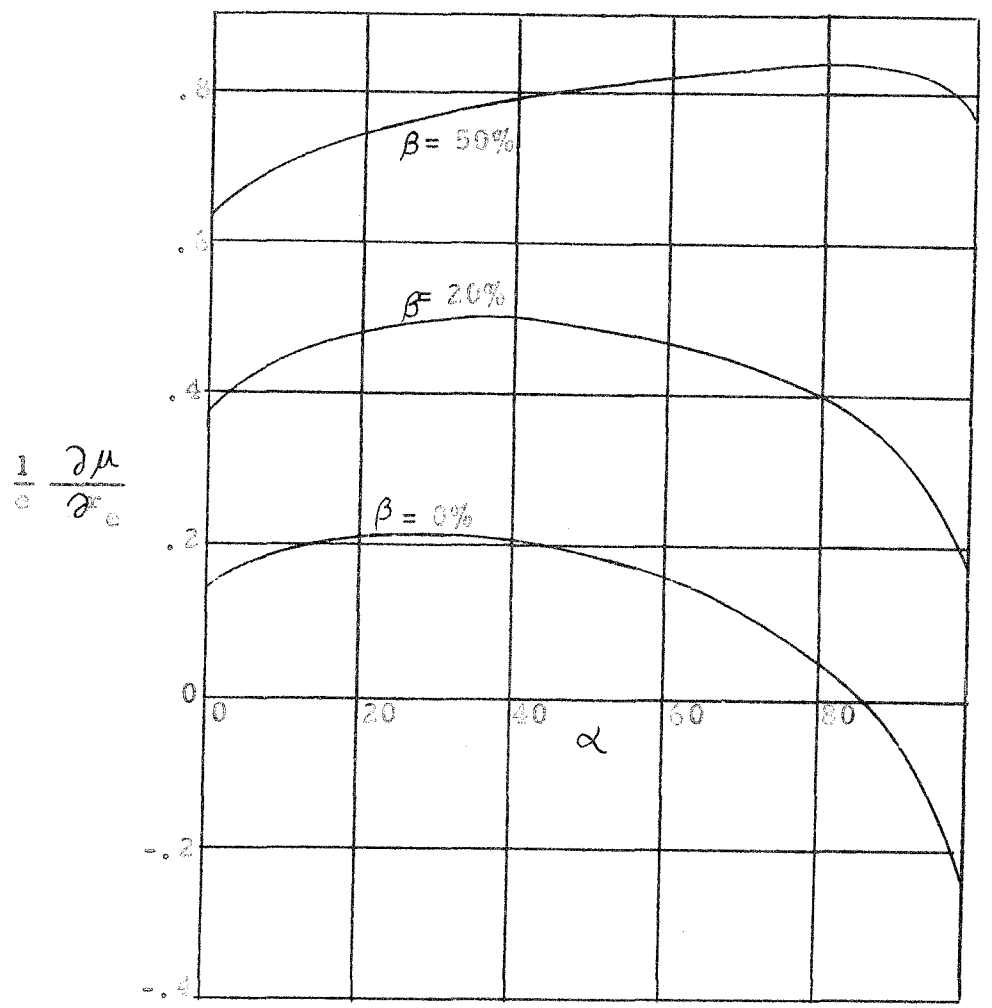

Fig. 3. The reduced effective charge $\frac{1}{e}\frac{\partial \mu}{\partial r_e}$ of HF as a function of the percentage s-p hybridization for different ionicities.

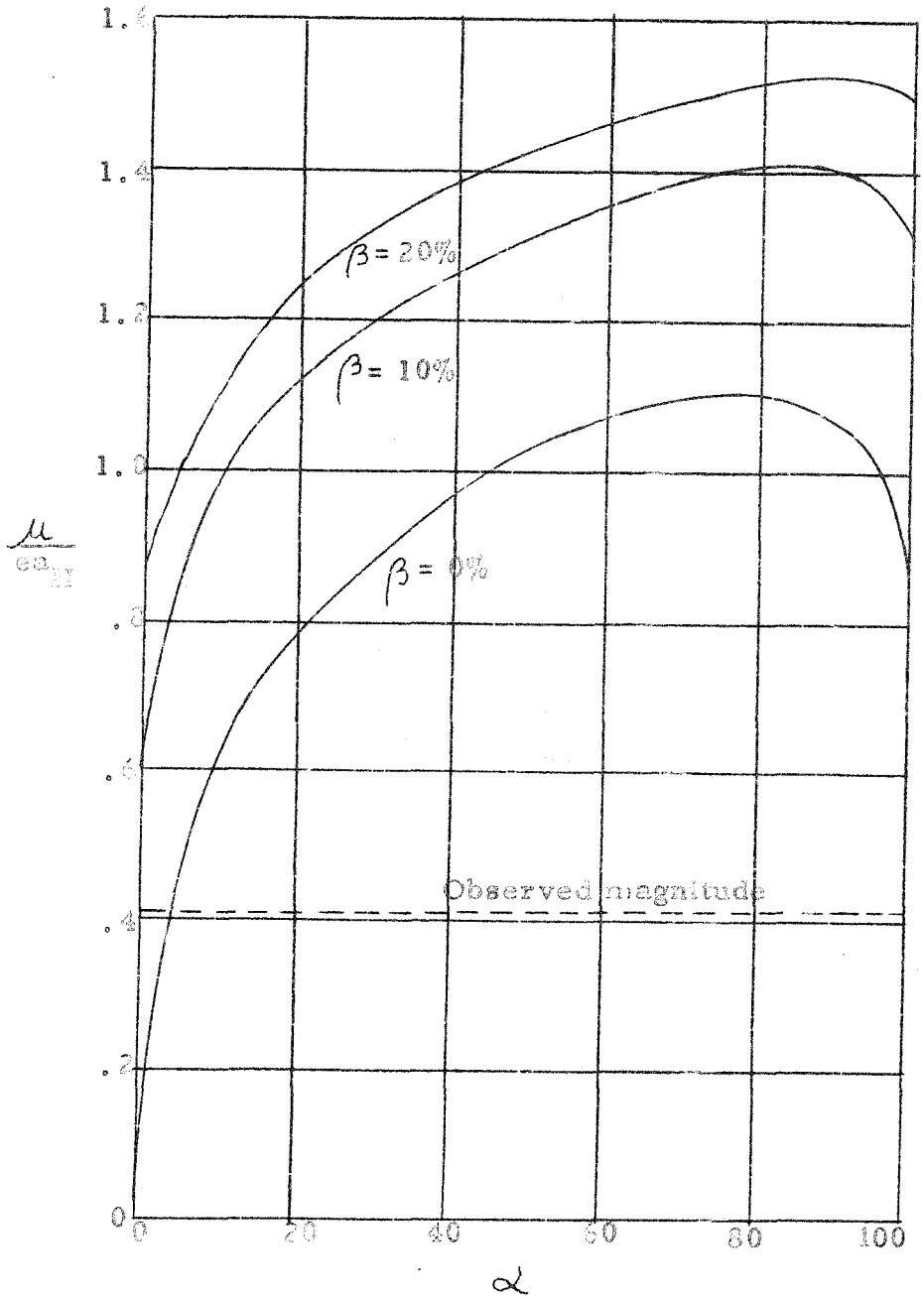

Fig. 4. The reduced dipole moment μ/ea_{xx} of HCl as a function of the percentage s-p hybridization for different ionicities.

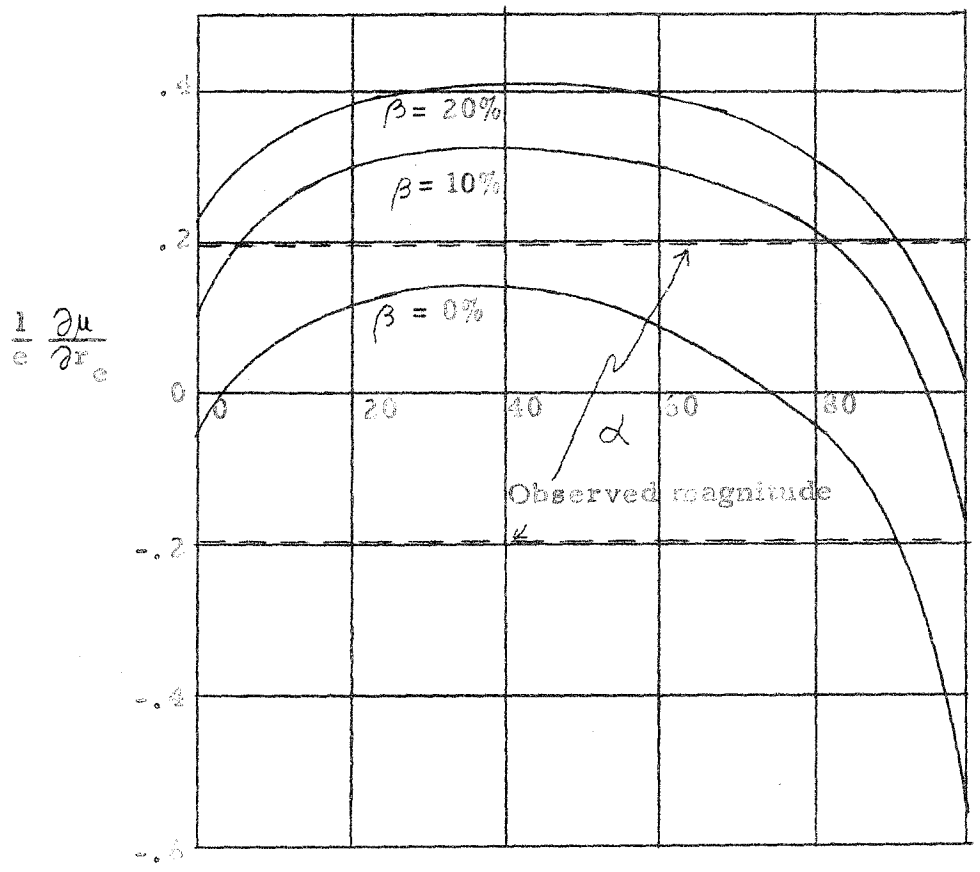

Fig. 5. The reduced effective charge $\frac{1}{e}\frac{\partial \mu}{\partial r_e}$ of HCl as a function of the percentage s-p hybridization for different ionicities.

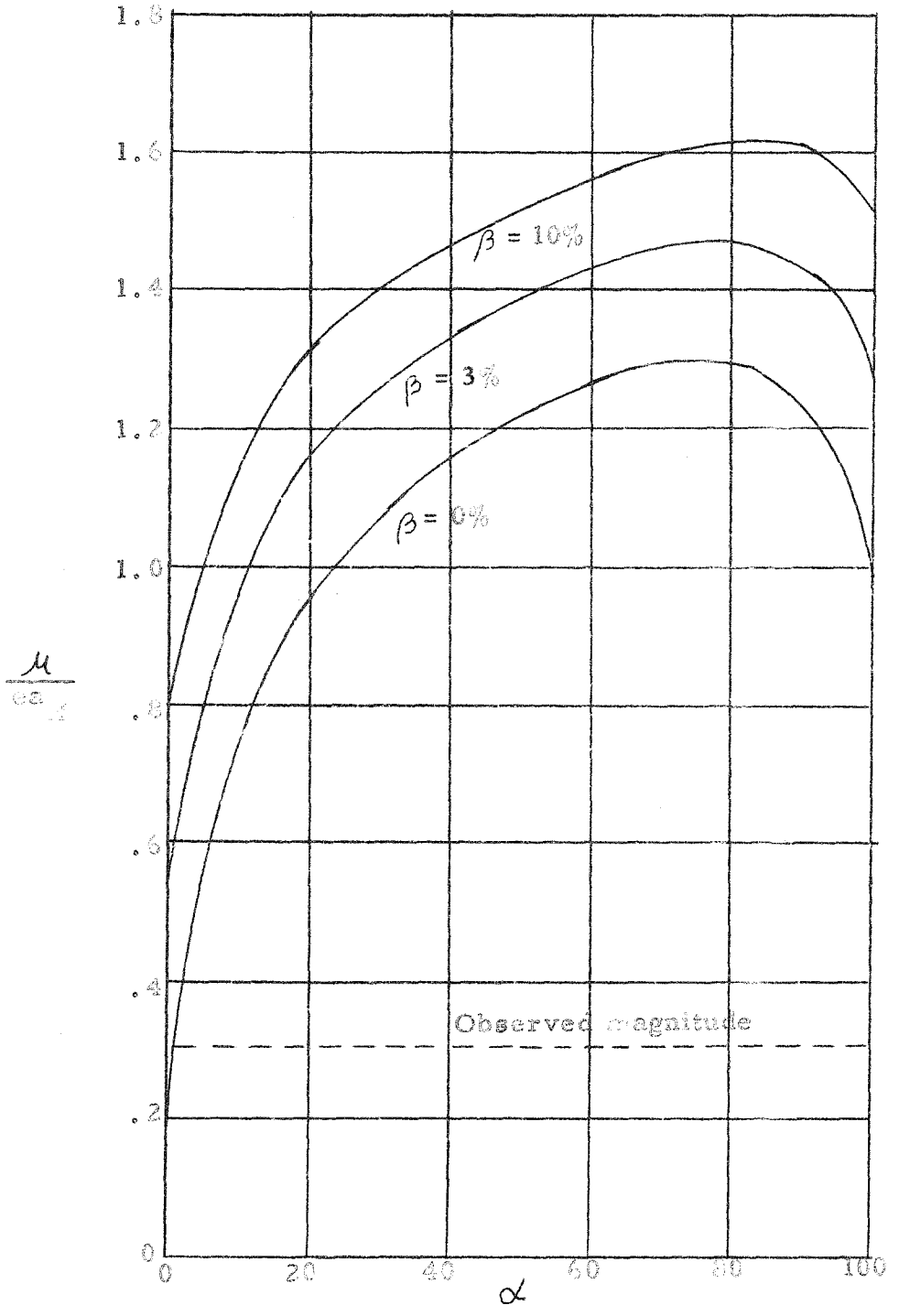

Fig. 1. The reduced dipole moment μ/ea_H of HBr as a function of the percentage s-p hybridization for different ionicities.

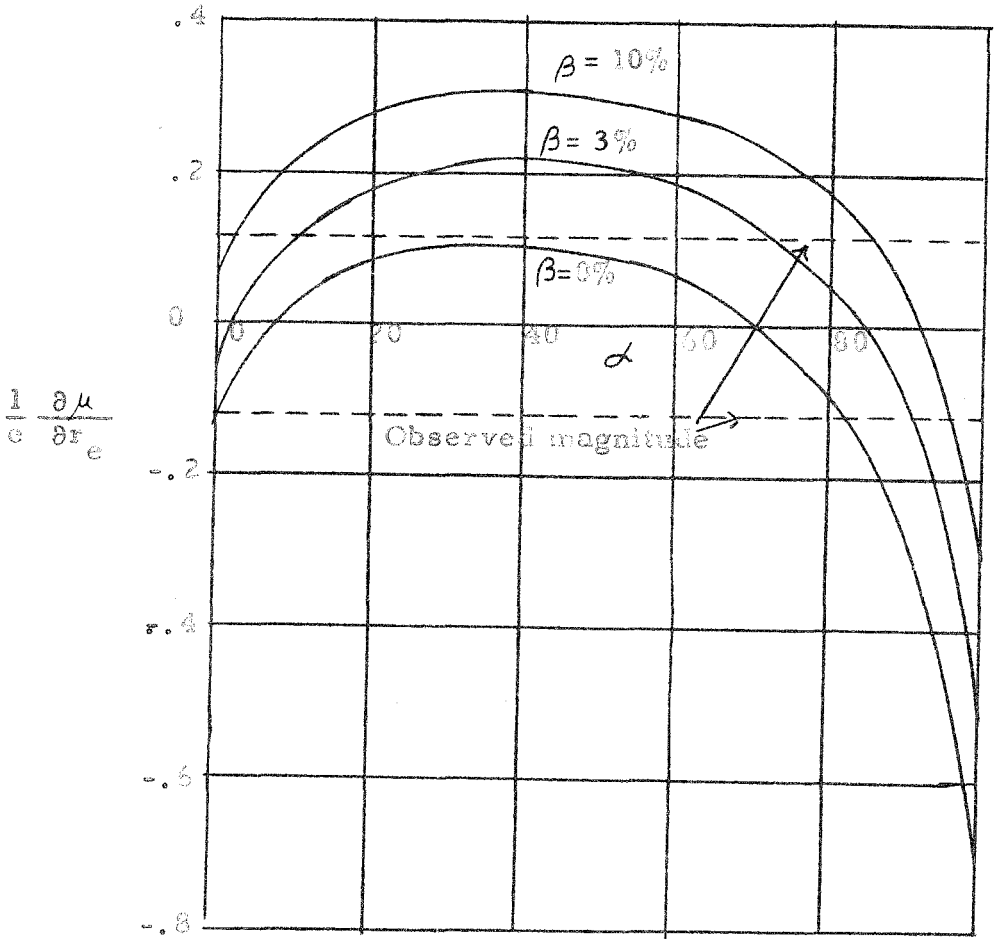

Fig. 7. The reduced effective charge $\frac{1}{e}\frac{\partial \mu}{\partial r_e}$ of HBr as a function of the percentage s-p hybridization for different ionicities.

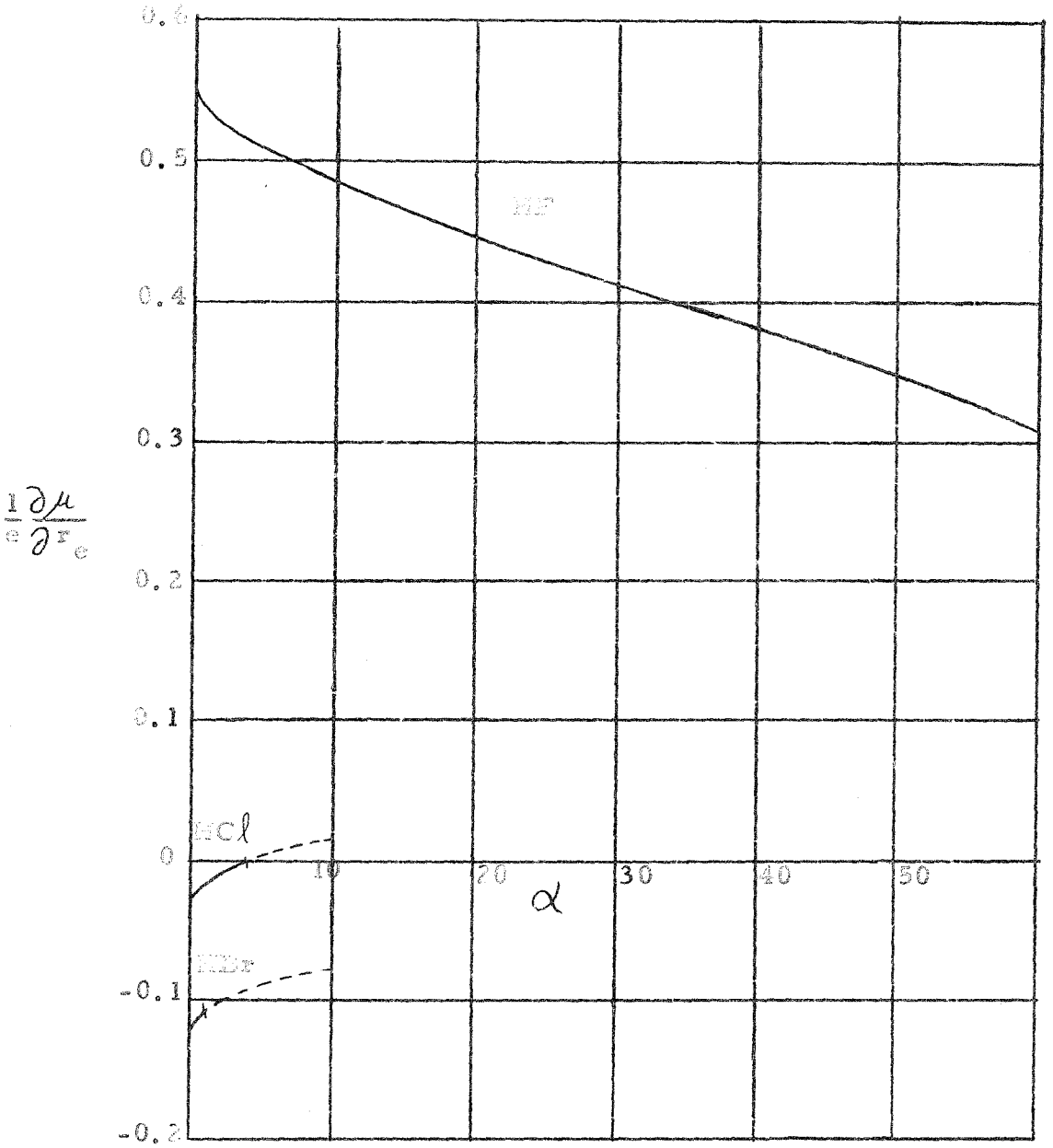

Fig. 8. The reduced effective charge as a function of the percentage s-p hybridization when the ratio α/β is chosen in such a way that the calculated values of the dipole moments agree with the measured values (the dashed portions of the curves correspond to negative values of λ).

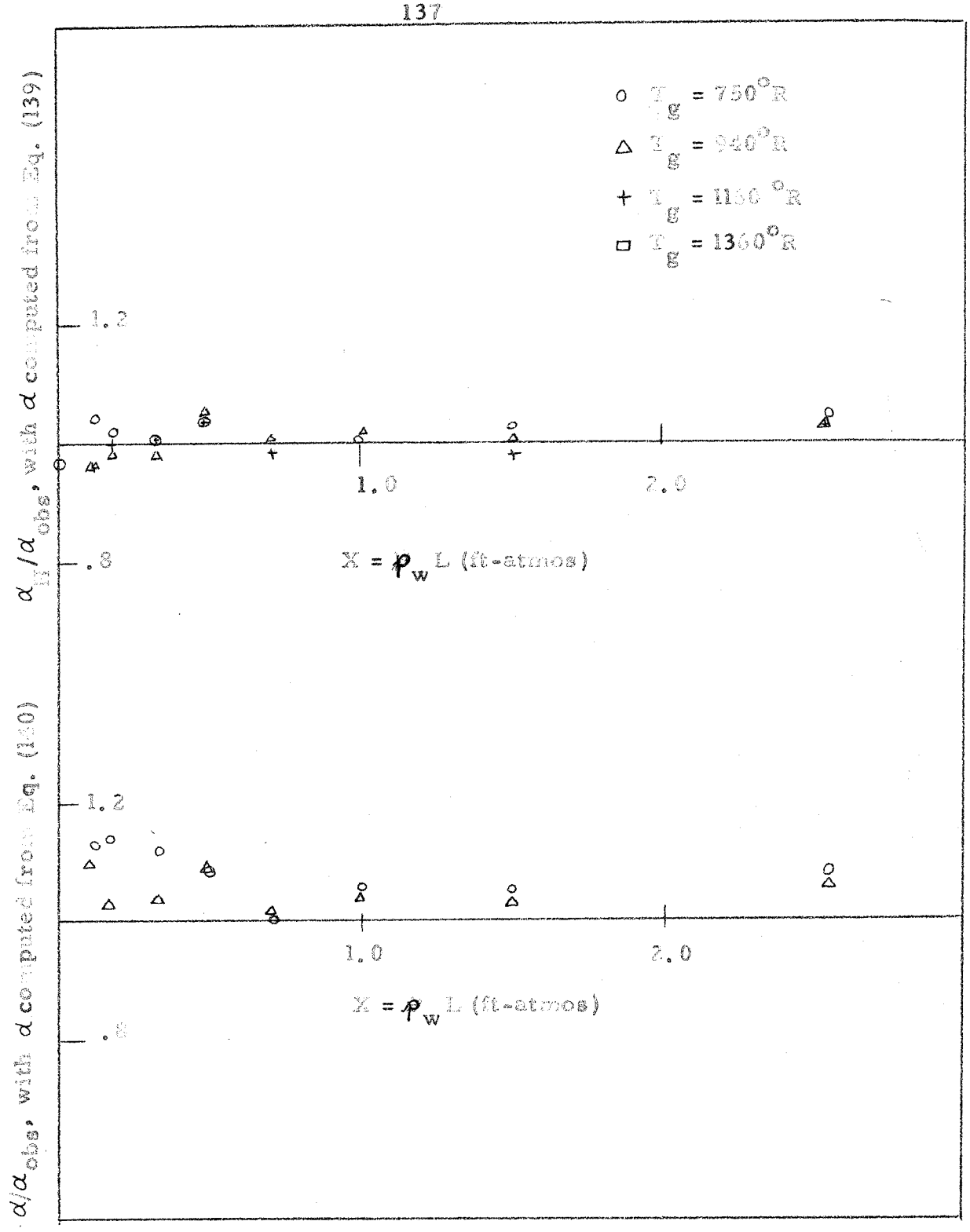

Fig. 9. The ratios α_H / α_{obs} and α/α_{obs} for blackbody radiation at a temperature T_s = 1160°R.

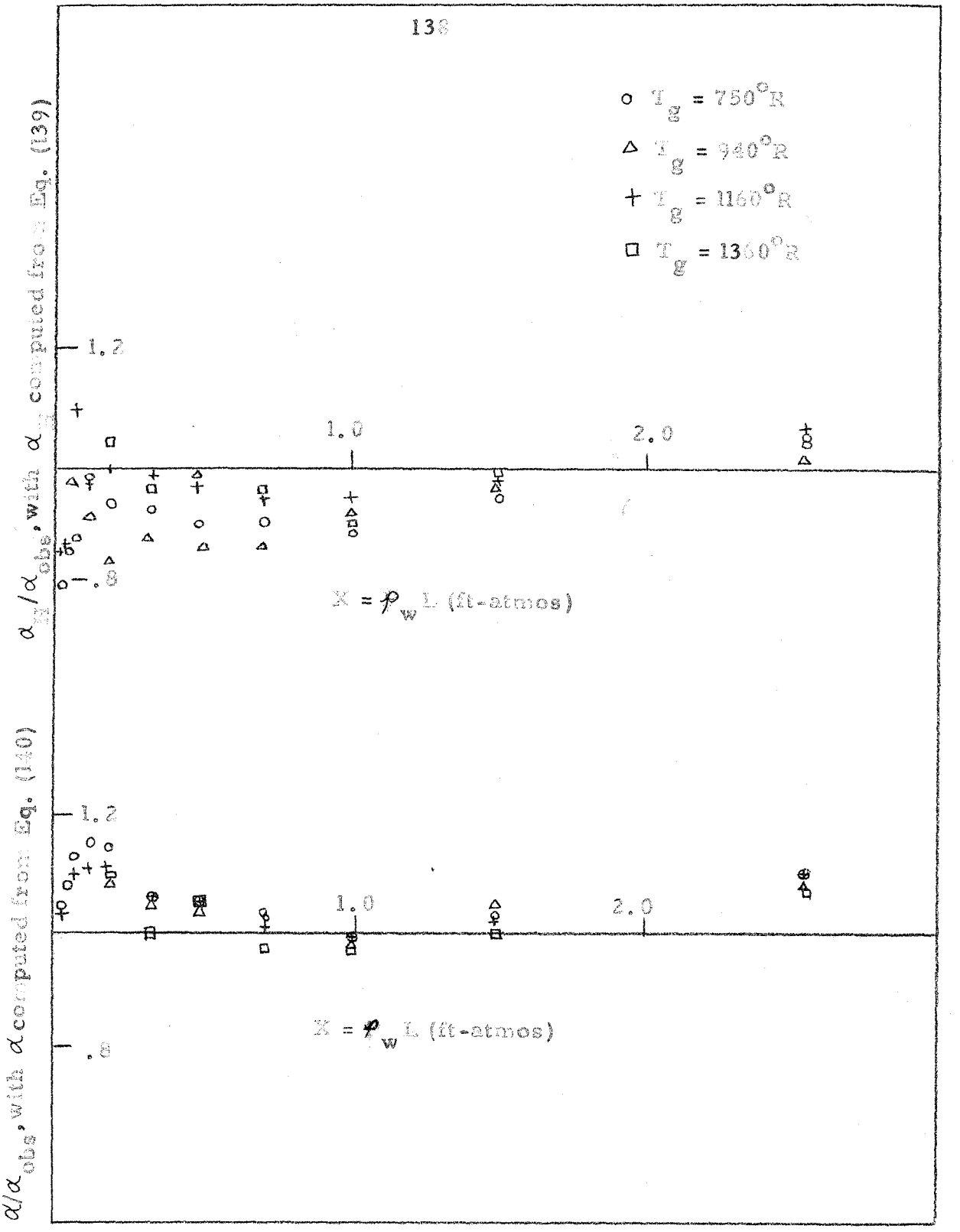

Fig. 10. The ratios α_H/α_{obs} and α/α_{obs} for blackbody radiation at a temperature $T_s = 1760^\circ R$.

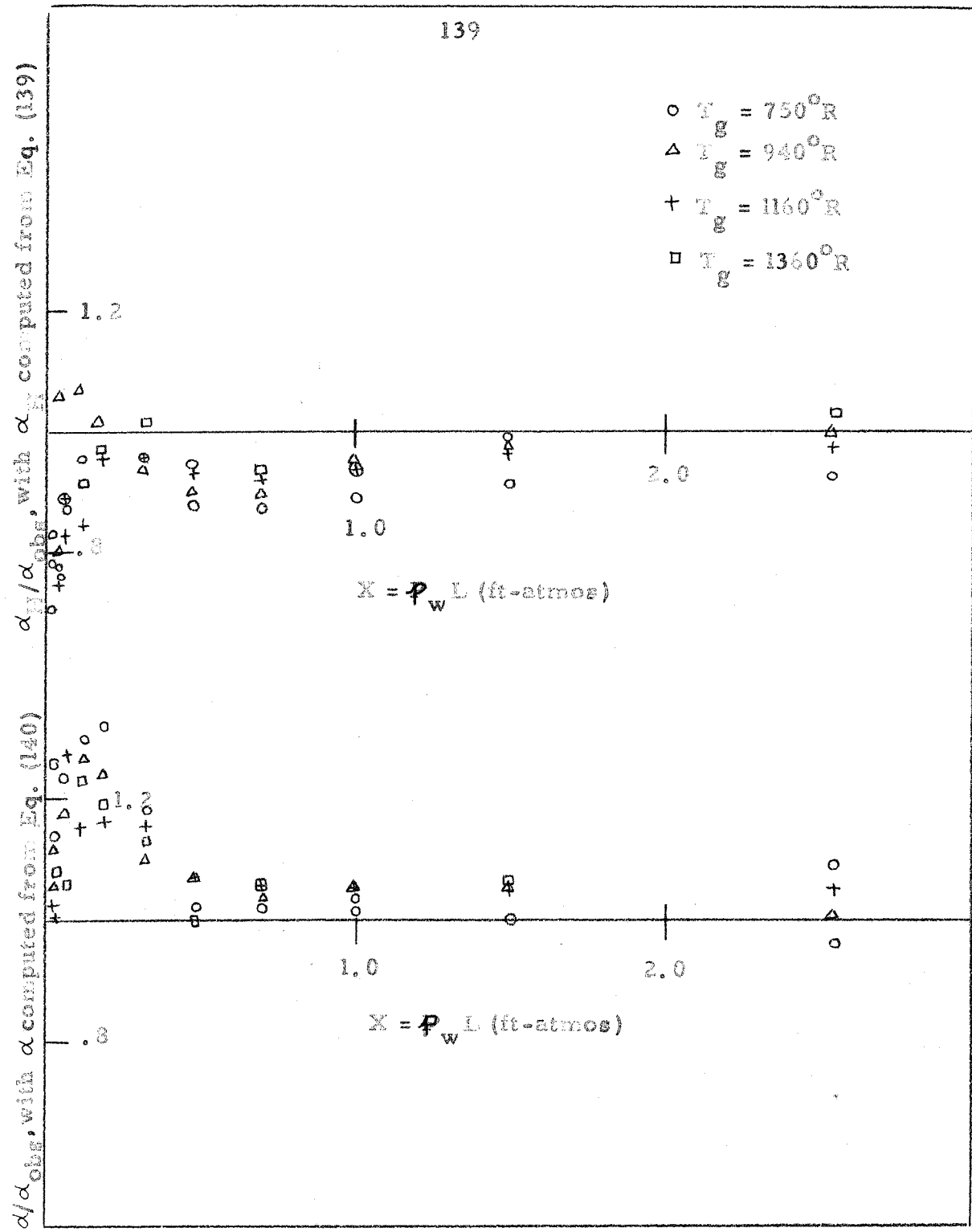

Fig. 11. The ratios α_{EY}/α_{obs} and α/α_{obs} for blackbody radiation at a temperature $T_g = 2500°R$.

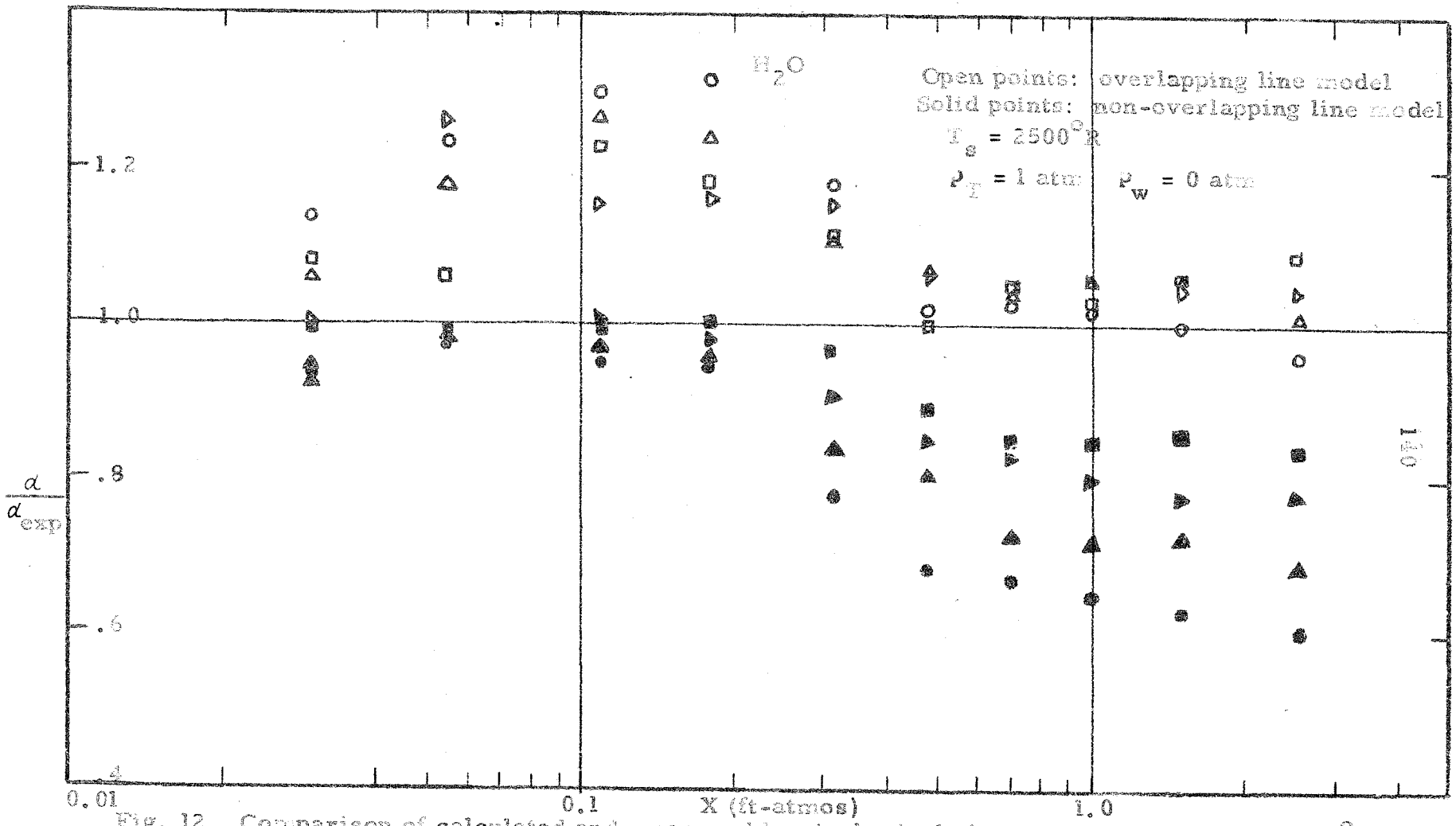

Fig. 12. Comparison of calculated and measured hemispherical absorptivity data for water vapor. The open points are calculated for an overlapping line model according to Eq. (140) and the solid points for a non-overlapping model according to Eq. (159).

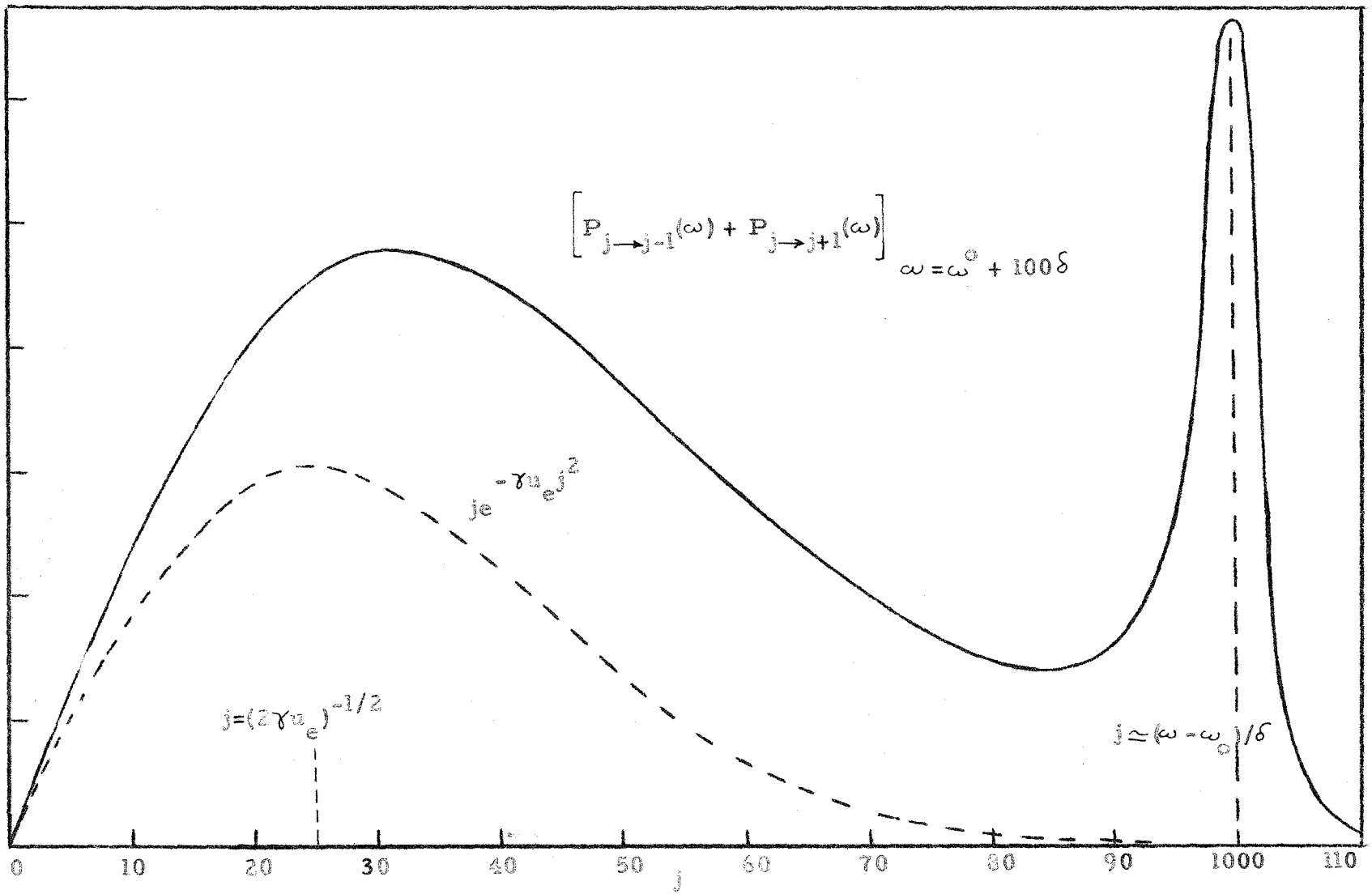

Fig. 13. The quantity $P_{j\to j-1}(\omega) + P_{j\to j+1}(\omega)$ evaluated at $\omega=\omega_o + 100\delta$ as a function of j for $b/\delta = 2.5$ and $(2\gamma u_e)^{-1/2} = 25$. The dashed curve represents $j \exp\left[-\gamma u_e j^2\right]$.

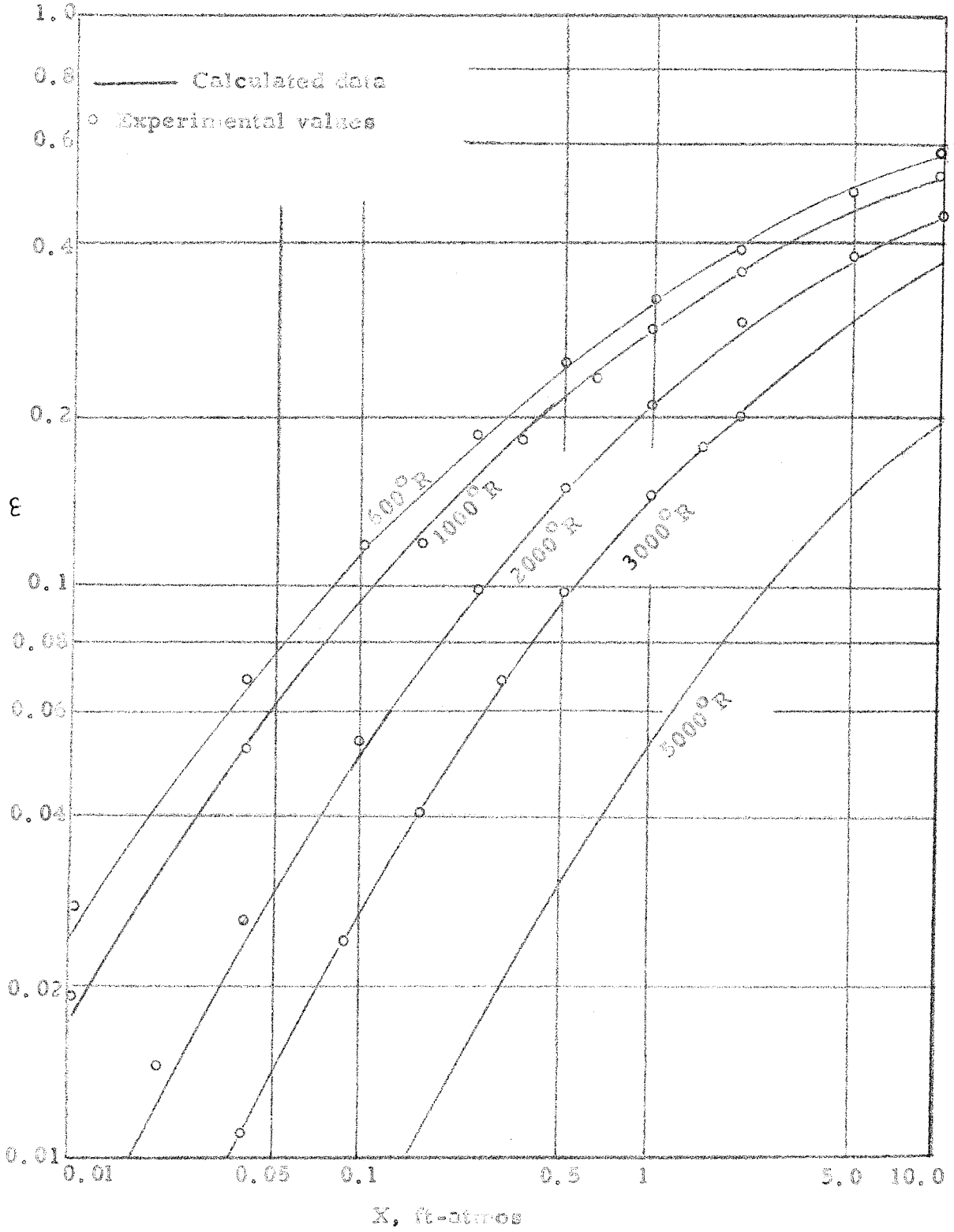

Fig. 14. The emissivity of water vapor calculated from Eq. (13f) by use of "best" values of the adjustable parameters. The circles represent experimental points according to Hottel[58] for pure water vapor at a pressure of 0.5 atmos.

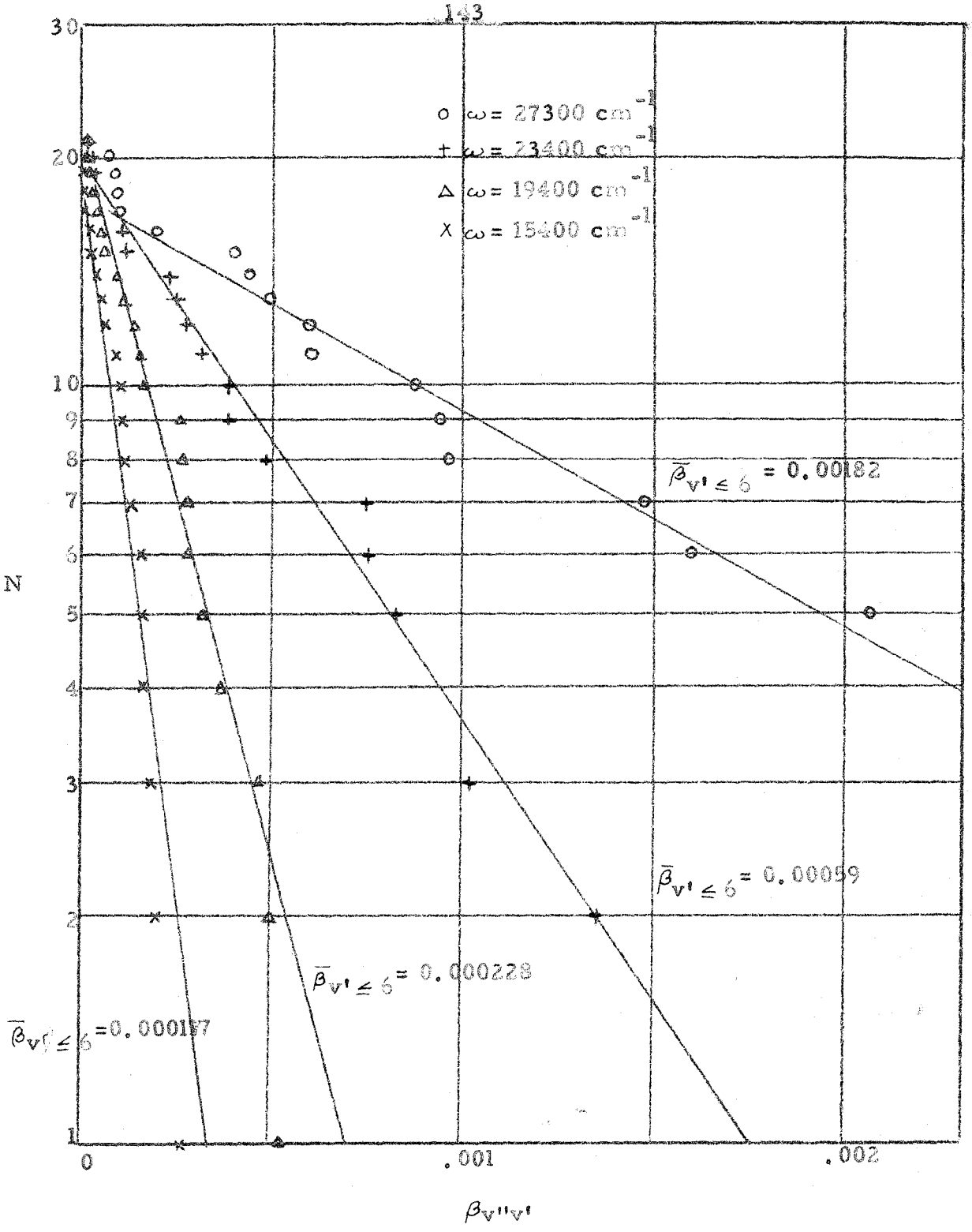

Fig. 15. Plot for determining the intensity distribution function $\rho(\alpha, \bar{\alpha})$ for the β-band system of NO at 8000°K. The solid curves correspond to the distribution $\rho(\beta, \bar{\beta}) = (\bar{\beta})^{-1} \exp(-\beta/\bar{\beta})$. The points are computed according to Eq. (257a) for $v' \le 6$ utilizing the values of $q^{v}_{v''v'}$ listed by Kivel, Mayer and Bethe.[26]

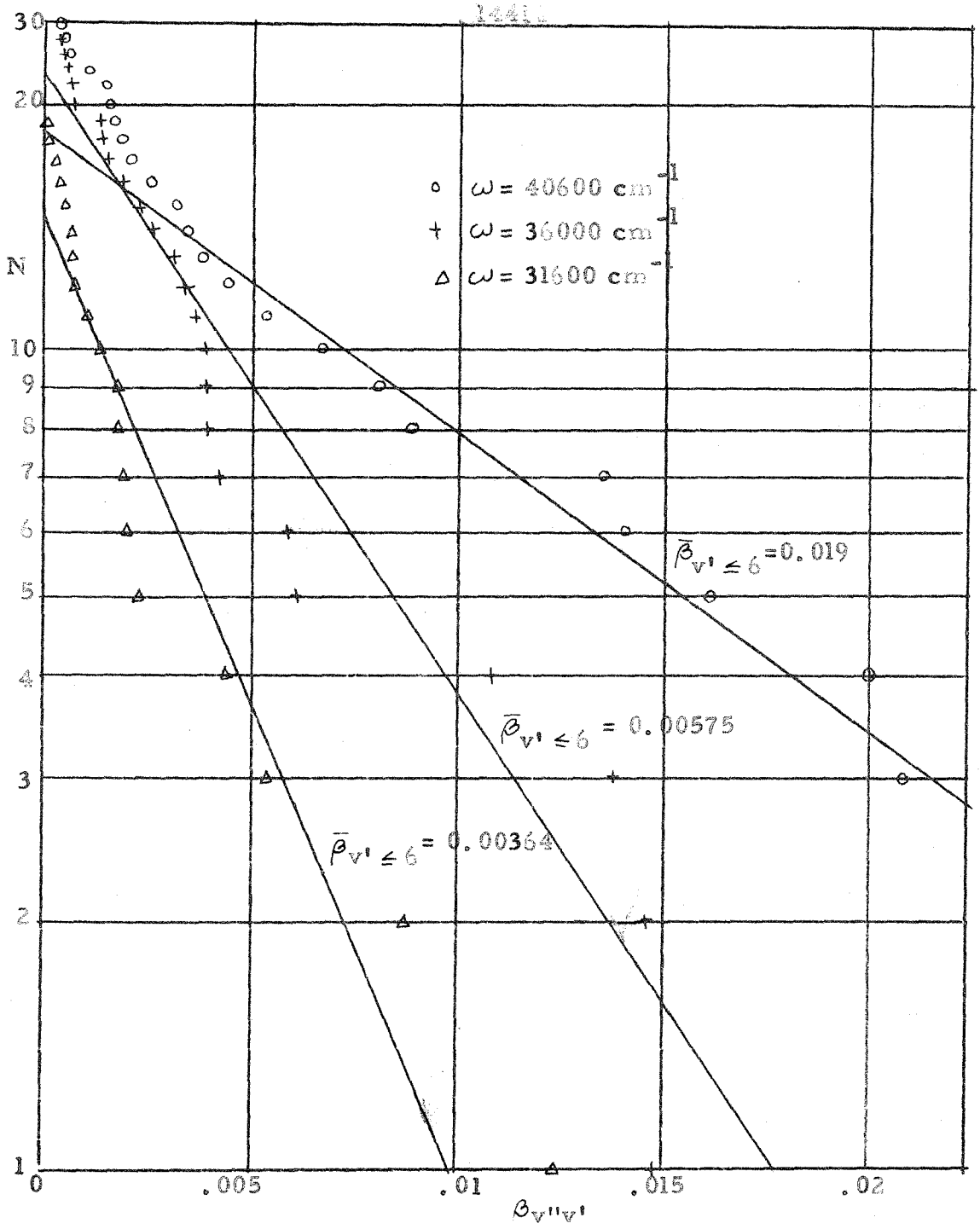

Fig. 16. Plot for determining the intensity distribution function $\rho(\alpha, \bar{\alpha})$ for the β-band system of NO at 8000°K. The solid curves correspond to the distribution $\rho(\beta, \bar{\beta}) = (\bar{\beta})^{-1} \exp(-\beta/\bar{\beta})$. The points are computed according to Eq. (257a) for $v' \leq 6$ utilizing the values of $q^2_{v''v'}$ listed by Kivel, Mayer and Bethe.[25]

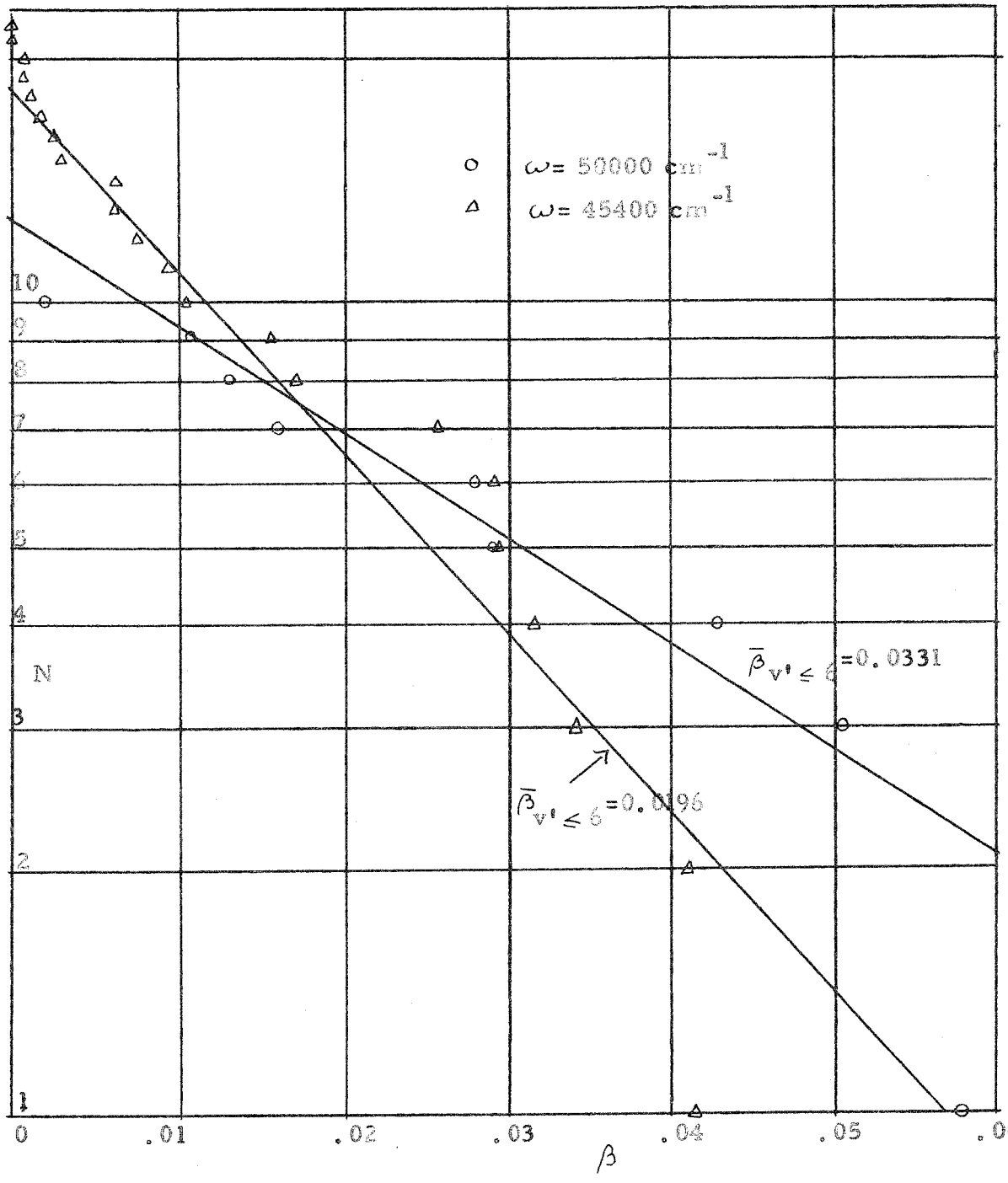

Fig. 17. Plot for determining the intensity distribution function $\rho(\alpha, \bar{\alpha})$ for the β-band system of NO at 8000°K. The solid curves correspond to the distribution $\rho(\beta, \bar{\beta}) = (\bar{\beta})^{-1} \exp(-\beta/\bar{\beta})$. The points are computed according to Eq. (257a) for $v' \leq 6$ utilizing the values of $q^2_{v''v'}$ listed by Kivel, Mayer and Bethe.[26]

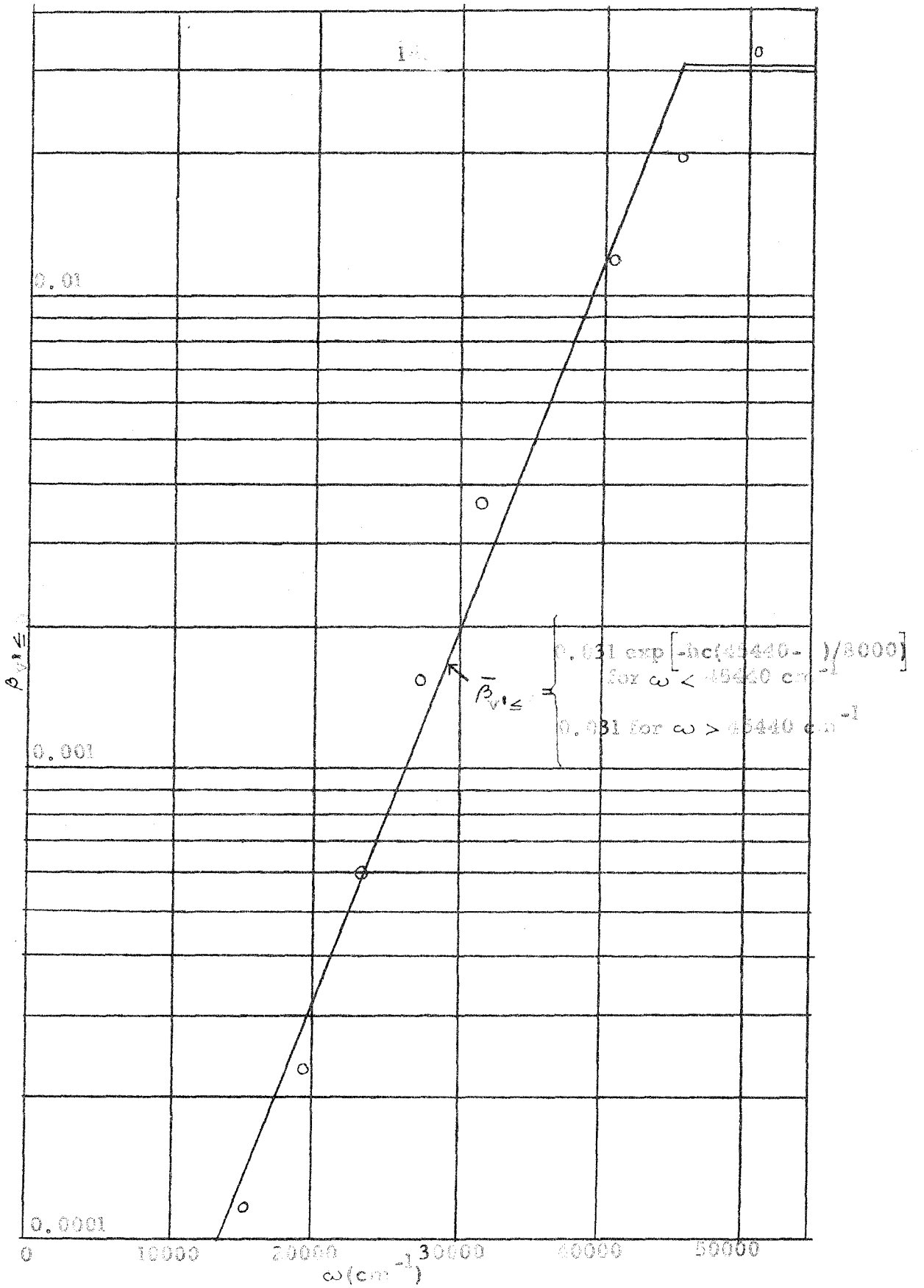

Fig. 18. The mean value of the parameter β for $v' \leq 4$ as a function of ω for the β-band system of NO at 8000°K.

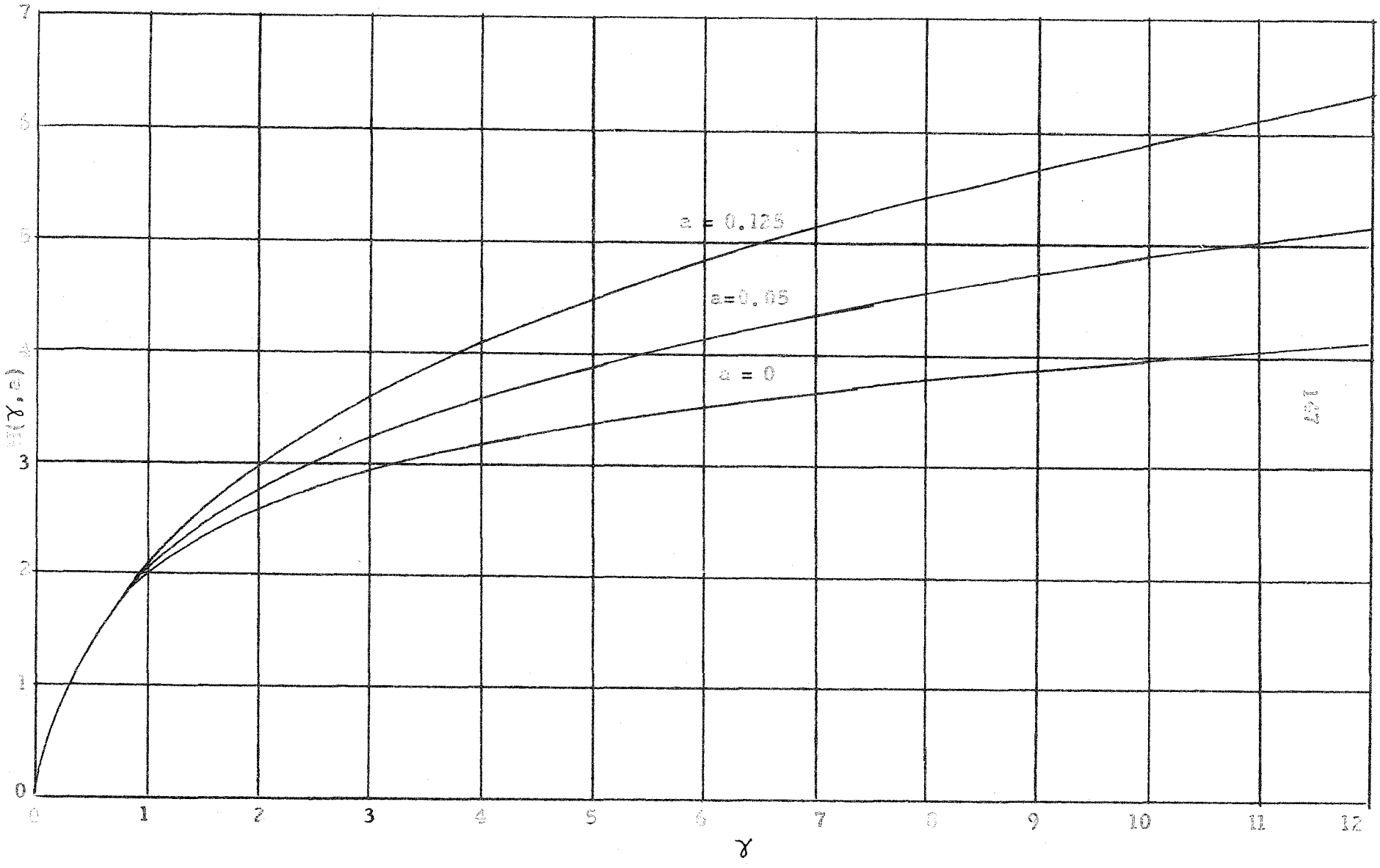

Fig. 19. The function $H(\gamma, a)$.

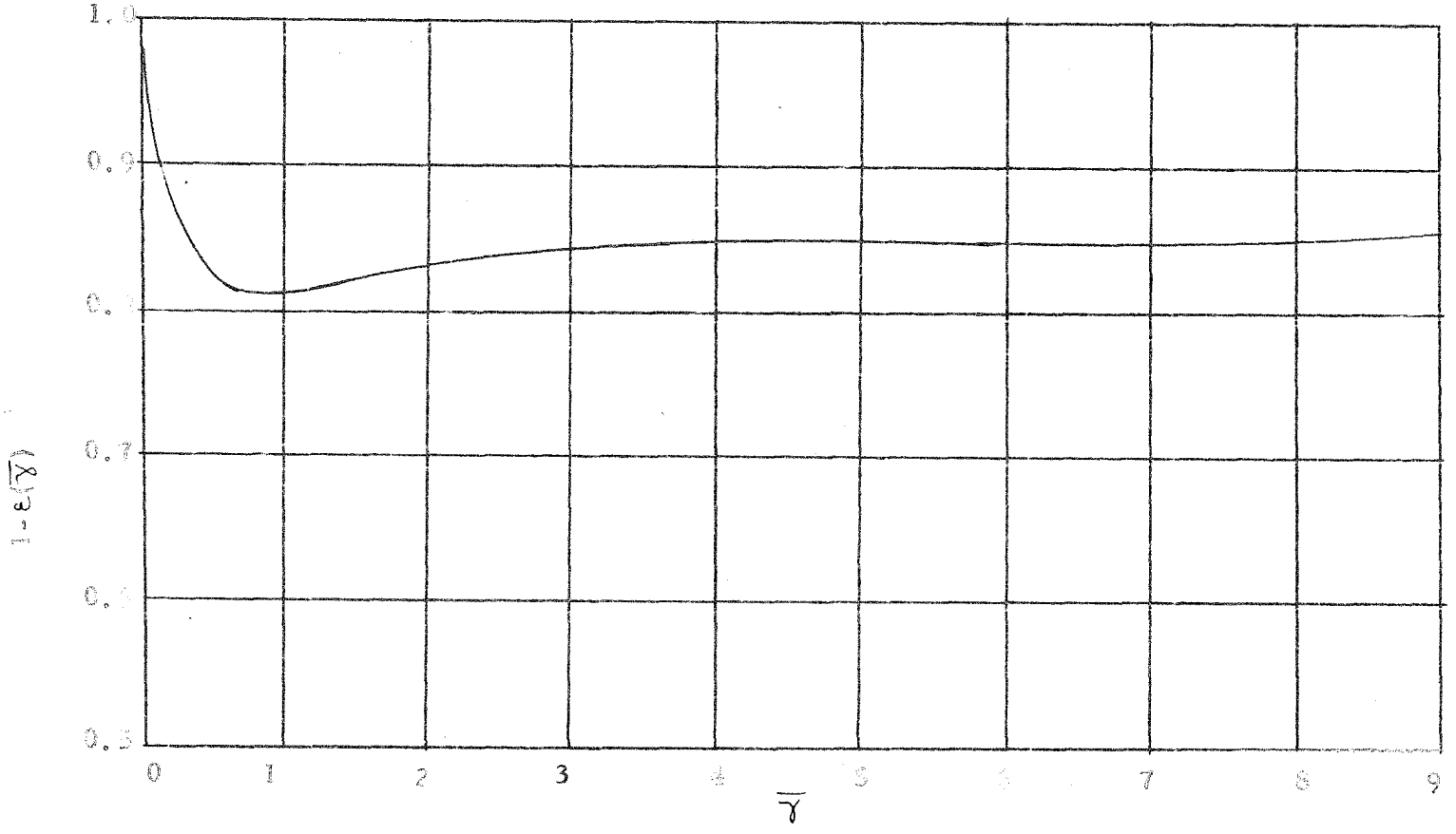

Fig. 20. The parameter $1-\varepsilon(\overline{\gamma})$ as a function of $\overline{\gamma}$.

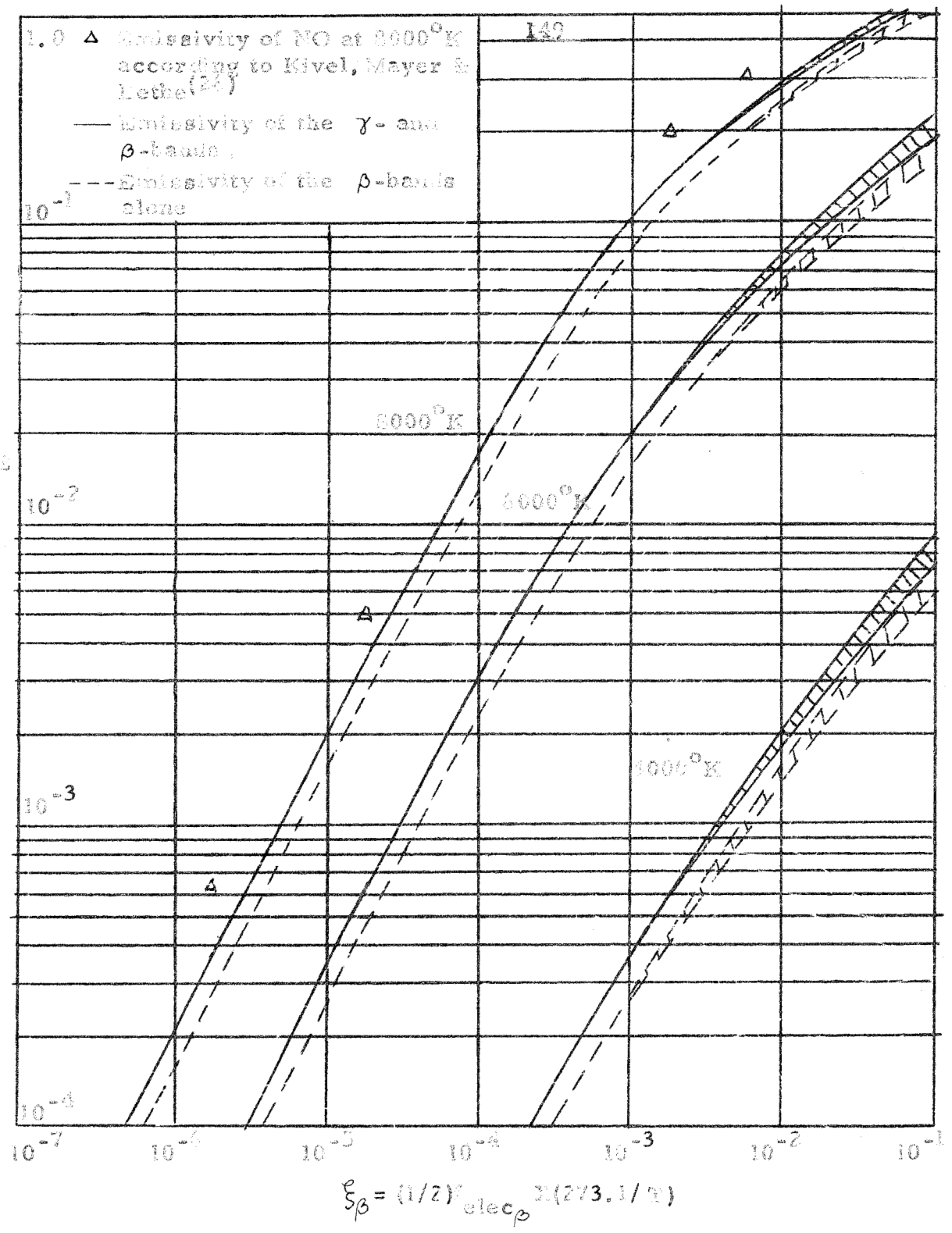

Fig. 21. The hemispherical emissivity of the γ- and β-bands of NO (for $T_{elec_\gamma} = 0.312\, T_{elec_\beta}$). The lower boundaries of the hatched regions refer to zero pressure and the upper boundaries to high pressure. For intermediate pressures the emissivity lies within the hatched regions.

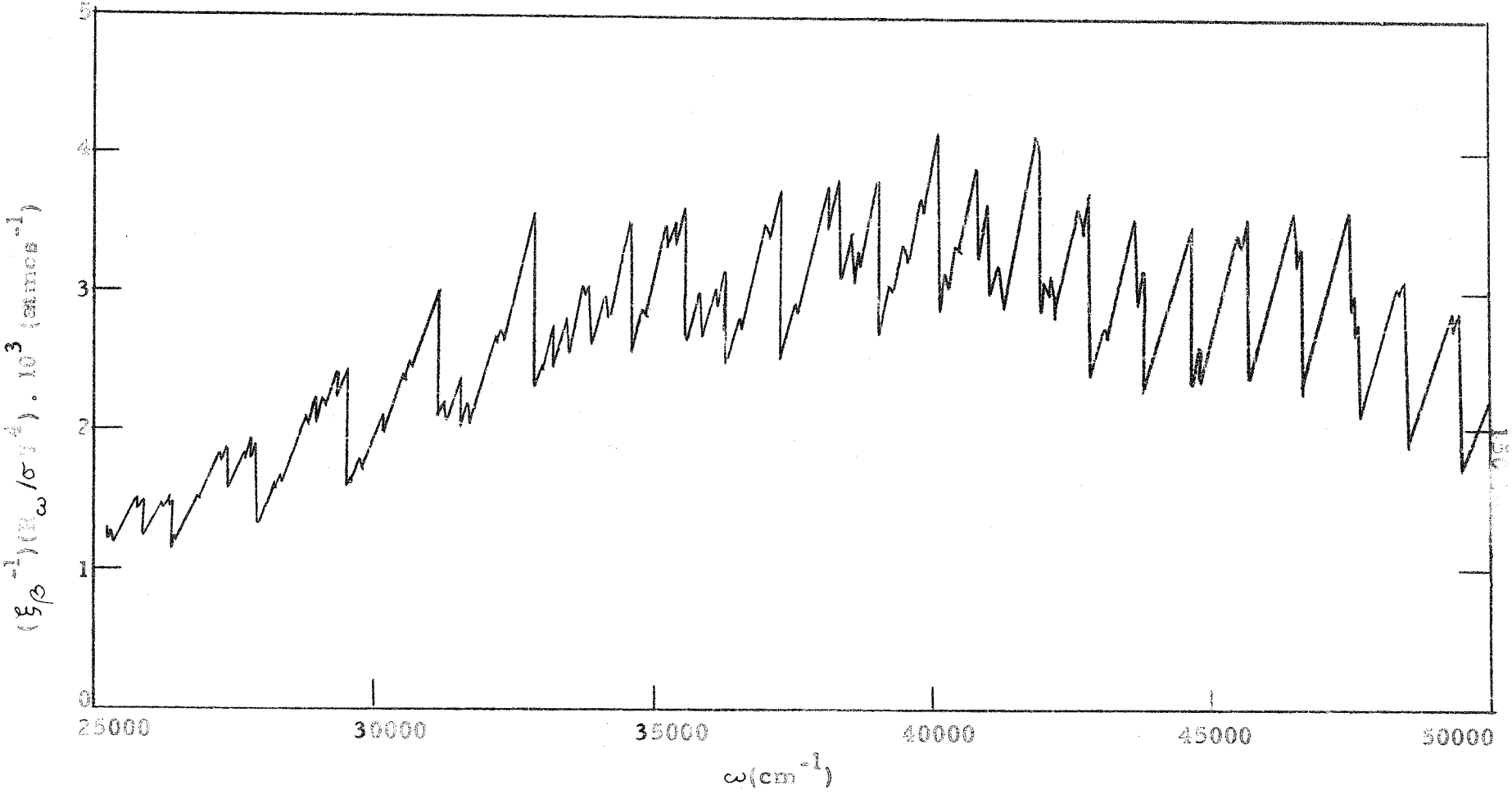

Fig. 22. Partial emission spectrum of the β-bands of NO at 8000°K and high pressure. Only transitions from the first six upper vibrational states have been included. The values of vibrational overlap integrals were taken from ref. (26).

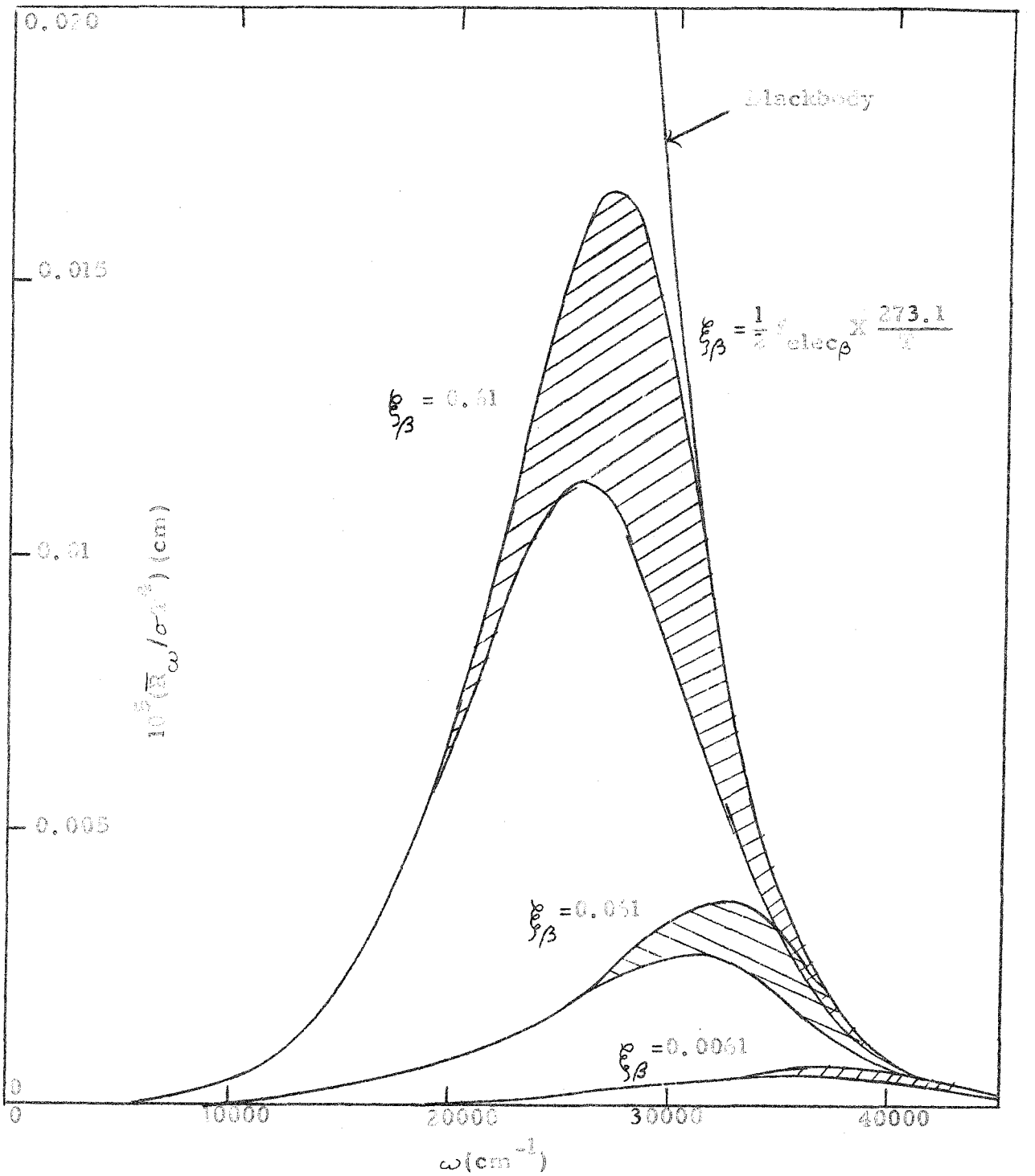

Fig. 23. The "smoothed" spectral radiancy $\bar{E}_\omega = \bar{\epsilon}_\omega E^0_\omega$ for the NO β-bands at 4060°K. The lower boundaries of the hatched regions correspond to zero pressure and the upper boundaries to very high pressure. For intermediate pressures the radiancy lies within the hatched regions.

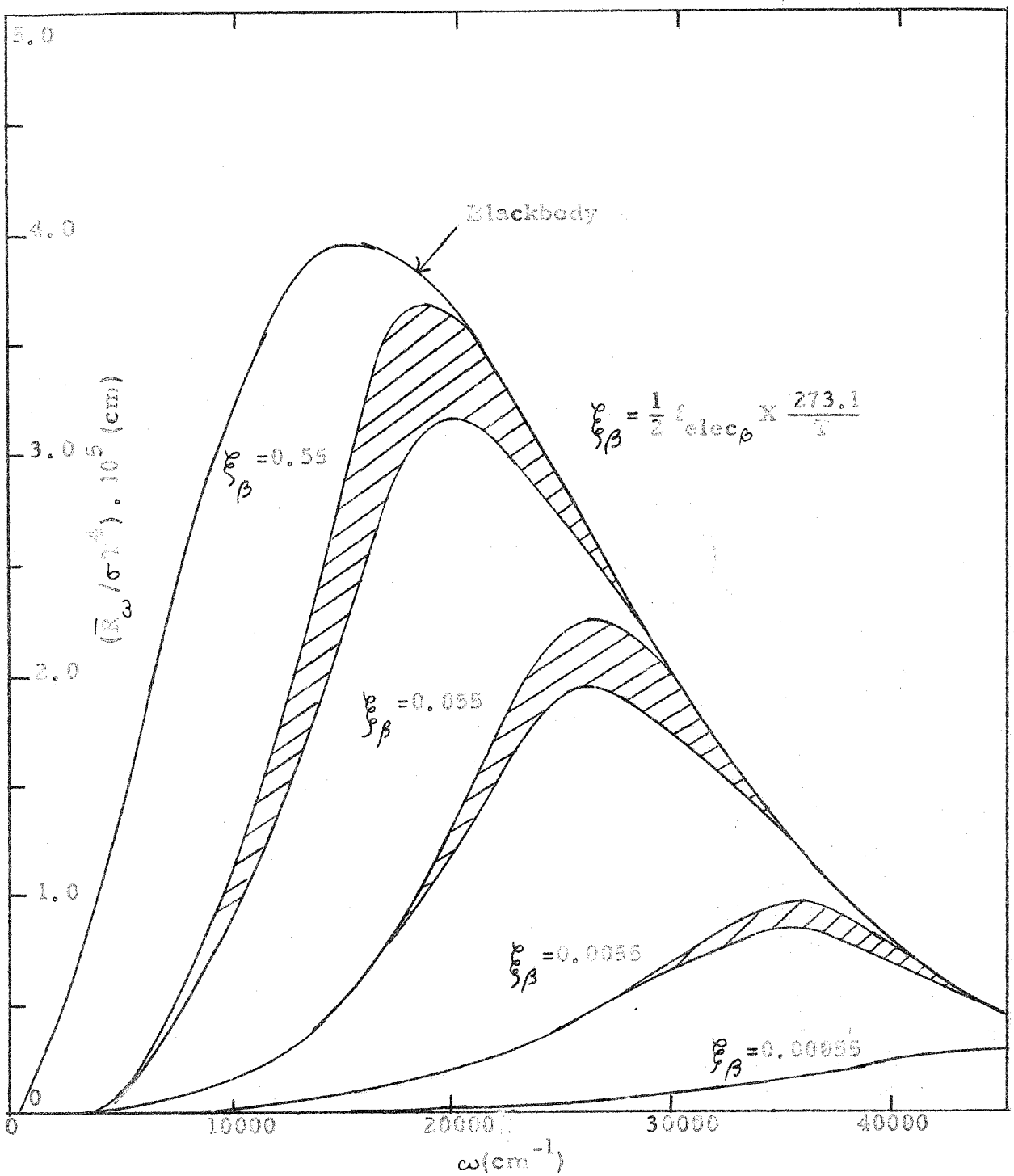

Fig. 24. The "smoothed" spectral radiancy $\bar{R}_\omega = \bar{\epsilon}_\omega R^o_\omega$ for the NO β-bands at 6000°K. The lower boundaries of the hatched regions correspond to zero pressure and the upper boundaries to very high pressure. For intermediate pressures the radiancy lies within the hatched regions.